Analysis of
Halogenated Trace Gases in Air
with Gas Chromatography -
Time-of-Flight Mass Spectrometry

Dissertation

zur Erlangung des Doktorgrades

Doctor rerum naturalium (Dr. rer. nat.)

Vorgelegt am Fachbereich 11

der Johann Wolfgang Goethe Universität

Frankfurt am Main

Vorgelegt von Florian Obersteiner aus München

Frankfurt, August 2016

D 30

Vom Fachbereich 11 der Johann Wolfgang Goethe Universität als Dissertation angenommen.

Dekan:

Prof. Dr. Peter Lindner

Gutachter:

Apl. Prof. Dr. Andreas Engel

Prof. Dr. Joachim Curtius

Datum der Disputation:

18. Januar 2017

Zusammenfassung

Ziel dieser Arbeit war es, die Flugzeitmassenspektrometrie als neue Analysemethode für die instrumentelle Analytik halogenierter Spurengase in der Luft zu etablieren. Die grundlegende Motivation dafür ist, dass anthropogene Emissionen vieler Vertreter dieser Substanzklasse einen negativen Einfluss auf die Umwelt zeigen: in der Atmosphäre agieren die Substanzen bzw. ihre Abbauprodukte als Katalysatoren für den stratosphärischen Ozonabbau und verstärken den Strahlungsantrieb der Erde durch Absorption elektromagnetischer Strahlung im sogenannten atmosphärischen Fenster. Um diese Effekte und deren Auswirkung quantifizieren zu können, ist es notwendig, Konzentrationen und Trends der Substanzen in der Atmosphäre zu überwachen. Nur so können Gegenmaßnahmen wie Produktionsreglementierungen geplant und bewertet werden. In Kombination mit inverser Modellierung können zudem Rückschlüsse über tatsächlich emittierten Mengen gezogen werden. Dies stellt den Anspruch an die Analytik, sehr geringe Mengen dieser Gase sehr präzise quantifizieren zu können, um auch schwache Trends zu erkennen. Zudem muss die Analysemethode die Möglichkeit zu bieten, mit der wachsenden Anzahl bekannter und zu überwachender Substanzen Schritt zu halten. Besonders für letzteren Aspekt bietet die Flugzeitmassenspektrometrie einen entscheidenden Vorteil gegenüber der „konventionellen" Methode der Quadrupolmassenspektrometrie: sie zeichnet das gesamten Massenspektrum auf ohne dadurch an Empfindlichkeit einzubüßen. Um das atmosphärische Mischungsverhältnis von Substanzen im Bereich von pmol mol^{-1} bis fmol mol^{-1} bestimmen zu können, muss das Quadrupolmassenspektrometer im Single Ion Monitoring (SIM) Modus betrieben werden – so wird zwar eine hohe Sensitivität erreicht, es wird aber auch nur die Intensität eines bestimmten Masse zu Ladungsverhältnisses (kurz: Masse) zu einem Zeitpunkt aufgezeichnet. Ein Flugzeitmassenspektrometer hingegen extrahiert Ionen mit einer Frequenz im Kiloherzbereich und zeichnet für jede Extraktion das vollständige Flugzeitspektrum (und damit Massenspektrum) auf.

Aufgabe dieser Arbeit war es, ein Flugzeitmassenspektrometer mit vorgeschalteter Probenanreicherungseinheit sowie Gaschromatograph zur Trennung des Subtanzgemisches vor der Detektion aufzubauen und Werkzeuge zur Datenauswertung zu entwickeln. Um einen zukünftigen Feldeinsatz vorzubereiten, sollte der Aufbau möglichst kompakt, mobil und vollständig automatisiert sein. Anschließend sollte Empfindlichkeit, Präzision

und dynamischer Messbereich geprüft, optimiert und die Anwendbarkeit zur Analyse halogenierter Spurengase gezeigt werden.

Nach gründlicher Marktrecherche wurden ein kommerziell erhältlicher Gaschromatograph der Firma Agilent sowie ein Massenspektrometer der Firma Tofwerk erworben und mit einer zuvor selbstentwickelten Probenanreicherungseinheit gekoppelt. Letztere stellt eine Weiterentwicklung des in der Masterarbeit des Autors vorgestellten Systems dar (Obersteiner, 2012). Die Ergebnisse aus der in der vorliegenden Arbeit präsentierten Geräteentwicklung finden sich in drei Publikationen wieder (siehe Abschnitt II), welche in thematischer Reihenfolge die Probenanreicherung (Obersteiner et al., 2016b), den Vergleich von Quadrupol- und Flugzeitmassenspektrometrie (Hoker et al., 2015) sowie Eigenschaften und Anwendung des neuen Aufbaus (Obersteiner et al., 2016a) behandeln.

Die erste in Abschnitt II aufgeführte Publikation diskutiert die Charakterisierung und Anwendung der selbstentwickelten, kryogenen Probenanreicherung. Eine solche ist für die Analyse vieler Spurengase essentiell, insbesondere in Kombination mit der Elektronenionisation in der Massenspektrometrie. Nach der Anreicherung auf adsorptivem Material bei $T \leq -80\,°C$ in einer kurzen gepackten Säule wird die Probe mittels Thermodesorption direkt in die gaschromatographische Säule injiziert. Das Anreicherungsverfahren zeichnet sich durch die Verwendung eines Stirlingkühlers aus, wodurch das System lediglich einer Stromversorgung bedarf und sich in Kombination mit dem kompakten Design und dem Verzicht auf bewegliche Teile und Vakuumisolation optimal für den wartungsfreien Feldeinsatz eignet. Diese Eignung wird durch den erfolgreichen Einsatz des Anreicherungsverfahrens als Teil des GhOST-MS, eines Messgeräts der Arbeitsgruppe Engel für flugzeugbasierte in-situ Messungen, eindrucksvoll bezeugt. Die Charakterisierung am Laborgerät zeigte, dass sich das System nahezu uneingeschränkt für die hochpräzise Analyse vieler halogenierter Spurengase in Luftproben eignet. Potentiell ist das Substanzspektrum z.B. um Kohlenwasserstoffe erweiterbar und ebenso für die Verwendung in Kombination mit anderen Detektionsmethoden geeignet. Zukünftig könnte die Methode um ein Verfahren zur Abscheidung von ungewünscht angereichertem CO_2 erweitert werden, was die Bandbreite der analysierbaren Substanzen um leichtflüchtige Gase wie CF_4 oder C_2H_6 ergänzen könnte.

Der erste Aufbau einer solchen Anreicherungseinheit im Labor war elementarer Bestandteil der zweiten hier aufgeführten Publikation, welche den Vergleich eines Flugzeitmas-

senspektrometers der Firma Markes (Modell BenchTOF-dx E24) mit einem Quadrupol-massenspektrometer der Firma Agilent (Modell 5975C) als Referenz beschreibt. Das BenchTOF-dx zeigte hier zwar eine herausragende Empfindlichkeit (Detektionsgrenze bis zu ~20 ppq in 1 L Probe) und vergleichbare Präzision bei der Substanzquantifizierung (bis zu ~0.2 %), blieb in punkto Trennung benachbarter Signale in der Massendimension (Massenauflösung) aber auf dem Niveau des Quadrupols ($m/\Delta m$ ~1000; nur Integermas-sen exportierbar) und erreichte dessen lineares Ansprechverhalten nicht. Insbesondere die signifikante Nichtlinearität im Detektorsignal schränkt die Einsatzmöglichkeit des BenchTOF-dx für die quantitative Analyse halogenierter Spurengase ein. Die bisher er-folglose Suche nach einer Ursache von und Korrekturmöglichkeit für die auftretende Nichtlinearität wurde durch ein proprietäres Datenformat erschwert, welches den Einsatz dieses Geräts für wissenschaftliche Fragestellungen generell einschränkt.

Die beschriebenen messtechnischen Limitierungen sollten mit dem in der vorliegenden Arbeit entwickelten Aufbau vermieden werden. Die wesentliche Neuerung auf techni-scher Seite ist ein Flugzeitmassenspektrometer der Firma Tofwerk (Modell EI-003), wel-ches eine höhere Massenauflösung und einen größeren dynamischen Bereich bietet. Zu-dem werden die Daten des Spektrometers in einem offenen Datenformat gespeichert, was eine deutlich tiefgreifendere Analyse erlaubt. Darauf aufbauend konnte mit geeigneten Verfahren bei der Datenauswertung ein lineares Ansprechverhalten bis hin zu einem Pro-benanreicherungsvolumen von 10 L gezeigt werden. Dies entspricht mit der genannten Anreicherungsmethode einem quantifizierbaren Konzentrationsbereich von ungefähr 10^{-13} bis 10^{-9} mol mol^{-1}. Die signifikant höhere Massenauflösung im Vergleich zum BenchTOF-dx von $m/\Delta m$ ~4000 ermöglicht eine hohe Empfindlichkeit durch die gewon-nene Selektivität für bestimmte Molekülfragmentmassen. Empfindlichkeit als auch Präzi-sion bei der Quantifizierung von Analyten sind vergleichbar mit der des Quadrupolspekt-rometers im SIM Modus, welches bereits in der vorangegangenen Publikation als Refe-renz diente. Die LabVIEW-basierte Steuersoftware der vorgeschalteten Probenanreiche-rung erlaubt zudem einen vollautomatischen Messbetrieb, da sie auch Gaschromatograph und Massenspektrometer ansteuern kann. So kann der Nutzer deutlich mehr Zeit in die Datenauswertung investieren.

Die Flugzeitmassenspektrometrie stellt ein wertvolles neues Werkzeug im Forschungsumfeld dieser Arbeit dar. Im Gegensatz zum hier typischerweise eingesetzten Quadrupolmassenspektrometer im SIM Modus können unbekannte Signale im Chromatogramm einfach identifiziert werden, da immer ein weitgehend vollständiges Massenspektrum vorliegt − ohne, dass dafür besondere Einstellungen bzw. Experimente notwendig wären. So können auch retrospektiv Signale ausgewertet werden, welche bei Aufzeichnung des Chromatogramms unbekannt waren und erst später identifiziert wurden. Das Massenauflösungsvermögen des Tofwerk-Instruments ist hierbei von besonderer Hilfe, da die Identifikation über die Zuordnung exakter Fragmentmassen verifiziert werden kann. In Kombination mit der hohen Messpräzision und −genauigkeit ist das Messgerät damit hervorragend für die quantitative Analyse halogenierter Spurengase geeignet. Die neue Messmethode förderte allerdings auch neue Probleme zutage, wie z.B. die Empfindlichkeit des Spektrometers gegenüber großer Mengen CO_2 und H_2O, welche mit dem verwendeten Anreicherungsverfahren zwangsweise den Detektor erreichen. Deren Signale können zwar unterdrückt aber nicht wie beim Quadrupol vollständig ausgeblendet werden. Ergebnisse der Arbeit mit dem BenchTOF-dx Massenspektrometer zeigen, dass lineares Ansprechverhalten und ein für die hier beschriebene Fragestellung wünschenswerter dynamischer Bereich von ~10^6 nach wie vor eine große technische Herausforderung darstellen.

Mit den in 2015 und 2016 veröffentlichten Aufsätzen ist die Arbeitsgruppe Engel weltweit die erste, welche hochpräzise Analytik halogenierter Spurengas routinemäßig mittels Flugzeitmassenspektrometrie durchführt. Der nächste Schritt ist der Übergang von der Laboranwendung zur Feldmessung, z.B. in Form von bodenbasierter in-situ Analyse troposphärischer Luftmassen am Taunus Observatorium auf dem Kleinen Feldberg. Da es bisher keine Messstation für die hier beschriebene analytische Fragestellung in Deutschland gibt, könnte eine deutliche Verbesserung der Überwachung halogenierter Treibhausgase und ozonzerstörender Substanzen in Europa erzielt werden. Weiterhin wäre eine Flugzeugapplikation in Zukunft denkbar, welche neben der durch das Flugzeitmassenspektrometer abgedeckten Substanzbandbreite auch von dessen hoher möglicher Spektrenrate profitieren könnte. In Kombination mit Hochgeschwindigkeitsgaschromatographie könnte eine bisher unerreichte Zeitauflösung der Beprobung der Atmosphäre mittels Gaschromatographie-Massenspektrometrie erzielt werden.

Content

Section II: Publications

List of Figures

List of Abbreviations

A/V	area-to-volmue ratio
ADC	analogue to digital converter
CFC	Chloro-fluoro-carbon
cRIO	compact, reconfigurable input-output
ECD	electron capture detector
EI	electron ionization
EMPA	Eidgenössische Materialprüfungs- und Forschungsanstalt
FASTOF	Fully automated in-situ GC-TOFMS
FID	flame ionization detector
FPGA	field programmable gate array
GC	Gas chromatograph / chromatography
GHG	greenhouse gas
GhOST	Gas chromatograph for observational studies using tracers
GWP	global warming potential
HCFC	Hydro-chloro-fluoro-carbon
HFC	Hydro-fluoro-carbon
IAU	Institut für Atmosphäre und Umwelt
IDL	interactive data language
IPCC	Intergovernmental Panel on Climate Change
LabVIEW	Laboratory Virtual Instrument Engineering Workbench
LAN	local area network
m/Q	mass-to-charge ratio
MCP	multi-channel plate
MHD	Mace Head Station
MS	mass spectrometer / spectrometry
NCI	negative chemical ionization
ODP	ozone depletion potential
ODS	ozone depleting substance
PC	personal computer
PFC	Per-fluoro-carbon
PID	proportional, derivative, integral (control algorithm)
ppq	parts per quadrillion; fmol mol−1 fraction
ppt	parts per trillion; pmol mol−1 fraction
QPMS	quadrupole mass spectrometer / spectrometry
S/N	signal-to-noise ratio
SFMS	sector field mass spectrometer / spectrometry
SIM	single ion monitoring
TO	Taunus Observatorium
TOF	time-of-flight
TOFMS	time-of-flight mass spectrometer / spectrometry
UV	ultraviolet (light)
VHOC	volatile halogenated organic compounds
VI	virtual instrument (LabVIEW)
WMO	World Meteorological Organization

Section I: Frame

Introduction

The evidence of the present change in earth's climate impressively demonstrates the impact of human activities on our planet. By changing physical variables like trace gas composition of the atmosphere, man causes a change of meta-level parameters like the increase of surface temperature (IPCC, 2013; therein e.g. Hartmann et al., 2013) or depletion of stratospheric ozone − on top of natural variability (WMO, 2011; therein e.g. Douglass et al., 2011). The target species of this work, halogenated trace gases, form a substance class of atmospheric trace constituents that plays an important role in both stratospheric ozone depletion and climate change.

The substance class of halogenated trace gases is dominated by volatile halogenated hydrocarbons or short "halocarbons". The history of environmentally harmful halocarbons began in the 1920s with the search for replacements of the toxic refrigeration agents used back then, e.g. sulphur dioxide (SO_2), methyl chloride (CH_3Cl) or ammonia (NH_3). Methane and ethane derivatives, fully halogenated with chlorine and fluorine (chloro-fluoro-carbons, CFCs), were the outcome of this search (Midgley, 1937; Midgley and Henne, 1930). CFCs are nontoxic, non-flammable and inert when e.g. used as refrigerants or aerosol propellants. Their molecular stability however also has a downside from a wider perspective: there is almost no degradation of CFCs in the troposphere (Burkholder et al., 2015) which means that the emitted amount will eventually reach the stratosphere (Fabian et al., 1981; Goldan et al., 1980; Volz et al., 1978). In the stratosphere, halocarbon molecules are degraded photochemically and inorganic halogens are released. The discovery of ozone depletion in the stratosphere catalysed by chlorine (Molina and Rowland, 1974) and bromine (Wofsy et al., 1975) and the phenomenon later called "ozone hole" over Antarctica by Farman et al. (1985) ultimately lead to a regulation of CFC production enforced by the Montreal Protocol in 1989 (e.g. UNEP, 2012a).

CFCs were intermediately replaced by partly chlorinated and fluorinated hydrocarbons (hydro-chloro-fluoro-carbons; HCFCs), which have shorter tropospheric lifetimes but can still partly reach the stratosphere (Burkholder et al., 2015). Today, HCFCs are replaced by a variety of fluorinated hydrocarbons (HFCs), which do not contribute significantly to stratospheric ozone depletion anymore (Ravishankara et al., 1994). However,

like CFCs and HCFCs, HFCs are potent greenhouse gases and therefore contribute to global warming (Hodnebrog et al., 2013). Continuous, accurate observations of these species are required for a quantitative understanding of processes like ozone depletion, ozone recovery and the contribution of the targeted species to climate change (Montzka et al., 2015). To keep track with the ongoing introduction of new compounds to the atmosphere (e.g. Laube and Engel, 2008; Mühle et al., 2009; Vollmer et al., 2015; Weiss et al., 2008), a continuous improvement of the observational methods is needed. The results of such an effort are presented in this work: A time-of-flight mass spectrometry instrument is characterised and applied as a quantification method for halogenated trace gases in ambient air. It is up to now the first time that the method is used in this field of research. The development includes a self-built cryogenic preconcentration system to achieve suitable detection limits and a gas chromatograph for analyte separation prior to detection.

This work consists of a framing chapter (section I) and three publications (section II). The overall focus lies on the instrumentation that was developed and applied for halocarbon trace gas analysis in ambient air samples. The publications listed in section II give a comprehensive picture of the technical development over the last three years (2012-2015, and partly 2016) in the working group of Prof. Andreas Engel at Goethe University, Frankfurt am Main. They build upon each other in the order that they are listed with regard to content; chronologically, they were published in a different order. The first publication treats the preconcentration method required for the analysis. This method has been applied in the second publication, which focuses on the comparison of the well-established quadrupole mass spectrometry as detection method with time-of-flight mass spectrometry. Efforts were then undertaken to set up a GC-TOFMS instrument (gas chromatograph coupled to a time-of-flight mass spectrometer) that fully meets the ambitious requirements of halocarbon analysis and incorporates the benefits of time-of-flight mass spectrometry. The achievements of these efforts are discussed in the third publication. All three publications are framed by section I that gives a brief scientific motivation in chapter 1, highlights key results from the publications alongside some additional background information in chapter 2, and gives a comprehensive summary and outlook in chapter 3. This summary can also be found at the beginning of this work in German.

1 General scientific background

Halogenated trace gases play an important role in atmospheric chemistry and physics, despite their very low atmospheric concentrations. This chapter gives a brief introduction to the scientific investigation of halogenated trace gases in the atmosphere to motivate the instrumental development described in chapter 2 and section II. After a general classification of halogenated trace gases in section 1.1, sections 1.2 and 1.3 summarise their relevance in stratospheric ozone depletion and climate change.

1.1 Halogenated trace gases: classification and atmospheric abundance

Volatile halogenated trace gases cover a wide range of individual compounds in the atmosphere; from exclusively anthropogenic substances like dichlorodifluoromethane (CCl_2F_2, CFC-12) to methyl chloride, which is mainly of natural origin. All these species are generally found in very low concentrations. Compared to CO_2, which reached a mole fraction of 400 ppm in 2015 (Mauna Loa, Hawaii; ppm: parts per million; after correction for the seasonal cycle; NOAA-ESRL, 2015), mixing ratios of halogenated trace gases are lower by approximately six to eight orders of magnitude. Even the most abundant anthropogenic halocarbon, CFC-12, is found at a concentration of only 520 ppt in the troposphere (2.5 ng·L^{-1} of ambient air at standard temperature and pressure), i.e. six orders of magnitude below CO_2. However, most halogenated gases are very stable in the atmosphere with lifetimes of a few years (e.g. CH_3CCl_3: 5 years) to several tens of thousands of years (e.g. CF_4: >50000 years) (Carpenter et al., 2014). Consequently, most halogenated trace gases are ubiquitous in the lower atmosphere. A brief overview of important species and their tropospheric trends from 1980 to 2010 is shown in Figure 1.
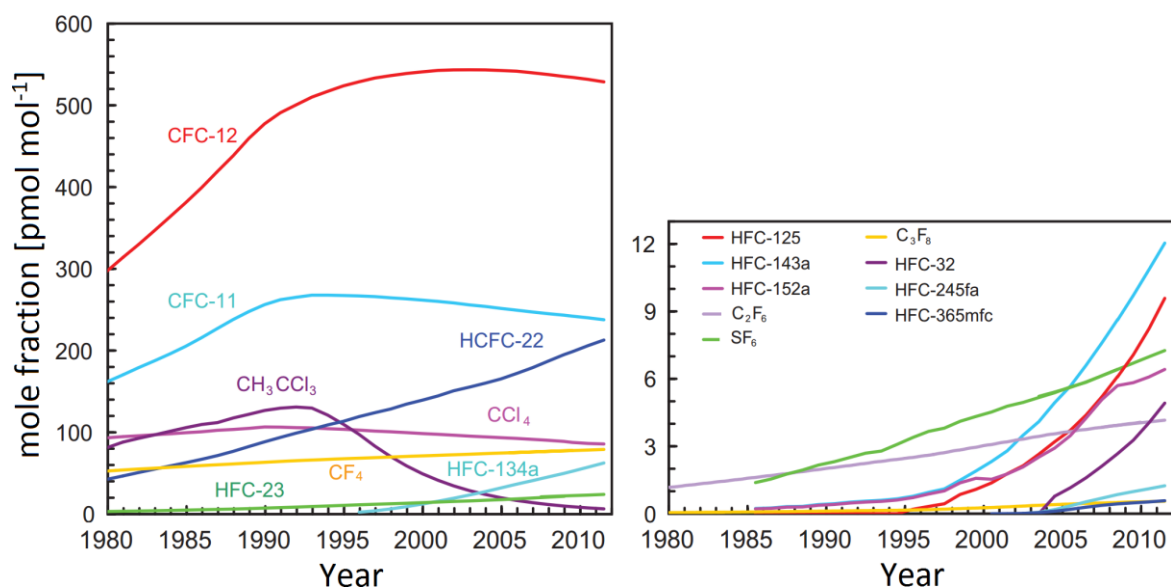
Figure 1. Mole fractions in parts per trillion (ppt, y-axis; both plots) of selected halogenated trace gases and the temporal evolution of their tropospheric concentration over the last three decades (1980 to 2010, x-axis). While most major species (left plot) controlled by the Montreal Protocol show a decline towards the end of the 20th century (e.g. CFC-12 or CH3CCl3), especially fluorinated gases (right plot) show a steep increase in concentration from the year 2000 onwards (e.g. HFC-125 or HFC-143a, right plot). Adapted from Hartmann et al. (2013).

Evolving from the discussion on stratospheric ozone depletion (see section 1.2), a useful classification into six subclasses relevant to atmospheric chemistry can be done:

I. **CFCs**. Chloro-fluoro-carbons. Fully halogenated with chlorine and fluorine.

II. **HCFCs**. Hydro-chloro-fluoro-carbons. Partly halogenated with chlorine and fluorine.

III. **Halons**. Haloalkanes that are partly or fully halogenated with bromine, chlorine and/or fluorine. Mostly used to refer to bromine-containing species.

IV. **HFCs** and **PFCs**. Hydro- and per- fluoro-carbons. Partly (HFCs) or fully (PFCs) halogenated with fluorine.

V. **Bromo-, Chloro-** and **Iodocarbons.** Halogenated with a single type of halogen except fluorine.

VI. **Natural, mixed halogenated hydrocarbons.** Distinguished by their natural origin and a short atmospheric lifetime < 6 month. Therefore referred to as "very short lived substances", VSLS.

Classes I to IV share an almost exclusively anthropogenic origin (Butler et al., 1999; Sturrock et al., 2002) and a high ozone depletion potential (ODP; UNEP, 2012a). (compared to CFC-11). The ODP is highest for Halons due to their bromine content and lowest for HCFCs due to their reduced capability to reach the stratosphere (degradation via OH in the troposphere). HFCs and PFCs, also exclusively of anthropogenic origin, do not contribute to ozone depletion. However, substances from classes I to IV have similar radiative efficiencies, much higher than CO_2, and therefor contribute to global warming (see section 1.3).

Natural production of some species from classes I to IV only occurs under very unique conditions like volcanic activity (CFCs: Isidorov et al., 1990). In regard to stratospheric ozone depletion, the biggest natural contributors to stratospheric chlorine and bromine are methyl chloride (CH_3Cl) and methyl bromide (CH_3Br). Stratospheric chlorine and bromine are strongly influenced by human activities: anthropogenic substances cause approximately 83% of the chlorine (mostly CFCs) and 42% of the bromine (mostly Halons) entering the stratosphere in 2008 (Fahey and Hegglin, 2011). A detailed assessment of observations, emissions and trends of substances that contribute to stratospheric ozone depletion can be found in Montzka et al. (2011) with subsequent updates in Carpenter et al. (2014). A review on tropospheric halogen chemistry has recently been given by Simpson et al. (2015). Other classifications like "volatile halogenated organic compounds" (VHOC) are also used in literature, however mostly to refer to species of natural origin (e.g. Gribble, 1992; Keppler et al., 2000). Not included in the classes above are halogenated sulphur compounds like SF_6, which do not play an important role in ozone depletion but for climate change. SF_6 is also an important tracer to study stratospheric transport (e.g. Bönisch et al., 2009; Engel et al., 2009) as it has no tropospheric or stratospheric sink but is only dissociated in the mesosphere (e.g. Totterdill et al., 2015).

1.2 Stratospheric ozone depletion

The stratospheric ozone layer found at 12 to 25 km above ground absorbs most of the short-wave ultraviolet light (UV-B) from the sun. Thereby, life on the earth's surface is protected from this harmful part of the sunlight. Ozone is formed by combination of oxygen atoms with oxygen molecules, a reaction first proposed by S. Chapman in 1930 (Chapman, 1930). Stratospheric ozone formation mainly takes place over the tropics where solar irradiation is highest. Ozone is then transported poleward via the Brewer-Dobson-Circulation (Brewer, 1949); a concept that was originally inferred from tracer observations (H_2O and O_3). Due to this large-scale atmospheric circulation, a concentration maximum is observed around the winter hemisphere pole.

Ozone is destroyed by photodissociation, reaction with atomic oxygen (Chapman mechanism) and naturally occurring catalytic loss cycles involving OH & HO_2 (HO_x) and NO & NO_2 (NO_x) (e.g. Crutzen, 1970). The halogens bromine and chlorine can also take part instead of HO_x or NO_x whereas fluorine is mostly inactive in the form of HF (Molina and Rowland, 1974; Stolarski and Rundel, 1975). The efficiency of ozone destruction is altered by the introduction of additional chlorine and bromine to the stratosphere by human activities, i.e. the release of volatile chlorine- and bromine-containing compounds. This eventually leads to the large-scale depletion of stratospheric ozone first observed over Antarctica in 1985 (Farman et al., 1985). Reviews of the mechanisms involved in the formation of the phenomenon were e.g. given by Lary (1997) or Solomon (1999).
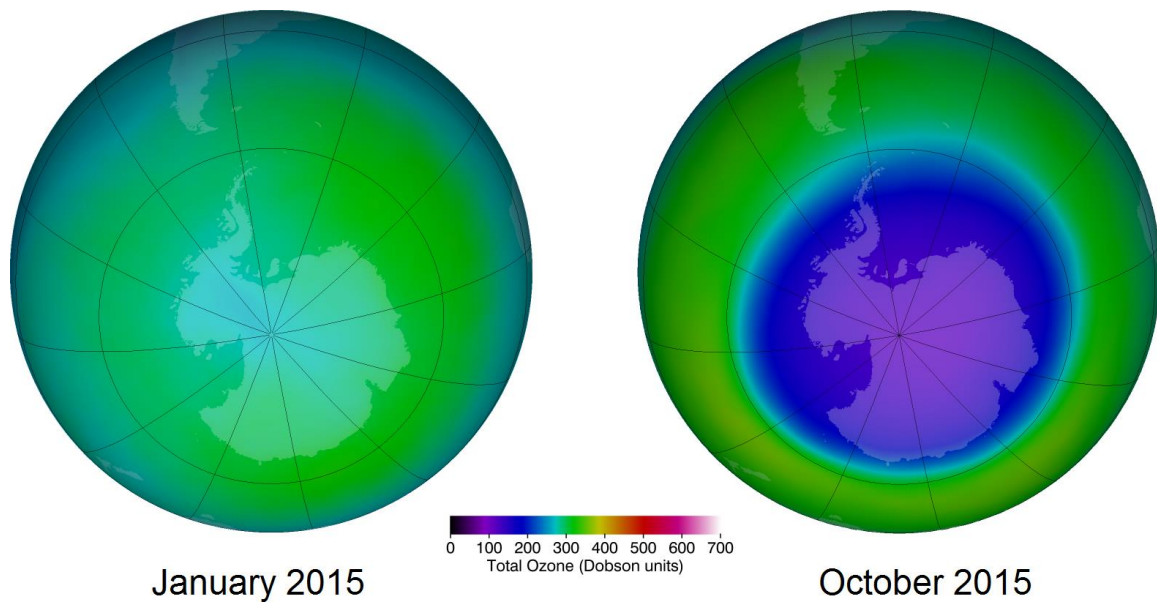
Figure 2. False colour image of ozone column thickness over Antarctica, showing monthly averages of January 2015 (southern hemisphere summer) and October 2015 (southern hemisphere spring). Units: 1 Dobson Unit (DU) equals a layer of pure ozone of 10 μm thickness at 273.15 K and 1013.25 hPa, colour code given on the image. In spring, ozone column thickness over the South Pole is reduced to approximately ⅓ of its summer value. Data from the OMI instrument (KNMI / NASA) on board the Aura satellite (NASA, 2015).

Although stratospheric chlorine loading peaked around the year 2000 (Engel et al., 2002 and update in Clerbaux et al., 2007), the ozone hole still appears over Antarctica in southern hemisphere spring as demonstrated in Figure 2. Over the north pole, large-scale ozone depletion can also be observed (e.g. Manney et al. (2011)), while the area of reduced ozone column thickness is not as confined as over the south pole. For the future, the analysis of multi-model time series projects a return to 1960s values of total ozone column thickness around the year 2050 in the global mean (Bekki et al., 2011). This return is actually earlier than the projected recovery of stratospheric chlorine and bromine levels as stratospheric ozone is not only affected by halogen-catalysed destruction but also changes in stratospheric temperatures, transport and dynamics (Bekki et al., 2011; Forster et al., 2011). Concluding, the Montreal Protocol and its CFC & HCFC production and usage regulations are working with respect to the purpose for which it was brought to life: the protection of the ozone layer (UNEP, 2012b). However, a strong interdependence with climate change is evident in model calculations. While ozone depleting substances are still the dominating influence factor on stratospheric ozone, future ozone projections mostly depend on the chosen greenhouse gas emission scenario (Pawson et al.,

2014) and feedback mechanisms of potential climate geoengineering measures (Nowack et al., 2016).

The Montreal Protocol also seems to be working with regard to the reduction of surface UV irradiance caused by reduced ozone column thickness. Especially at southern hemispheric, unpolluted measurement sites, irradiances were decreasing as reported in Bais et al. (2007). The overall effect of the Montreal Protocol on surface UV is however difficult to quantify, e.g. due to scarce availability and limited spatial coverage of measurements and large measurement errors. Furthermore, stratospheric ozone is not the only influencing factor – other important factors are e.g. changes in cloud coverage (the dominant influence factor), surface albedo (land usage) or aerosol particle concentration and tropospheric ozone (air pollution) (Douglass et al., 2011).

1.3 Radiative forcing of halogenated trace gases

Halogenated trace gases not only contribute to the catalytic destruction of stratospheric ozone – they are also strong greenhouse gases. Again, despite their low concentrations, they are very efficient: compared to CO_2, e.g. CFC-12 has a radiative efficiency higher by a factor of approximately $2.3 \cdot 10^6$ (calculated in W m^{-2} ppb^{-1} based on Hartmann et al., 2013). Due to absorption of electromagnetic waves within the so-called atmospheric window between wavelengths of 7-14 µm or wavenumbers 700-1300 cm^{-1} respectively, halogenated gases attenuate the outgoing radiation of earth's energy balance – more energy gets stored within the system. An illustration is given in Figure 3.
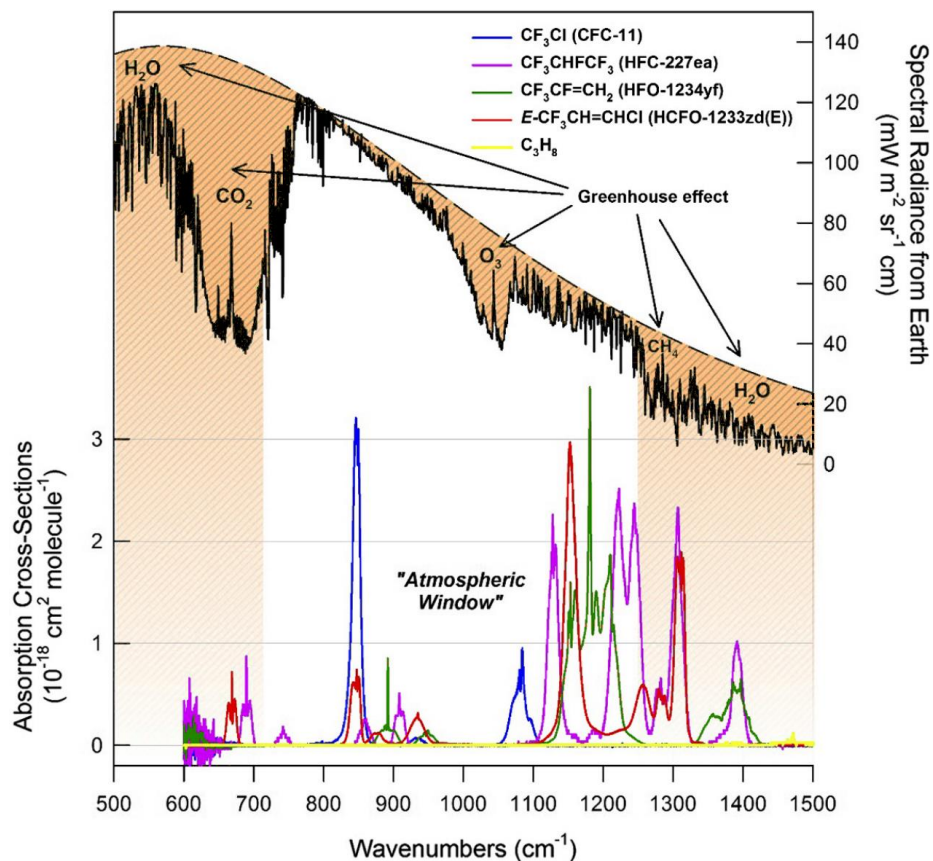
Figure 3. Net upward atmospheric radiance spectrum at the tropopause (black solid line, based on model calculations) and ideal Planck function for a blackbody emission at 290 K (black dashed line) within a wavenumber section from 500 to 1500 cm^{-1} (x-axis). The difference between the two indicates the so-called greenhouse effect caused by the absorption of certain trace gases (reduction of the outgoing radiation, marked by the orange colouring). Blue, purple, green, red and yellow line: infrared spectra of selected halocarbons as well as propane (C_3H_8) for comparison. A strong absorption of the halocarbons in the atmospheric window region is observed. Adapted from Wallington et al. (2015); therein adapted from Sulbaek Andersen et al. (2012).

This positive radiative forcing as defined by the Intergovernmental Panel on Climate Change (IPCC; Ramaswamy et al., 2001; briefly: increase in radiative heating of the troposphere) was already published in 1975 by Ramanathan (1975) and further elaborated on e.g. by McDaniel et al. (1991) or Highwood and Shine (2000) and recently by Hodnebrog et al. (2013). According to up-to-date calculations (Myhre et al., 2013), halogenated trace gases contribute to radiative forcing with 0.337 W m^{-2} in total, which is 12 % of the 2.83 (2.54 to 3.12) W m^{-2} from all well-mixed greenhouse gases combined (excluding H_2O). The contribution of individual halogenated species to radiative forcing is illustrated in Figure 4.
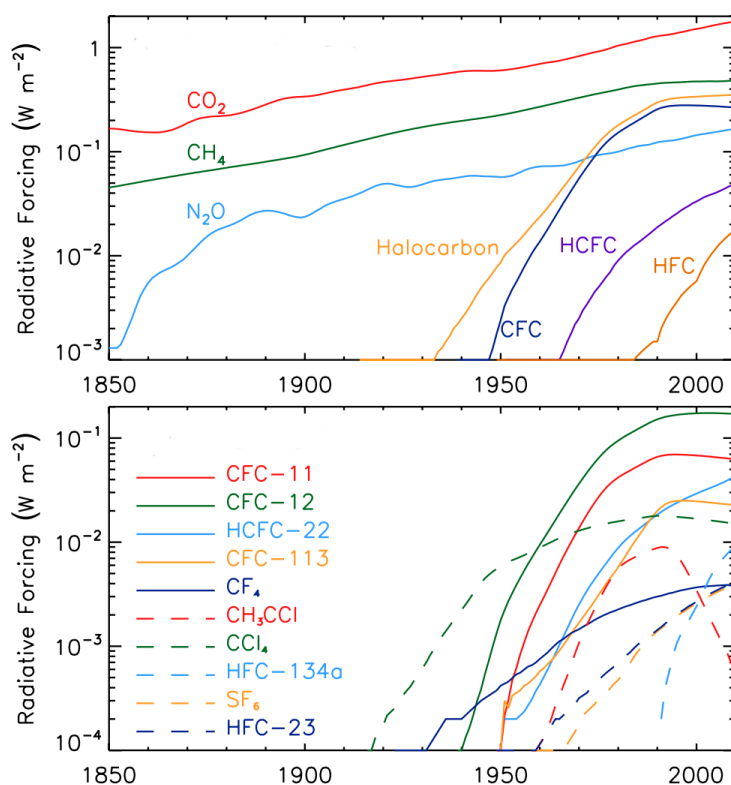
Figure 4. Contribution of individual trace gases to radiative forcing (y-axis, logarithmic scale) from 1850 to 2011 (x-axis). The upper graph shows the contribution of different classes of halogenated species in comparison to the three major well-mixed greenhouse gases CO_2, CH_4 and N_2O. The lower graph shows the individual contribution of ten halogenated greenhouse gases. Adapted from Myhre et al. (2013).

The overall increase in radiative forcing caused by halogenated species has declined since approximately 1990 thanks to the reduction of CFC emissions. However, the contributions of individual classes, especially HFCs, show a strong positive trend with HFC-134a being the dominant contributor.

Considering the halocarbon emissions that were avoided by the regulations of the Montreal Protocol, the Protocol also represents a very successful step in climate protection, even exceeding the greenhouse gas reduction target of the first commitment period of the Kyoto Protocol (Velders et al., 2007). The next step would now be a phase-out of HFC consumption – calculations by Velders et al. (2009) show that without mitigation, HFC radiative forcing might otherwise increase by 0.25 to 0.4 W m^{-2} until 2050 relative to the year 2000.

2 Analysis of halogenated trace gases in air with gas chromatography – time-of-flight mass spectrometry

The assessment of quantitative contributions of halogenated trace gases to ozone depletion and climate change as well as their use for studying atmospheric transport and dynamics fundamentally relies on high-quality measurement data and accurate calibration. A specialized instrumental setup is necessary for this task and a thorough characterisation forms the backbone of any newly developed instrument. During this work, efforts were undertaken to further improve existing methods and introduce a detection method new to this field of research; time-of-flight mass spectrometry. A schematic of the method GC-TOFMS for detection and quantification of trace gases is shown in Figure 5.
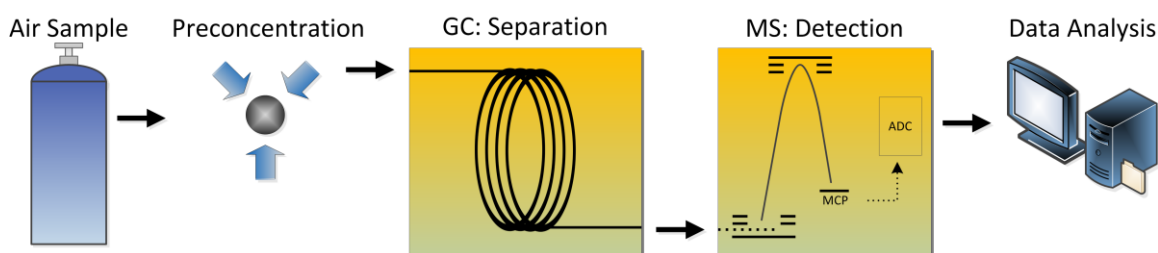
Figure 5. Simplified schematic of the instrumental method used for trace gas analysis. Analytes are preconcentrated on adsorptive materiel prior to analysis to elevate detection limits to a suitable level for the MS. Preconcentrated analytes are injected onto a GC column to achieve a temporal separation of the vast amount of compounds found in a typical air sample. Analytes are detected by the MS (schematic of an orthogonally extracting TOFMS shown; see also Figure 13). MS data are then analysed to qualify and quantify compounds of interest.

The following section 2.1 briefly describes the historical development of the analysis of halogenated species in air. Coming from this background, present-day development is described in sections 2.2 to 2.4, which outline important results from the three publications that constitute this work. The basis of the analytical method, the preconcentration technique, is described and discussed in section 2.2 (Obersteiner et al., 2016b). Sample preconcentration and gas chromatographic separation are followed by detection, which is the topic of sections 2.3 and 2.4. Section 2.3 is dedicated to the comparison of the established detection method quadrupole mass spectrometry with the new method time-of-flight mass spectrometry (Hoker et al., 2015). Section 2.4 describes the development and characterisation of a new, fully automated GC-TOFMS setup (Obersteiner et al., 2016a).

2.1 Instrumental background

The analysis of halogenated trace gases in the atmosphere began in the 1960s when James E. Lovelock developed the electron capture detector (ECD) for the direct determination of electron affinities (Lovelock, 1963; Lovelock and Lipsky, 1960). Although the ECD's response is not limited to molecules containing halogens, it is where it excels most in sensitivity (depending on the number of halogen atoms) due to the high electron affinity of especially chlorine and fluorine (Clemons and Altshuller, 1966). Instrumental development was then pushed by the findings of Molina and Rowland (1974) and lead to many analytical setups published in literature (e.g. Bassford et al., 1998; Elkins et al., 1996; Wang et al., 1999). The ECD is selective to a high degree, i.e. it is very sensitive to certain compounds while being insensitive to others. Its response is furthermore non-linearly proportional to the injected amount of analyte (Crescentini et al., 1981; Lovelock and Watson, 1978) and the ECD signal of one compound cannot be distinguished from another, meaning that a powerful and reliable separation method is necessary for analyte mixtures. Despite these limitations, the ECD became a wide-spread detector due to its small size and competitive price: compared to a few thousand € ECD, a GC plus quadrupole mass spectrometer cost more than 500000 € in the early 1970s translated to today's price (Finnigan, 1994). The ECD found application in many innovative analytical setups, especially in-situ airborne instruments where size and weight are desired to be as small/low as possible. Noteworthy instruments are NOAA's ACATS and later PANTHER setup (PANTHER additionally incorporates an MS channel; Elkins et al., 2002; Elkins et al., 1996; Romashkin et al., 2001), the LACE instrument and the similar HAGAR (Moore, 2003; Riediger, 2000), the GhOST (Bönisch, 2005; Bujok et al., 2001) and the battery-powered μDIRAC (Gostlow et al., 2010). Detectors other than ECD and MS are rarely applied for quantifications of halogenated tracers – the only other detector used is the flame ionization detector (FID) e.g. for the quantification of methyl chloride in air samples by Andreae et al. (1996) or the analysis of different volatile chlorinated and brominated halocarbons in drinking water by Djozan and Assadi (1995).

Although all quoted analytical setups use a gas chromatograph to separate the vast amount of substances in the sample (see also Helmig, 1999), an inherently 1-dimensional detector that only records intensity at a given time like the ECD or the FID poses a limi-

tation to the number of quantifiable substances within a chromatogram and makes the identification of unknown compounds very difficult. Furthermore, high sensitivity of the ECD is only given for certain compounds, i.e. chlorinated and fluorinated species with a preferably high number of halogen atoms in the molecule. These limitations can be overcome by mass spectrometry: if ionized, molecules form a number of specific ion fragments. The fragmentation patterns are specific for each molecule and can be detected by the mass spectrometer in the form of mass-to-charge ratio (m/Q or short "mass" with Q being one elementary charge) of the ions, in addition to their abundance (intensity). With m/Q, a second data dimension is gained that simplifies substance identification and allows quantification of compounds that are only partially separated by gas chromatography. The mass spectrometer was reported to be used for the analysis of halogenated trace gases in air samples about 10 years later than the ECD (Bruner et al., 1981; Cronn and Harsch, 1979; Grimsrud and Rasmussen, 1975). Both Grimsrud & Rasmussen and Cronn & Harsch used quadrupole mass spectrometers (QPMS) for their studies; Bruner et al. used a sector field mass spectrometer (SFMS).

A QPMS in general is smaller and lighter than a typical SFMS, which makes the QPMS much better suited for field applications. However, SFMS offers significantly higher resolving power of the m/Q dimension, i.e. for the separation of neighbouring ion signals. The QPMS, due to its competitive price and ease of operation, is undoubtedly the most wide spread type of instrument in mass spectrometry, with countless applications including the analysis of halogenated trace gases. A prominent example of an analytical setup developed for that task is the Medusa GC-MS described by Miller et al. (2008). Relatively small size and low weight make the QPMS also well suited for in-situ applications, like e.g. airborne instruments like the PANTHER named above or the GhOST-MS used by Sala et al. (2014). Applications of the SFMS on the other hand are limited to ex-situ, i.e. laboratory setups (e.g. Bruner et al., 1981; Laube et al., 2012; Lee et al., 1995; Sturges et al., 2000). For quantitative analysis of halogenated traces gases in air, no other applications than the ones presented in this work have been published to the author's knowledge up to now that use other types of mass spectrometers.

2.2 The prerequisite: sample preconcentration

Publication I: "A versatile, refrigerant free cryofocusing thermodesorption unit for pre-concentration of traces gases in air", Obersteiner et al. 2016, AMTD

While the ECD is sensitive enough to detect and quantify specific substances based on a direct injection of a few mL of air, most mass spectrometers are not sensitive enough, at least for trace gas analysis on a ppt-level. For example, a CFC-12 peak detected by a GC-MS with a typical signal-to-noise ratio of 30000 from the CFC-12 molecules in 1 L of air would be reduced to a signal with a signal-to-noise ratio of 3 if using a typical direct injection volume of 100 µL of air, i.e. just above detection limit (assuming linear detector response and noise being independent of sample volume). As 1 L of air cannot be injected instantaneously into the MS or directly onto a chromatographic column, the volume has to be reduced by removing the most volatile components, mainly nitrogen, oxygen and argon. This critical step in the analysis is referred to as preconcentration. The following sections provide additional information on the method, supplementary to Obersteiner et al. (2016b). The automated GC-TOFMS developed during this PhD thesis is used as an example here – similar hardware components, software control structures etc. are implemented in both the in-situ aircraft instrument GhOST-MS (Sala et al., 2014) and the laboratory instrument (Hoker et al., 2015; Obersteiner, 2012).

2.2.1 Principle

The principle used is preconcentration on adsorptive material, a common technique in trace gas analytics. The adsorptive material is contained in some form of tubing, i.e. forming essentially a packed chromatographic column. By flushing a defined sample volume over the adsorptive material, sample molecules physically interact with the adoptive material and a certain fraction of the sample will is retained ("trapped") on the surface of the material, depending on its type and surface properties. A review on sorbent tubes used for air composition monitoring was e.g. given by Woolfenden (2010). If the adsorptive material is cooled additionally, the steady-state between adsorption and desorption can be shifted further towards adsorption. The procedure is then termed "cryofocusing" or "cryotrapping" to indicate that sub-ambient temperatures were used during

adsorption, achieved by active cooling. Cooling the adsorptive material prior to desorption offers another advantage besides the possibility to trap analytes with higher volatility: a less powerful adsorbent can be used as it would be necessary for trapping at ambient temperatures. This again enables lower desorption temperatures which can be beneficial to the lifespan of the adsorptive material and avoid thermal decomposition of analytes. Furthermore, active cooling ensures that adsorption temperatures can be re-established quickly after desorption.

For analysis, analytes have to be desorbed from the adsorptive material, which is done by heating the material and thereby shifting the steady-state towards desorption ("thermodesorption"). During thermodesorption, a carrier gas transports analytes to further refocusation steps or directly to the detection instrument. Both adsorption and desorption have to be quantitative and repeatable to ensure high accuracy and precision. In the cryofocusing-thermodesorption unit used in this work, a built-in sorbent tube, i.e. the sample loop containing the adsorptive material, is used for the preconcentration of any sample directly before analysis by GC-MS. As the adsorptive material is permanently installed in the instrument and is only exchanged when degraded, the sample has to be "brought to the instrument" in the form of canisters that are analysed in the laboratory or the instrument has to be "brought to the sample" for in-situ operation e.g. at a monitoring station.

2.2.2 Instrumentation: cooling and heating

Two principal operations of the preconcentration system have to be implemented: cooling for cryofocusation and heating for thermodesorption. For cooling, three basic methods are available: (1) the use of a liquefied gas as a refrigerant that evaporates and gets lost in the process, (2) a compression cooler with a closed refrigerant loop or (3) a pure electrical cooler. Although being very powerful coolants and good laboratory solutions, liquid gases such as nitrogen or argon are relatively difficult to handle in continuous operation at remote location or in aircraft instruments. Compression coolers only require electrical power but are also relatively large in size and high in weight as well as power consumption. Electrical cooling solutions such as Peltier elements only require electrical power and are small in size and low in weight as well as power consumption and therefore a wide-spread cooling implementation in commercially available (cryofocusing-)

thermodesorbers from e.g. PerkinElmer or Markes. Stirling coolers are another, purely electrical cooling option and provide much lower minimum temperatures and higher cooling rates. A Stirling cooler was therefore chosen as cooling solution; Figure 6 shows a photograph of the Stirling cooler used in the setup described in Obersteiner et al. (2016b).
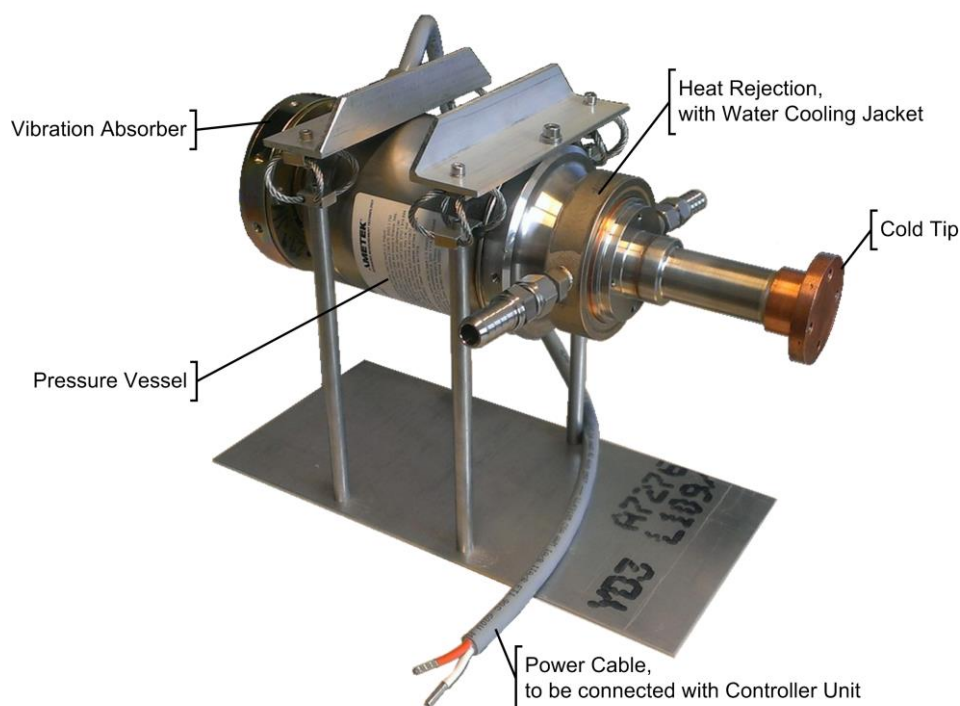
Figure 6. Free piston Stirling cooler from Sunpower (Ametek Inc., USA; CT model shown). The "reversed" Stirling engine transports heat from the cold tip to the heat rejection. A removable water cooling jacket is used to remove heat from the heat rejection. Vibrations from the moving parts inside the pressure vessel are mostly cancelled out by the vibration absorber at the back. A flexible mounting of the pressure vessel is still required. Sunpower Stirling coolers are also available with active vibration absorption, air fins for heat removal at the heat rejection and different cooling capacities.

Attached to the cold tip of the Stirling cooler is an aluminium block consisting of three separate plates holding two sample loops. Figure 7 shows a schematic drawing of this so-called coldhead. A photograph of the current setup of the preconcentration unit developed during this work is shown in Figure 8. The coldhead is insulated towards ambient air with 45 mm of Aeroflex HF material (Aeroflex GmbH, Germany; not shown in Figure 7). A better insulation can be achieved by a vacuum chamber around the coldhead (e.g. Eyer et al., 2016; Miller et al., 2008). However, some of the simplicity of construction would thereby be sacrificed.
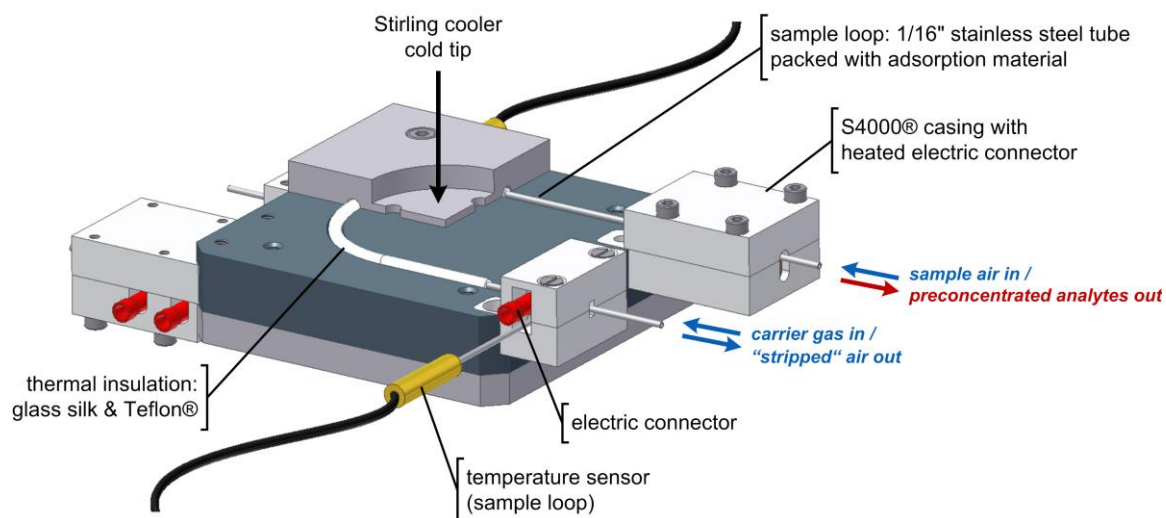
Figure 7. Drawing of the coldhead and sample loop placed inside. Three plates of anodized aluminium can hold two sample loops. The Stirling cooler's cold tip is screw-mounted to the coldhead and removes heat for cooling. Heat for sample desorption is generated by a current directly applied to the sample loop. The electric connector in the direction of sample flow (upper right side of the drawing) is heated constantly to 150 °C to avoid a cold point due to the mass of the electric connector and its proximity to the coldhead (S4000® insulation material: Brandenburger, Germany). As shown in Obersteiner et al. (2016b).
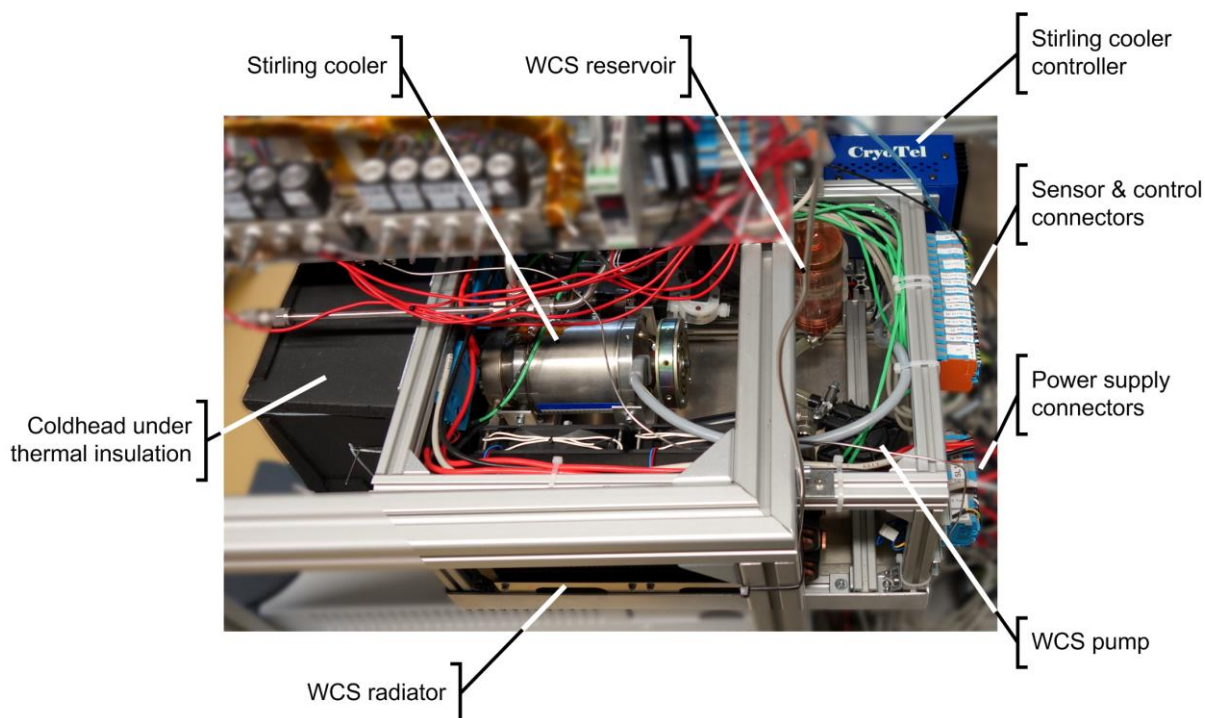
Figure 8. Photograph of the preconcentration unit (GC-TOFMS). Stirling cooler and water coolant system (WCS) are held inside an aluminium frame (width/length/height: 30/40/21 cm, excluding coldhead) which is placed on top of the GC of the analytical instrument. The aluminium frame is placed inside an aluminium tray to contain water spill in case of a leak in the water coolant system.

Desorption heating is implemented by applying a direct current to the sample loop tubing. By using a 12 V power supply with a maximum output of 40 A, desorption temperature can be reached very rapidly, ensuring a high injection quality of highly volatile species. As the sample loop is kept within the coldhead during desorption, heat transfer from sample loop to coldhead has to be reduced to a tolerable measure. Figure 9 shows the thermal insulation of the sample loop, which also isolates it electrically.

Layer 4-6: Teflon

3rd Layer: Glass Silk

2nd Layer: Teflon

1st Layer: Glass Silk

1/16" Stainless Steel Tube
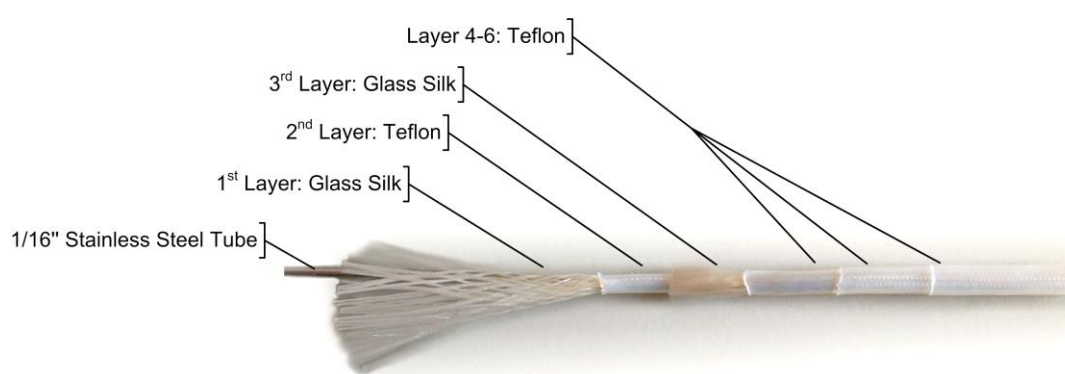
Figure 9. Sample loop insulation. Glass silk is used as a base layer due to its high heat tolerance. In combination with the Teflon shrinking hose, a relatively homogeneous insulation can be achieved although assembled by hand and repeatedly for every sample loop.

The sample loop insulation is a key parameter in the chosen setup. On the one hand, it determines heat transfer into the coldhead during desorption. Any warm-up of the coldhead during desorption has to be removed by the Stirling cooler to re-establish adsorption temperature. Cool-down time of the coldhead can be the limiting factor for the overall cycle time, i.e. preconcentration-thermodesorption steps and therefore number of sample analysis per time. On the other hand, if the insulation is too efficient, cool-down of the sample loop can become a limiting factor to cycle time. In summary, the optimal solution for sample loop isolation as well as desorption temperature and duration etc. are application-dependent and might rely on other parameters such as runtime of the GC.

2.2.3 Software control

The preconcentration unit is controlled by a self-written, embedded design LabVIEW (National Instruments Inc., USA) code. The operating software running on the host PC sends commands and receives data via LAN from a cRIO realtime controller, which uses

the LabVIEW Scan Engine to read and write input/output (IO-) variables like voltages, digital outputs etc. on the controller's chassis. The host PC does not interact directly with the hardware but only through the cRIO controller, which hosts the network variables. Individual LabVIEW control loops ("virtual instruments", VIs) are running on host PC as well as cRIO. LabVIEW functions and processes on the host PC are compiled into one runtime executable (.exe) that runs on the host PC, connected via LAN to the cRIO. Control loops on the cRIO are compiled into a realtime executable (.rtexe), which is called whenever the cRIO is powered on. The cRIO therefore operates basically independent of the host PC. The software structure and variable exchange (commands, data) via the LabVIEW Shared Variable Engine is illustrated in Figure 10. This implementation of software control offers the advantage of being user friendly as there is only one operating VI on the host PC, which avoids handling errors and ensures reliable operation due to a limited range of user interaction. Furthermore, the relatively expensive LabVIEW development environment license is not required for operating the preconcentration unit but only the LabVIEW runtime engine (available free of charge). However, no direct interaction of the user with individual control loops is possible which can be unsuitable for development purposes. The LabVIEW development environment would then be required, allowing the developer to interact with individual components of the control structure.
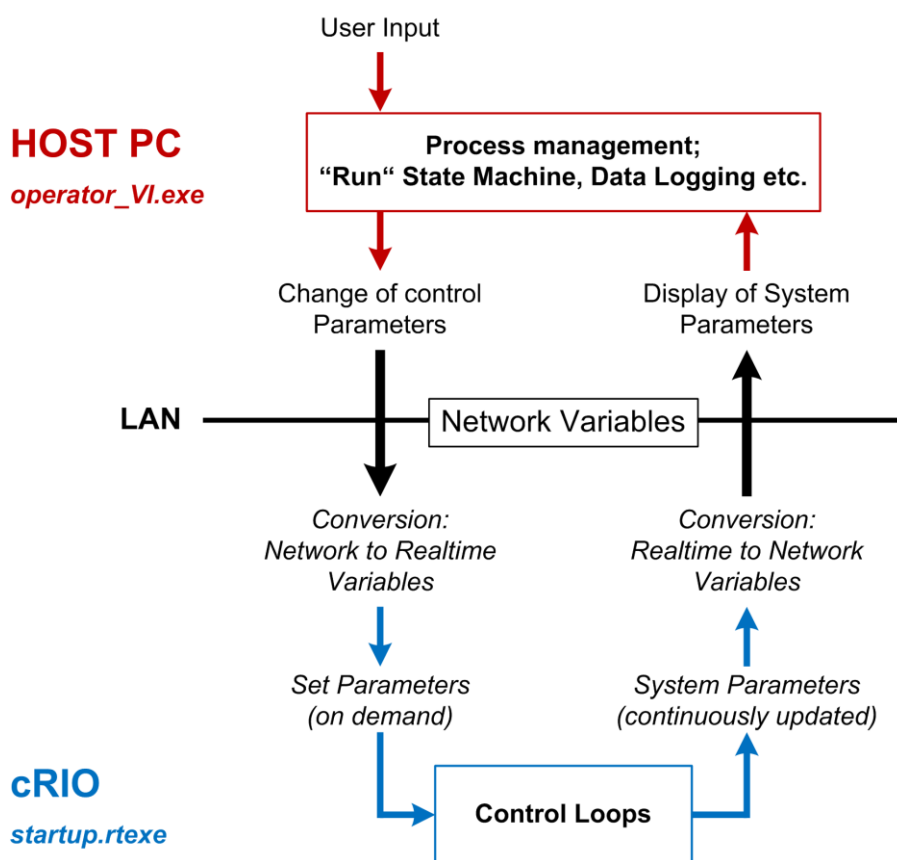
**Figure 10. LabVIEW software control structure of the preconcentration unit (GC-TOFMS). Host PC
and cRIO communicate via network exchange variables which are exchanged via a LAN con-
nection. User input (e.g. start of a measurement) are managed by the state machine and pro-
cess loops running on the host PC (operator_VI.exe) and converted to changes of specific pa-
rameters in the control loops running on the cRIO (startup.rtexe). Both host PC and cRIO
use separate variable libraries for operation; the network variable library is used for data ex-
change.**

The key concept implemented in the LabVIEW code is state machine programming (au-
tomata-based programming). The system and each of its subsystems has a finite number
of possible states. A state has a defined entry point and is updated during runtime in each
execution of the control loop cycle. Depending on if predefined conditions are met, it is
kept or changed. Each state also has one or a set of prescribed transitions to other states.
This concept can be applied to subroutines like e.g. the state of thermodesorption ("idle",
"heat & hold setpoint" etc.) up to meta-states like e.g. the system operation mode
("standby", "sleep" etc.). The advantages for programmer and user e.g. in comparison to
sequence-based programming lie in the definition of state transitions and the simplicity in
determining the current state and the respective system parameters constituting the state
of the (sub-)system.

2.2.4 Characterisation of the preconcentration unit

The preconcentration unit is an essential part of the instrumental setup as it defines measurement quality even before gas chromatography or mass spectrometry. Quality can only be as good as preconcentration and injection of the sample allow, assuming optimal performance of GC and MS. The technical assembly as well as adsorption and desorption of analytes were therefore studied in detail.

Technical assessment

Before any air sample can be preconcentrated and analysed, some technical challenges have to be met. While the cooling process is relatively easy to handle due to the Stirling cooler, the implementation of sample loop heating is a much more difficult task. Key features of the chosen setup are the direct injection, which means no refocusation of analytes and a sample loop that is kept in the coldhead permanently. This configuration offers some distinct advantages like the simplicity of construction and the absence of mechanical, moving parts. However, it also brings with it three main difficulties to be handled which are centred on sample loop heating for thermodesorption and will be discussed in the following paragraphs.

(1) Insulation. The idea of keeping the sample loop inside the coldhead brings the necessity to limit heat flow from sample loop to coldhead. This is done by insulating the sample loop. During heating, the homogeneity of this insulation becomes critical to the temperature distribution along the sample loop. Inhomogeneity of insulation potentially results in inhomogeneity of thermodesorption temperature. (2) Power supply. Although the sample loop is insulated, a relatively large amount of energy has to be at hand for a fast initial increase of temperature at the beginning of thermodesorption. For that purpose, a voltage is applied to the sample loop through the electric connectors (see Figure 7). The chosen high-current, low-voltage DC power supply offers a large amount of power, but is also hard to control precisely as the sample loop essentially is a short circuit due to its low electrical resistance of approximately $0.5 \, \Omega$. A pulse-width modulation with short period and very small minimum increments (μs range at a period of approximately ≥ 1 kHz) is necessary to allow for a fine adjustment of the large amount of power from the power supply. Heater characteristics also inherently depend on power supply charac-

teristics; in this case e.g. a very low inner resistance of the power supply is necessary to deliver the specified maximum power over a longer period of time. (3) Feedback control. Temperature inside the sample loop cannot be determined directly; only indirectly by a sensor at the outside wall of the sample loop tubing. However, due to its proximity to the coldhead and its thermal mass, this sensor will only give a proxy for actual sample loop temperature; this aspect was already discussed in Obersteiner, 2012.

The results from heater characterisation experiments can be summarized as follows. The temperature sensor welded to the sample loop tubing wall does not give an accurate value of the temperature of the adsorptive material inside the sample loop. The key quantity to characterise is the temperature difference $\Delta T_{|in-out|}$ of sensed temperature (T_{out}) and actual temperature (T_{in}), which is a function of the insulation, thermal mass of sensor & tubing and of time. The insulation, although slightly different from sample loop to sample loop, can be considered a constant. The thermal mass of the temperature sensor (although being a constant itself), causes $\Delta T_{|in-out|}$ to be very large at the beginning of thermodesorption and then decrease to an equilibrium value over time, almost exclusively determined by the insulation. An illustration of this temporal evolution is shown in Figure 11.
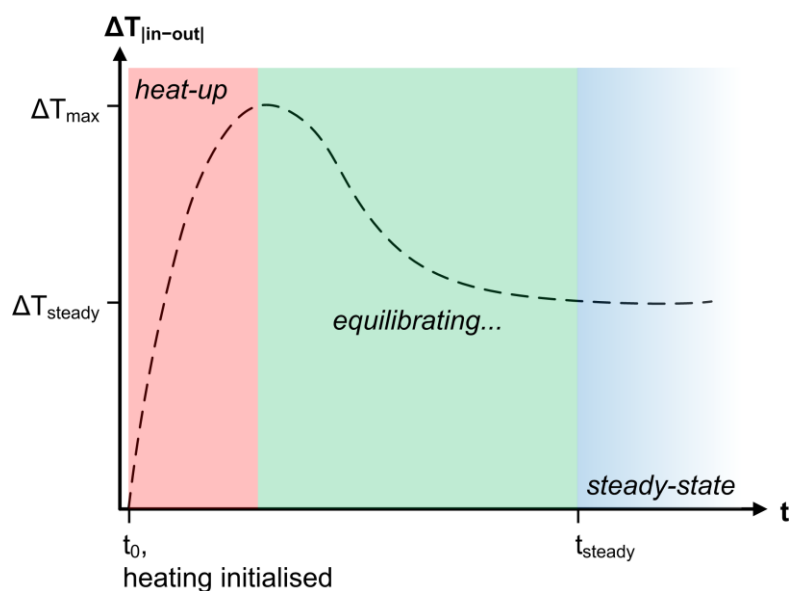
Figure 11. Illustration of the temporal evolution of $\Delta T_{|in-out|}$ during heating of the sample loop (thermo-desorption). In the initial heat-up phase, the temperature difference between inner sample loop temperature and sensed temperature at the outside tubing wall (T_{out}) is rapidly increasing, then decreases and reaches a steady-state value after some time. Experimental values are e.g. ΔT_{max} ~200 °C, ΔT_{steady} ~100 °C after Δt_{steady} ~120 s.

To account for this time-dependency and use the sensed temperature in a feedback control algorithm (i.e. PID controller), heater output has to be strictly limited (P_{lim}) during the initial heat-up phase (Δt_{hu}), causing a slow increase of the sensed temperature towards the setpoint (T_{set}) of the controller. Thereby, overshooting of the actual (inner) sample loop temperature (which could degrade the adsorptive material) can be reduced. At the time the setpoint T_{set} is reached, $\Delta T_{|in-out|}$ should have reached its minimum over the heating period. This heater characteristic can also be implemented by using a 2-stage, constant power output setting (P_1 and P_2 with $P_2 < P_1$). A constant power heater brings the advantage of not relying on an inaccurate process variable, the quality of a control algorithm (PID tuning) and work-arounds like limiting heater output to avoid overshooting of the actual temperature inside the sample loop.

Considering heater characterisation, i.e. determination of the parameters Δt_{hu}, P_{lim} and T_{set}, (PID control) or P_1, P_2 and Δt_{hu} (2-stage, constant power), a dummy loop with a temperature sensor of low thermal mass placed inside has proven to be a method that gives good approximate values. However, results are not directly conferrable due to potential variations in insulation (dummy vs. actual sample loop), thermal mass (including adsorptive material) and electrical resistance (variations in tubing wall thickness, carbon content etc.). After obtaining estimates of Δt_{hu}, P_{lim} and T_{set} or P_1, P_2 and Δt_{hu} in the dummy loop experiment, the actual sample loop has to be installed. Heater parameters have then to be adjusted, first by placing a temperature sensor inside the sample loop up to the point where the adsorptive material is held in place by a frit. After the parameters have been tuned for the installed sample loop, final adjustments can be made based on GC-MS results of actual sample thermodesorption.

Quality assessment of Adsorption and Desorption

The ultimate test for the preconcentration-thermodesorption assembly is the quality determined in GC-MS measurements. The parameters of interest are (1) analyte breakthrough in regard to adsorption and (2) injection quality and (3) analyte residues in regard to desorption. (1) To determine the mixing ratio range that can be covered by the preconcentration setup, analyte breakthrough has to be analysed. This can be done experimentally by increasing the preconcentrated volume of a reference air sample. Assuming

that there is no detector saturation and the detector responds proportionally (linearly), breakthrough will be indicated by a decreased detector response in comparison to a response obtained from a preconcentration volume where no breakthrough occurs. (2) Injection quality can be judged based on peak shape and retention time stability of substances eluting early from the GC; the lowest retention time possible implies that these analytes are least influenced by chromatographic separation (i.e. "focusing"). The peak shape is then essentially determined by the injection from thermodesorption. (3.1) To ensure accurate results, analyte residues from preceding samples ("memory effect") or system contaminations have to be accounted for. Contaminations are by definition always present in any sample measurement. If they represent a constant background, they might be accounted for; if however they are variable in concentration and this concentration is significantly above measurement precision, reliable analyte quantification is impossible. Contaminations undoubtedly are a worst-case and should be avoided by appropriate selection of materials (tubing, valve membranes etc.) and gases (carrier gas purification etc.). (3.2) Analyte residues from preceding sample measurements are likely to occur positively correlated with substance boiling point and concentration. Such a memory effect is indicated by an amount of residue decreasing to zero within one to a few measurements of blank gas. If the residue persists, it can be considered a contamination. The origin of the memory effect can be separated into "system", i.e. all parts like tubing, valves, sample dryer etc. prior to preconcentration and "preconcentration", i.e. the sample loop (non-quantitative thermodesorption) as well as tubing and valves between sample loop and GC column. Experimentally, preconcentration residues can be tested by repeated thermodesorptions subsequent to the preconcentration of an ambient air sample. Gas flow is thereby unchanged, i.e. the sample loop is kept in line with the GC column. Anything that appears in the chromatogram after that of the ambient air measurement is preconcentration residue or "preconcentration blank". After the preconcentration blank has been characterised, the "system blank" can be determined by preconcentrating a "blank gas" known to be free of detectable analytes after the measurement of the reference air sample with known analyte mixing ratios. For such experiments, TOFMS is a very well suited detector, due the acquisition of full mass spectra with high sensitivity which ensures that a large substance range is covered.

Results from characterisation experiments presented in Obersteiner et al. (2016b) assure applicability of the preconcentration setup for the quantitative analysis of a wide range of halocarbons and potentially also hydrocarbons after further characterisation experiments. The simplicity of design, low weight, small size and refrigerant-free operation of the set-up have proven to be very beneficial for a field application like the in-situ aircraft instrument GhOST-MS. Reliability of performance during field- and laboratory operation is underpinned by results from three different instrumental setups (Hoker et al., 2015; Obersteiner et al., 2016a; Sala et al., 2014). The analyte range of highly volatile species is limited by the unintended but unavoidable preconcentration of large amounts of CO_2 (sublimation point: $-78.5\,°C$) at an adsorption temperature of $-80\,°C$. Future development of the setup could therefor attempt to overcome this limitation by a CO_2-removal step prior to preconcentration. The preconcentration setup could then also be suited for the analysis of compounds like CF_4 or C_2H_6.

2.3 Gas chromatography – mass spectrometry: from quadrupole to time-of-flight MS

Publication II: "Comparison of GC/time-of-flight MS with GC/quadrupole MS for halo-carbon trace gas analysis", Hoker et al. 2015, AMT

The following sections 2.3.1 to 2.3.4 give a general background and summary of results of the detector comparison published by Hoker et al., 2015. More details and an application of the GC-QPMS/-TOFMS instrument to ambient air samples; a time series collected at Taunus Observatory, Kleiner Feldberg, Germany, can be found in J. Hoker's dissertation (Hoker, 2015).

2.3.1 Instrumental motivation

The QPMS is essentially a mass filter; a direct voltage and an alternating voltage between two concentric pairs of metal rods are chosen so that ions accelerated into the generated electric field can only pass through if they have a specific, "resonant" m/Q. The sector field mass spectrometer (SFMS) relies on the separation of ions of different m/Q while passing through a combination of magnetic and electric fields. To acquire a mass spectrum in a specified mass range, in QPMS as well as SFMS, a sequence of different configurations (e.g. voltages, frequency, etc.) are necessary to record each desired m/Q within the mass spectrum – both QPMS and SFMS are scanning techniques. Consequently, molecules from a continuous analyte source such as a gas chromatograph are sampled with the spectra acquisition rate of the MS. If the area of the chromatographic signal is required to be representative for the amount of the analyte in the sample (quantitative analysis), the number of ions from that analyte (i.e. analyte outflow from the GC) must not change significantly during the time that is needed to acquire the mass spectrum. Otherwise, "spectral skewing" occurs and the chromatographic peak area is not a quantitative representation of the analyte concentration. To avoid spectral skewing, the spectra acquisition rate must be sufficiently high to characterise the chromatographic peak. Because longer acquisition times generally result in better sensitivity, scanning instruments are limited by a minimum acquisition rate imposed by the necessity to avoid spectral skew in quantitative analysis while at the same time guaranteeing sufficient sensitivity

depending on the application. In applications that demand high sensitivity like trace gas analysis, QPMS and SFMS are monitoring only specific ions during the elution of their parent molecules from the GC (single ion monitoring, SIM). SIM mode on the other hand limits the capability of the mass spectrometer for substance identification as only specific parts of the mass spectrum are recorded. Well-established scanning mass spectrometers (QPMS, SFMS) therefore stand in contrast to the vast number of species found in a chromatogram of an ambient air sample – the search for a non-scanning, "full spectra" technique seems obvious. This development in measurement technology is also encouraged by the continuous introduction to and/or discovery of new compounds in the atmosphere, namely replacements for formerly used refrigerants etc. (Kloss et al., 2014; Laube et al., 2014; Mühle et al., 2009; Schoenenberger et al., 2015; Vollmer et al., 2015; Weiss et al., 2008).

More sophisticated quadrupole mass analyser applications like tandem MS (MS-MS; e.g. quadrupole – collision cell – quadrupole) provide higher selectivity but still suffer from a very limited spectral acquisition range at a given time. A relatively new type of mass spectrometer, the orbitrap MS which is basically a Fourier transform mass spectrometer with an electrostatic ion trap, intrinsically acquires full mass spectra at very high mass resolution and spectra rate suitable for conventional gas chromatography. This technology is however also reported to be limited to a dynamic range (10^3 to 10^4) which is decreased if the spectra acquisition rate is increased (Hu et al., 2005; Zubarev and Makarov, 2013). In contrast to orbitrap MS, TOFMS is actually a quite old method, developed in the 1950s (Cameron and Eggers, 1948; Wiley and McLaren, 1955; Wolff and Stephens, 1953), shortly before the QPMS (Paul and Steinwedel, 1953). TOFMS relies on the simple fact that at constant acceleration energy, ions of different mass need different times to travel a specific distance through a field-free region. After the heaviest ion has reached the detector, each acceleration event provides a full mass spectrum with a potentially large mass range. The first application of TOFMS to capillary column gas chromatography was published in 1962 (Gohlke, 1962), important technical improvements like the introduction of an electrostatic ion mirror followed (Mamyrin et al., 1973), as well as many applications like protein analysis (review by Bonk and Humeny, 2001), aerosol composition analysis (e.g. Drewnick et al., 2005) or high-speed gas chromatography

(Wollnik et al., 1994). A discussion of TOFMS principles can be found in Guilhaus (1995) or Mamyrin (2001). Although still more expensive than quadrupole mass analysers (about a factor of 2-4), TOFMS became more affordable in recent years and manufacturers claim that limits in dynamic range are overcome. Nevertheless, there is a reason why established technology became established in the first place and TOFMS has to prove that it can compete with QPMS in terms of precision, dynamic range and ease of operation. If so, TOFMS could enable a step forward from scanning the mass spectrum to full spectra acquisition in mass spectrometric analysis of trace gases.

2.3.2 Analytical setup

The setup used to evaluate the performance of a TOFMS in the analysis of halogenated trace gases comprises a sample preconcentration system described in Obersteiner (2012), an Agilent Technologies 7890A gas chromatograph and a split at the end of the GC column that splits the column effluent approximately equally into two detectors; an Agilent Technologies 5975C quadrupole mass analyser as reference and a Markes International Bench TOF-dx time-of-flight mass analyser (former ALMSCO; model no. E24). The original GC-MS setup (QPMS only) was described, characterised and applied by Laube (2008) and Brinckmann (2011). The split allows a direct comparison of both detectors, excluding possible effects of sample preconcentration or gas chromatography on e.g. precision of detection. A flow diagram of the instrumental setup is shown in Figure 12.
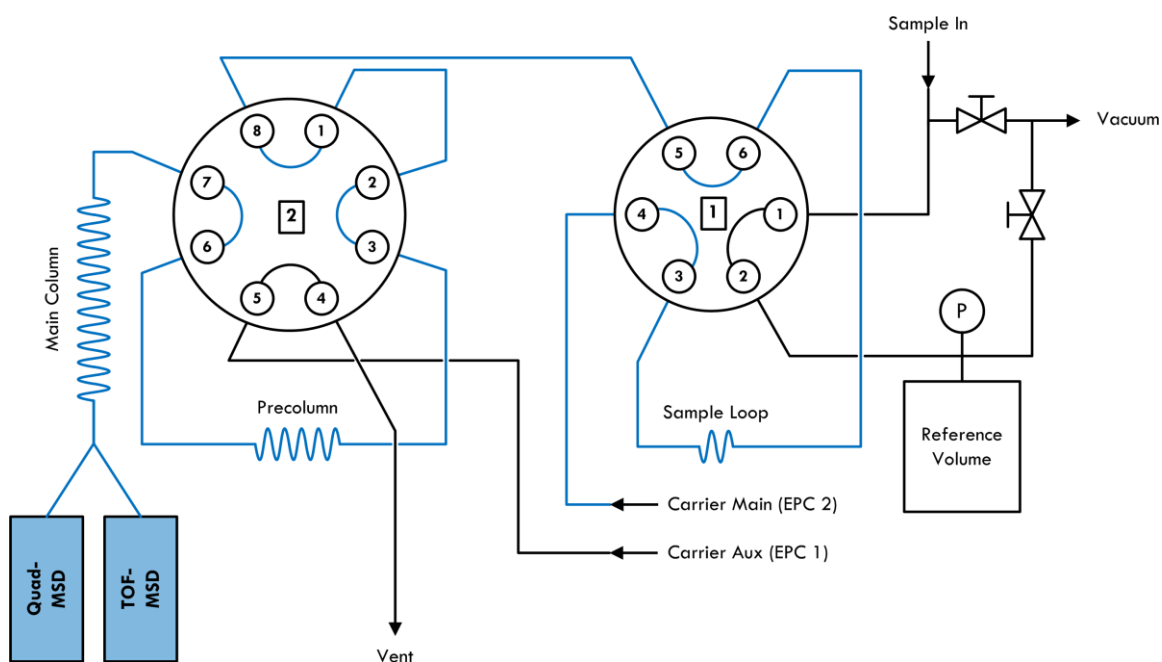
Figure 12. Flow diagram of the GC-MS setup used for the experiments conducted for the publication Hoker et al. (2015). The flow path of the preconcentrated sample during injection into the GC column is marked by the blue line.

The simultaneous operation of two mass spectrometers attached to the same GC has proven to be a valuable tool for a first characterization of a new type of spectrometer. However, a redundant detector is of no benefit for routine measurements. Therefore, the original plan was to operate the QPMS in negative chemical ionization mode (NCI; highly selective and sensitive to e.g. brominated and mixed halogenated hydrocarbons; see e.g. Sala et al., 2014 or Worton et al., 2008) and the TOFMS in electron ionization mode (EI) to combine sensitivity (NCI QPMS) with a large substance range (EI TOFMS).

2.3.3 Technical basics of TOFMS

The reference instrument, the Agilent MSD, is a very wide-spread instrument and QPMS is common in general. In contrast, the TOFMS used in the comparison is more "specific", namely a direct extracting instrument. Direct extraction means that all ions formed in the ion source are extracted pulse-wise from the ion source into the drift tube. Except for the ion mirror (reflectron; and detection electronics of course), this configuration is close to the historic setup by Wiley and McLaren (1955). The general advantage is the high transmission rate (most ions formed can be detected) resulting in high sensitivity; the

downside is a reduced space- and time-focusing of the ions resulting in low mass resolving power. The other TOFMS configuration, which was used in Obersteiner et al., 2016a, is orthogonal extraction (e.g. Chernushevich et al., 2001; Guilhaus et al., 2000) in which a continuous ion beam is extracted from the ion source, of which packets of ions are pulse-wise pushed orthogonally into the drift tube. Thereby, a better space- and time-focusing of the ions is achieved, resulting in a higher mass resolving power but also reduced transmission rate. A schematic of a TOFMS is given in Figure 13. A quadrupole mass filter can additionally be introduced into the ion beam before extraction into the drift tube to serve e.g. as a high-pass filter that supresses low m/Q so that e.g. the GC carrier gas signal can be suppressed. Such a high-pass filter in direct extraction TOFMS can be implemented by an electrical "deflector" field in line with the extracted ion beam. The deflector field which is normally used to ensure a correct flight path of the ions can be switched off and on again during each ion extraction to deliberately exclude ions from hitting the detector.
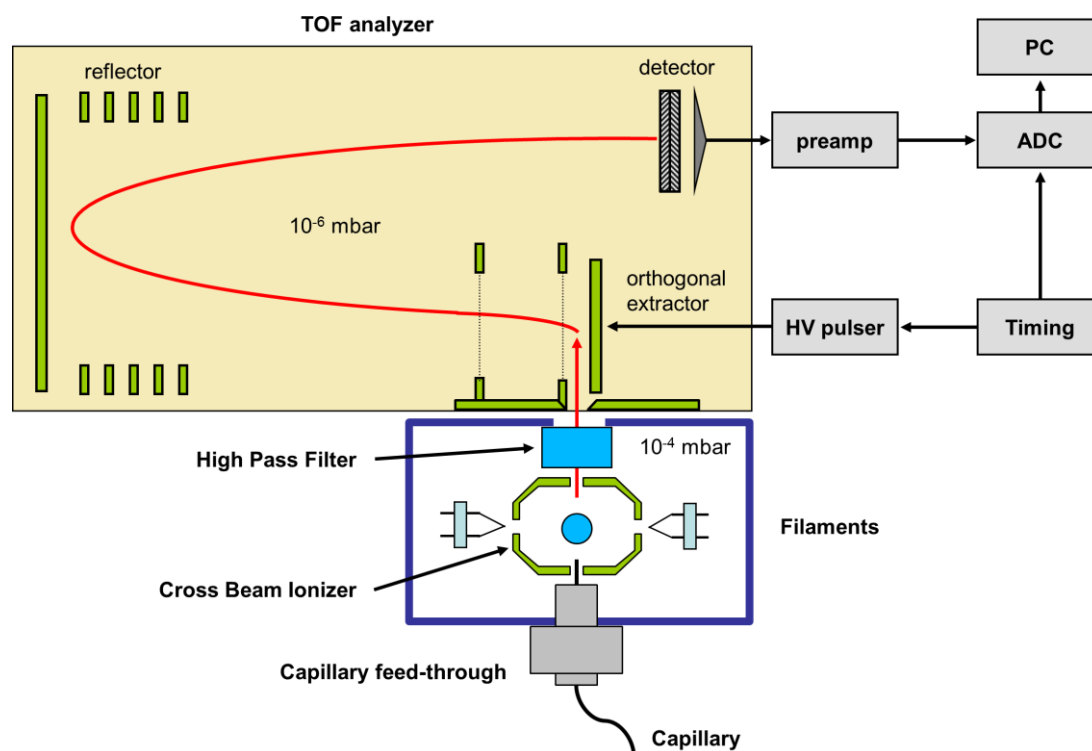
Figure 13. Schematic of an orthogonally extracting TOFMS, including a capillary GC interface (EI ion source). Adapted from Tofwerk AG, Switzerland. In comparison to the direct extracting TOFMS, ions are formed outside the TOF analyser and introduced to the ionizer via the quadrupole high-pass filter. A schematic of a direct extracting TOFMS is shown in Fig. 2, Hoker et al. (2015).

The heart of a TOFMS is its timing and detection electronics. The time-of-flight mass analyser fundamentally relies on a precise measurement of the time interval between ion extraction and arrival at the detector. The detector itself is e.g. a multi-channel-plate (MCP; electron multiplier array) that amplifies signals of arriving ions. To resolve ions of different m/Q from an ion extraction, the MCP has to reach its baseline voltage after each m/Q. The time between extraction and signal can then be used to calculate the mass-to-charge ratio of the ion; the signal intensity can be used to calculate the number of ions of equal m/Q contained in the extraction. If the number of ions of equal m/Q in consecutive extractions exceeds a certain limit, MCP saturation can occur. The MCP signal in this case is not representative anymore for the number of ions; a quantitative measurement is not possible anymore.

The analogue signal of the MCP has then to be converted to a digital representation by an analogue-to-digital converter (ADC) for further data processing. The ADC bandwidth (sampling frequency) determines the digital mass resolving power of the TOFMS; the physical mass resolving power is determined by space- and time-focusing of ions of equal m/Q as well as the total flight distance. Longer travel time also reduces the demand for ADC bandwidth. The signal intensity resolving power is determined by the ADC memory size. If the MCP voltage exceeds the input voltage range of the ADC, ADC saturation can occur. To achieve a suitable signal-to-noise ratio (S/N) of the mass spectrum, recorded waveforms of multiple ion extractions are averaged to form one mass spectrum. More waveforms averaged means better S/N; however also reduced spectra rate. This consideration has to be taken into account if the TOFMS should be used for fast GC.

2.3.4 The comparison experiment: results and motivation for further development

The direct comparison of the state-of-the-art Agilent 5975C QPMS with the relatively affordable Markes International BenchTOF-dx E24 revealed some distinct differences of both instruments and even though two specific instruments were compared, some results can be considered general for the respective mass analyser technique. Handling and stability of performance is exceptionally good for the QPMS, which is manifested in a small drift of sensitivity during measurement series, high precision in dedicated experiments as

well as routine air sample analysis and no hardware failures during years of continuous operation. This finding is further supported by the experience gained by using a similar 5975C QPMS in aircraft in-situ operation (Sala et al., 2014). The BenchTOF-dx, although performing reliably most of the time with equally good results in instrument drift and precision, caused some down time of the GC-MS due to hardware failures (defective voltage supply modules). On the other hand, the BenchTOF-dx showed unmatched sensitivity (e.g. Tab. 5, Hoker et al., 2015), considering that it was providing full mass spectra at a spectra rate comparable to that of the 5975C (~3.5 spectra per second). The QPMS could only compete in SIM mode, exclusively monitoring quantifier ions of selected analytes. The mass filtering of the QPMS however is an advantage in some cases, when large amounts of non-target species, namely CO_2 and H_2O (also trapped during preconcentration), threaten to saturate the detector. While the QPMS can easily suppress those ions by quadrupole filter settings, the TOFMS suffers a loss of sensitivity and mass range. To deal with the large amount of CO_2 that is eluting from the GC column, ions up to m/Q 44 (CO_2^+) have to be deflected by the deflector field (see 2.3.3). This deflector setting cannot be changed during the chromatographic run; consequently, a lot of information is cut from all mass spectra like e.g. signals from CF^+ (m/Q 31, typical HFC or PFC ion) or $C_2H_5^+$ (m/Q 29 typical hydrocarbon ion). A part of this problem is of course caused by the preconcentration setup (direct injection without removal of CO_2; see 2.2). The other part has to be attributed to the direct extraction technique and a limited dynamic range of the spectrometer's MCP. Additionally, the deflecting electric field needs a certain time to be established; this attenuates signals further along the TOF-axis (e.g. m/Q 49 from $CH_2^{35}Cl^+$ or m/Q 51 from CHF_2^+). The signal of H_2O is completely suppressed by this deflector setting. However, presumably due to the expansion of water when introduced into the ion source and flight chamber thereupon, a dampening effect occurs that influences all other ion signals. As a consequence, measurement precision is significantly decreased for analytes that elute with or after water from the GC column. This problem can only be avoided if samples are dried extremely well and also have equal water content, what is almost impossible when analysing ambient air samples that are dried with magnesium perchlorate. Besides the restriction of limited dynamic range (CO_2) and the dampening effect of water, the BenchTOF-dx showed another limitation in characterisation experiments with regard to quantitative analysis of trace gases: sub-

stance-specific and partly significant non-linearities (e.g. Fig. 6, Hoker et al., 2015). These are characterised, at least for analytes that are measured with high precision (CFC-12, CFC-11 etc.), by a systematic under-prediction of low intensity signals and a systematic over-prediction of high intensity signals. Despite our efforts, we could not identify a reason that caused this non-linear detector response. The manufacturer of the TOFMS tried to solve the issue by instrument (software) tuning, but did neither make significant progress towards a linear response nor gave away any information on possible reasons. Furthermore, the data format that was made available to us was proprietary, meaning that we did not have a chance to investigate the actual time-of-flight spectra but only pre-processed mass spectra (1 amu centroided "line" spectra).

In summary, the BenchTOF-dx leaves a two-sided impression. On the one hand, the instrument is performing very well in regard to precision and especially sensitivity. Precision was found to be comparable to that of the QPMS and as good as 0.2% depending on substance and preconcentration volume. Limits of detection were calculated to be around 20 ppq for selected substances in 1 L sample volume, which is exceptionally low for a mass spectrometer with an electron ionisation (EI) source and a mass resolving power of approximately 1000 $m/\Delta m$. Detection limits of the BenchTOF-dx are therefore comparable or even better than with a QPMS in SIM mode, monitoring only one specific ion. On the other hand, a deviation of up to 10% from linear response at a measurement precision of 0.2% render the instrument unsuited for accurate, quantitative trace gas analysis without further correction steps in data processing. A post-correction of non-linearity would introduce an additional error source. The encountered non-linearity in combination with restricted data accessibility of the BenchTOF-dx is unsatisfactory from a scientific perspective, especially for the intended application. This type of TOFMS therefore cannot replace the QPMS unconditionally.

2.4   The automated GC-TOFMS instrument *FASTOF*

Publication III: "An automated gas chromatography time-of-flight mass spectrometry instrument for the quantitative analysis of halocarbons in air", Obersteiner et al. 2016, AMT.

The experience gained with the BenchTOF-dx suggests that TOFMS definitely has potential for analysis of halogenated trace gases. The full range mass spectra open up the possibility to create a "digital air archive"; chromatographic signals of substances that were not target species at the time of measurement can in principal be analysed in retrospect. As mentioned in section 2.3.4, the BenchTOF-dx provides high sensitivity and very good precision; however, it has some deficits with regard to dynamic range and non-linearity. Furthermore, the mass resolving power as well as mass accuracy of the instrument is insufficient to gain selectivity by separation of neighbouring ion signals of equal nominal (integer) *m/Q* but differing exact *m/Q*. The FASTOF project, for "Fully Automated in-Situ GC-TOFMS", is the attempt to address these issues with a TOFMS from another manufacturer, Tofwerk AG, and to undertake steps towards an independently operating in-situ instrument for e.g. online monitoring. The following sections 2.4.1 to 2.4.6 give additional information on the instrument development and characterisation published in 2016 and summarise results.

2.4.1   Component selection and final setup

Planning of the assembly began in the end of 2012. Significant time was devoted to the selection of a suitable mass spectrometer based on the first results from the Bench-TOF-dx. A visit at Tofwerk AG in Thun, Switzerland, including a test of one of their TOFMS attached to the in-situ GC-MS GhOST, gave promising results regarding non-linearity and suitability of the instrument. The choice was made to obtain a TOFMS with significantly higher mass resolving power (~4000 *m/Δm*) than the BenchTOF-dx to achieve selectivity despite using electron ionisation. Although this is only a medium mass resolving power compared to other TOFMS or SFMS and orbitrap MS, it is sufficient to separate many ion signals with matching nominal *m/Q* but differing exact *m/Q*. Examples are ions from halocarbon molecules whose *m/Q* is slightly below nominal *m/Q*

and ions from hydrocarbon molecules whose *m/Q* is slightly above nominal *m/Q*. An example is shown in Figure 14: A signal from $C_6H_{13}^+$ (*m/Q* 85.1012) could be mistaken for a $CF_2{}^{35}Cl^+$ signal (*m/Q* 84.9651) if only the "nominal signal" (nominal mass interval) is considered.
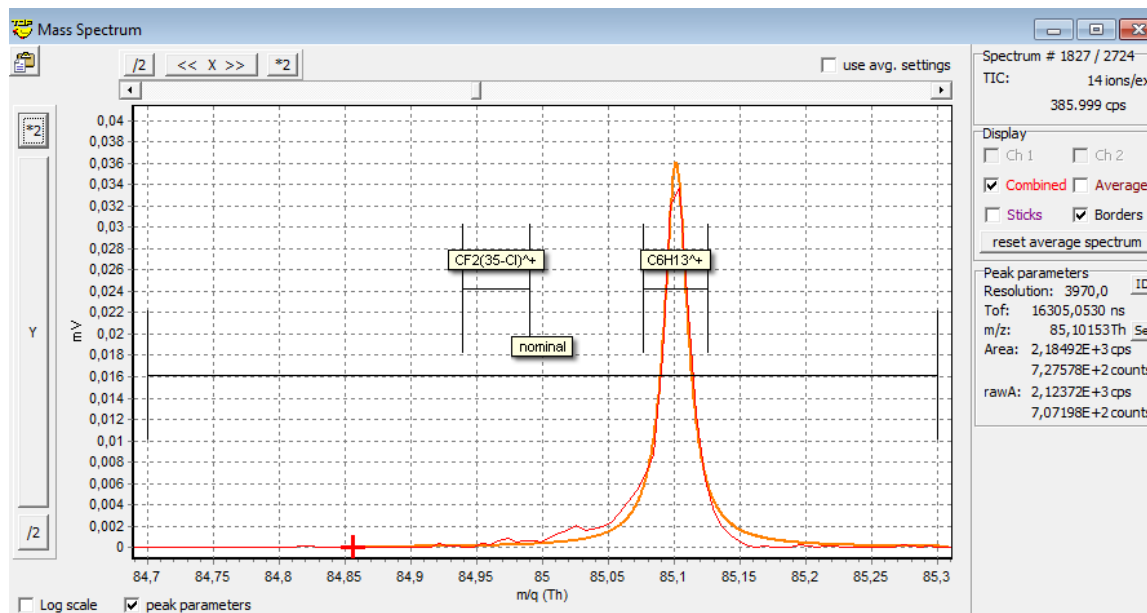
Figure 14. Screenshot from TofDaqViewer (Tofwerk AG) showing a signal on the mass axis (x-axis) from the $C_6H_{13}^+$ ion (red curve, intensity in mV on the y-axis). The signal identity is confirmed by the measured *m/Q* of 85.10153 at the curve fit apex (orange curve; deviation versus calculated *m/Q*: 3.9 ppm). *m/Q* intervals shown: integer *m/Q* ±0.3 (nominal interval) and calculated *m/Q* ±0.025 (narrow intervals). Summed intensity per interval and mass spectrum over the chromatographic runtime gives the temporal evolution of each specified signal; see also section 2.4.2.

A further example was given in Figure 7 of Obersteiner et al. (2016a) which shows the compensation of a coelution of two substances from the GC with matching nominal masses but differing exact masses. Mass resolving power therefore brings a plus in selectivity, i.e. gain in sensitivity. As an illustration, Figure 15 shows the noise reduction for the quantifier ion signal of bromoform ($CHBr_3$). Sensitivity is increased in this case by a factor of approximately 5.
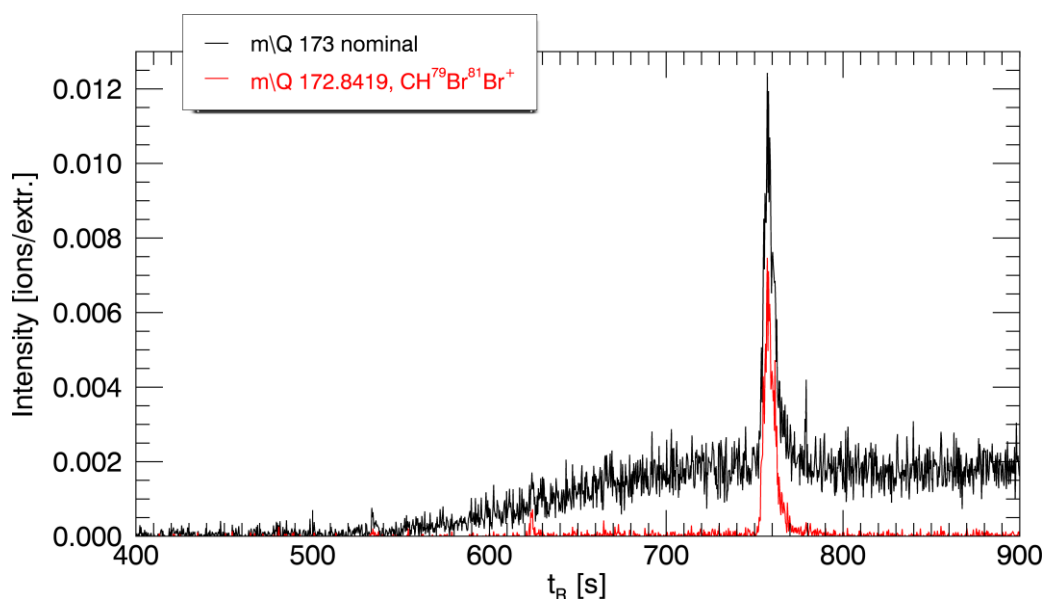
Figure 15. Chromatographic signal of the quantifier ion of bromoform (CHBr$_3$). X-axis: retention time t_R in seconds, y-axis: signal intensity in ions per extraction. Black curve: nominal signal, m/Q 173 ± 0.3. Red curve: accurate m/Q window, m/Q 172.8419 ± 0.025. Signal-to-noise ratio of the bromoform signal at t_R = 758 s is increased from ~7 to ~35 if the narrow m/Q interval is used instead of the nominal m/Q interval.

After the selection of the mass spectrometer was completed, a laboratory GC (Agilent Technologies 7890B) was purchased as the intended operation of the instrument does not involve high-speed in-situ measurements what would be the case for an aircraft instrument. In parallel, a revised version of the preconcentration unit was designed and assembled as described in section 2.2. The gas flow of the setup was chosen similar to that of the laboratory setup presented in the previous section 2.3, Figure 12. To prepare for an in-situ deployment in the future, the GC-MS setup was placed on a movable table as shown in Figure 16.
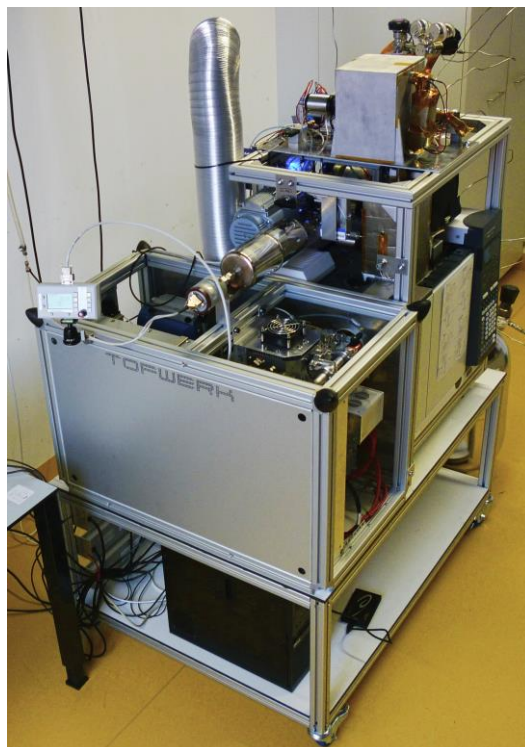
Figure 16. Photograph of the instrumental setup *FASTOF*, completed and fully operational in November 2014. Lower part of the table construction: Data acquisition PC and power supply. Upper part, left side: TOFMS; right side: GC. On top of GC: Stream selection and preconcentration. Back of GC: preconcentration unit control (NI cRIO).

2.4.2 Data structure and processing in IDL

The TOFMS (Tofwerk EI-TOF 003) data acquisition hardware is processing data at a frequency of 1.6 GS per second and a sample size of 14 bit – even though not every bit is recorded, a lot of data is generated during each measurement. Every mass spectrum consists of approximately $6 \cdot 10^4$ individual data points in full resolution, which makes ~$2.3 \cdot 10^8$ data points for each chromatogram with a runtime of 16 minutes. The data acquisition software already offers the possibility to process high resolution data and generates specific *m/Q* or "mass" traces at runtime, i.e. temporal evolution of *m/Q* during the chromatogram. These mass traces only contain one data point per spectrum and represent a user-specified interval of the mass axis around the specified *m/Q*, summed up into one data point. All TOFMS data including predefined mass traces and housekeeping data (temperatures, pressures, voltages) are saved and compressed into hdf5 file format, which is fully accessible to the user. IDL (Interactive Data Language, Exelis VIS / former RSI Research Systems Inc.) was chosen as a programming environment to handle the

TOFMS data. The existing, self-written and widget-based software ("IAU_Chrom") for the integration of chromatographic peaks was extended to work with the hdf5 file format and the TOFMS data. To integrate chromatographic signals, mass traces have to be generated from the high resolution spectra. This can either be done by directly importing the predefined mass traces from the hdf5 files (fast in computation) or by reading the high resolution data from the hdf5 file and then calculate specific mass traces (slower in computation). IAU_Chrom offers three models to integrate chromatographic signals (baseline integration, Gaussian fit, Gumble fit) and was extended to include viewer functionality, i.e. overlay of one mass trace and multiple chromatograms or multiple mass traces in one chromatogram, visualisation of TOFMS housekeeping data, calculation of signal-to-noise ratio of chromatographic signals and calculation of the ratio of different ion signals from one parent molecule.

2.4.3 From air sample to mixing ratio

A relative calibration scheme is used to assign a mixing ratio to an analyte found in an air sample. Relative means that a calibration gas (reference air sample) with known mixing ratios is measured in alternating sequence with air samples. The amount of an analyte in a sample is represented in GC-MS by the chromatographic peak area A. This detector response of the analyte has to be corrected for the analysed (i.e. preconcentrated) volume V from the sample by calculating A/V. Each A/V ratio of an analyte in a sample is then referenced against a corresponding A/V of the analyte in the calibration gas measurement. The $(A_{sample}/V_{sample}) / (A_{cal}/V_{cal})$ ratio gives the relative detector response rR. rR can in case of a linear detector simply be multiplied with the mixing ratio of the analyte in the calibration gas to yield the mixing ratio of the analyte in the sample. To account for a drift in sensitivity of the system during a measurement sequence, multiple calibration gas measurements are performed within the sequence. An illustration of the applied calibration and drift correction scheme is shown in Figure 17. The automated operation of the GC-TOFMS provides the possibility to run long, unattended measurement sequences that e.g. comprise two calibration points in series after a sample block size of five (depending on sample- and calibration gas availability). Consequently, data evaluation also gets more complicated if e.g. decisions have to be made like discarding specific measurements of one sample that lie out of the typical precision range.
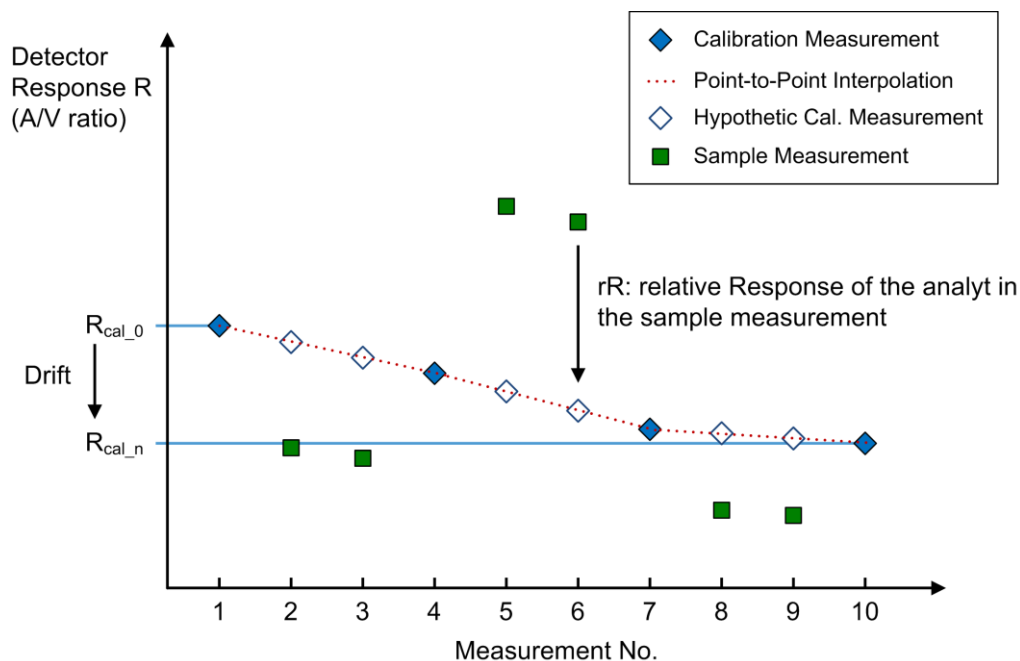
Figure 17. Illustration of the calibration scheme. An alternating sequence of calibration gas and air sample is measured; calibration points are interpolated linearly point-by-point to account for a possible detector drift between calibration points that are bracketing a block of sample measurements. Alternation sequence and number of measurements per sample can be different than displayed here; depending on the experimental task, stability of the detection system etc.

A mixing ratio assigned to a sample becomes meaningful only after an error estimate has also been provided. Measurement precision is an important part of such an error estimate and relatively easy to derive in most cases. In canister measurement series with multiple measurements of the same sample in one block, measurement precision can be approximated based on the relative standard deviation (rSD) of rR within the sample blocks. As block size is too small in most cases to deliver a significant rSD in a statistical sense, the rSD of multiple sample blocks has to be averaged to yield a meaningful value. This "intra-block" precision describes the variability within a block of measurements of the same sample. In case of online, in-situ measurements, there is only one measurement per sample and therefore measurement precision has to be derived experimentally by a dedicated experiment. This precision experiment consists of repeated measurements of the same reference air; the sequence should be as long as a typical measurement series. The experiment is then evaluated treating a subset of the measurements as calibrations and another subset as samples. The mean rSD of all virtual samples gives the "inter-block" precision of the instrument and describes the variability among blocks of measurements of the

same sample. In case of flask measurement series, the inter-block precision from the idealized precision experiment can be compared to the intra-block precision of the actual measurement series. To get a conservative estimate, the worse of both precision should be assigned to the mixing ratio. While intra-block precision can be calculated for every measurement series, precision experiments have to be repeated from time to time to account for changes of measurement quality over time (reproducibility). To get a reliable error estimate of a calculated mixing ratio, precision is not enough as a measurement can be very precise but inaccurate. Uncertainty regarding mixing rations in the calibration gas also has to be taken into account. Such uncertainties can e.g. originate from the original, gravimetrical calibration of the primary calibration gas (scale uncertainty) and errors during intercalibration and transfer of mixing ratios to secondary (ternary etc.) calibration gases (transfer uncertainty). An estimate of transfer uncertainty can e.g. be obtained by cross-referencing multiple secondary calibration gases that derive from the same primary carlibration gas against each other. Another way is to compare results from different instruments which all depend on the same primary calibration. Note that this procedure still excludes the error of the primary calibration scale itself.

2.4.4 Extension of the substance range

The TOFMS opens up new possibilities regarding substance identification and the number of routinely analysed species. No dedicated mass filter settings are necessary like with the quadrupole; identification can be performed in principal in any chromatogram. The unambiguity of identification benefits from mass resolution and a suitable mass accuracy (depending on mass resolution), as more mass resolution means more selectivity for specific molecule fragments. With the GC-QPMS setup established by Laube (2008) and Brinckmann (2011), 30 substances were detectable in regular samples; this qualified substance range was significantly extended by 65 compounds (+217 %), making 95 in total, with some unidentified signals still remaining in chromatograms. Figure 18 shows the identification of H_2S which appeared in blank gas measurements after installing a new sample loop as an example. Table 1 provides a comparison of calculated and measured mass spectrometric data of the respective H_2S signal.
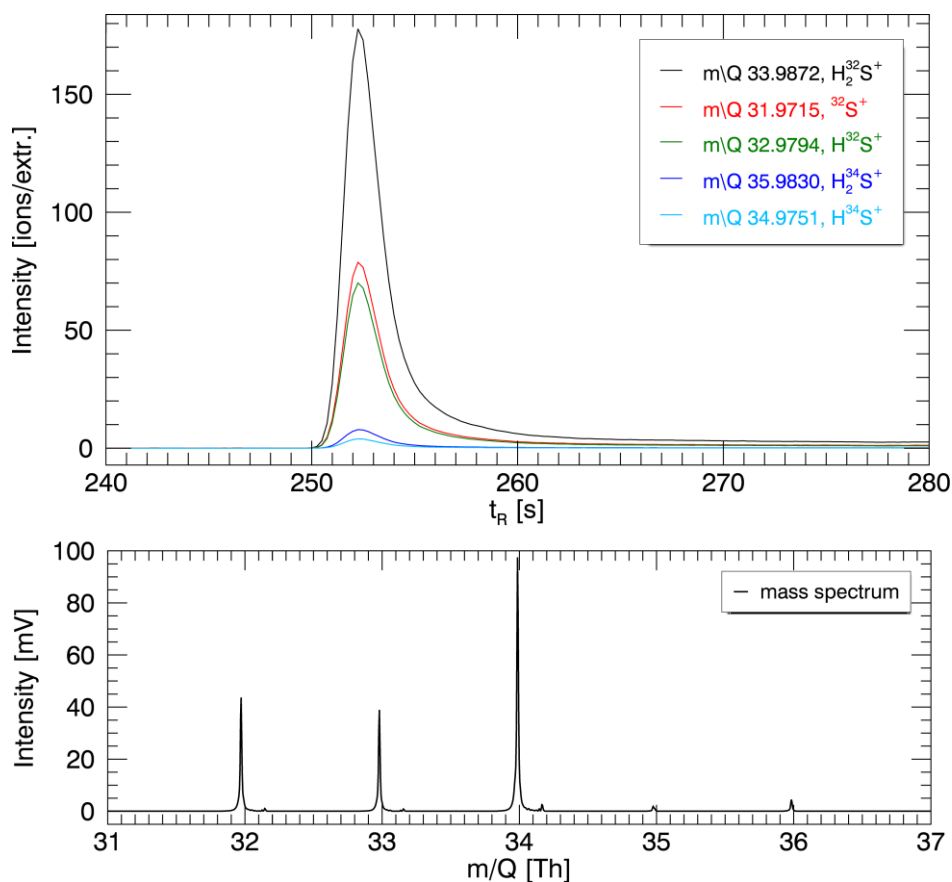
**Figure 18. Chromatographic signal of H$_2$S (upper part) as found in large abundance in a blank gas
measurement after installing a new sample loop in the preconcentration unit, and according
mass spectrum at the chromatographic peak apex (lower part). The tailing of the chromato-
graphic peak indicates a continuous injection during desorption, which is typical for residues
that originate from the adsorptive material or sample loop tubing. The small signals to the
right of the actual H$_2$S mass spectrum are detector artifacts, i.e. the signal reflection discussed
in sect. 3.4 of Obersteiner et al., 2016a.**

**Table 1. Comparison of calculated and measured data of the H$_2$S signal. The underlying mass spectrum is
shown in Figure 18, lower part.**

Ion	calculated m/Q	measured m/Q	m/Q deviation [ppm]	rel. abundance (NIST 2011)	rel. abundance (measured)
H$_2^{32}$S$^+$	33.9872	33.9874	6.7	1	1
^{32}S$^+$	31.9715	31.9717	5.5	0.444	0.444
H^{32}S$^+$	32.9793	32.9794	2.8	0.420	0.386
H$_2^{34}$S$^+$	35.9830	35.9833	8.7	0.042	0.040
H^{34}S$^+$	34.9751	34.9773	61.1	0.025	0.021

Identification is significantly facilitated by the TOFMS in comparison to QPMS. However, to make the step from identification to routine analysis, the limiting factor is quantification. Calibration gases that contain accurately known mixing ratios of nearly 100 species are hard to obtain. Uncalibrated signals can still be utilized in relation to other species if e.g. only the slope of a correlation is of interest.

2.4.5 Measurement quality and application

The goal of halocarbon trace gas analysis is high-precision quantification to reveal very small trends of analytes like CFCs to calculate future atmospheric burden and to quantify e.g. the budget of HFCs in the atmosphere for emission surveillance. This implies that a high-quality calibration gas is at hand and that the instrument is capable of not only qualification but also and more importantly precise quantification. A general quality assurance of the GC-TOFMS instrument is shown by the intra-laboratory comparison discussed in section 3.5, Obersteiner et al., 2016a. Unfortunately, an inter-laboratory comparison based on the round robin samples is not possible yet as no results from the In-GOS (Integrated non-CO_2 Greenhouse gas Observation System) Halocarbon Round Robin Intercomparison (IHRRI) had been publish at the time this dissertation was written. Results obtained with the instrument have also been compared to an external instrument, an in-situ Medusa GC-MS at Mace Head Station (MHD), Ireland. Results for the quantification of CFC-12 are discussed in section 4.1 of Obersteiner et al., 2016b. The instrument has been used furthermore to analyse air samples which were collected routinely at Taunus Observatory (TO) at Kleiner Feldberg in Germany. The comparison with other instruments, i.e. our GC-QPMS and the in-situ Medusa instrument at Mace Head Station, shows very promising results with regard to analyte quantification. Figure 19 shows additional results from the quantification of the most abundant HFC in the atmosphere, HFC-134a (CF_3CH_2F), in samples from Mace Head (left graph) and the Taunus Observatory (right graph). All three instruments agree very well, mostly within the 1-fold error bar. The comparison to the external instrument, the Medusa GC-MS, involves different calibration gases which are based on the same primary calibration scale but involve different chains of intercalibration which are a potential error source. The good agreement is therefore a very satisfying result as it confirms the correct propagation of mixing ratios from primary to secondary and tertiary calibration gases.
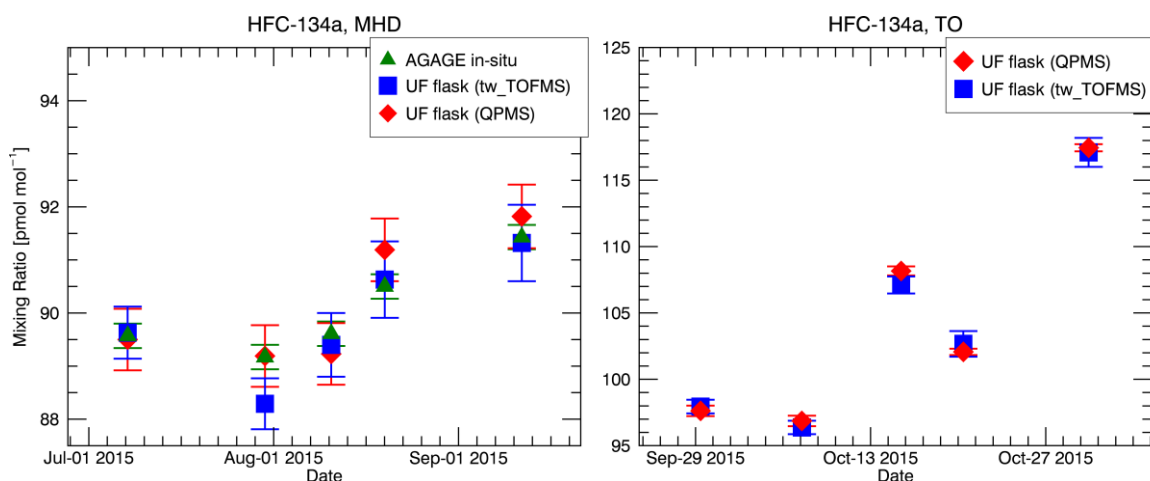
Figure 19. HFC-134a mixing ratios at MHD (left plot) and TO (right plot). Primary calibration scale, all instruments: SIO-05. Sampling: 2 L stainless steel flasks, ~4 bar abs. Blue squares: GC-TOFMS (FASTOF), red diamonds: GC-QPMS; our reference instrument, green triangles: in-situ data of the Medusa GC-MS at MHD (hourly sampling, value selected ± 1 hour around the time of flask filling). Error bars: 1-fold measurement precision of each instrument. Medusa system: typical precision taken from Miller et al. (2008). MHD samples were collected at meteorological background conditions, which implies that the elevated concentrations observed at TO resemble tropospheric sources of HFC-134a in the direction of air mass transport towards TO.

In comparison to the GC-QPMS laboratory setup, precision of the FASTOF instrument is comparable and also stable over time (multiple measurement series). It is furthermore sufficient to cover e.g. trends of CFCs in the atmosphere with only a few exceptions like CFC-114 and the comparison of absolute values (Obersteiner et al., 2016b, section 4.1 and Figure 19 of this work) ascertains a high level of accuracy. However, overall precision stays slightly below that of the laboratory GC-QPMS instrument despite a higher degree of automation of the FASTOF instrument. In contrast to the comparison of QPMS and BenchTOF-dx in Hoker et al., 2015, it is impossible here to determine if this difference in precision is only detector-related or if other parts of the instrumental setup, e.g. GC or preconcentration, play a major role. Similar to the BenchTOF-dx, a correlation of sample water content and measurement precision was found – the more water, the worse precision. This applies especially to analytes that have retention times around or greater than water. The correlation of water content and precision in combination with a detector that is very sensitive towards water directs attention to the sample drying method. Heated magnesium perchlorate removes most of the water while interfering only marginally with other sample components and is therefore well-suited in general. However, the drying process gradually reaches saturation if the sample water content is too high or the sample

44

volume that is dried is too large. Measurement precision in general is correlated with the signal-to-noise ratio of the chromatographic signal of an analyte; the higher *S/N*, the better precision. This is however only true below a specific preconcentration volume (approximately 1 L), above which e.g. the effect of water as discussed above begins to deteriorate precision. A remaining issue of the TOFMS is non-linearity. In case of the Tofwerk TOFMS, the source of the non-linearity could be identified in cooperation with the manufacturer and corrected by means of data processing. This is a big step forward compared to the state of understanding described in Hoker et al., 2015. A hardware-based method to solve the issue would be preferable and is a task for the manufacturer of the TOFMS.

2.4.6 Future development

Possible future applications of the GC-TOFMS instrument include a field deployment at the Taunus Observatory, Kleiner Feldberg, Germany. A ground-based field application could deliver important insights for another, aircraft-based application of TOFMS for online trace gas analysis. Online measurements inherit a significant difference compared to flask measurements: flasks mostly contain enough gas for a repeated analysis; an online sample can only be measured once. Therefore, measurement performance under these circumstances would have to be assessed before field deployment. Field tests would have to include instrument stability analysis under "non-laboratory" conditions, i.e. the response of the analytical system to changes in ambient temperature, humidity etc. A hardware limitation of the current setup is the sample stream selection manifold, which suffers from a very limited input pressure range (max. 4 bar abs.) and more importantly valve leakage, which was verified for helium already at 2.5 bar abs. input pressure at certain ports. For field application, a revision of the sampling manifold would therefore be desirable to ensure high measurement precision. The online sampling manifold would have to include a sample dryer that can be flushed with a specific amount of sample air before preconcentration. Hardware control, currently based on a LabVIEW realtime system that utilizes the LabVIEW Scan Engine for read/write operations of input/output variables could be improved in terms of control cycle speed and processing efficiency by programming the FPGA of the cRIO chassis.

3 Summary and outlook

The aim of this thesis was to establish the technique of time-of-flight mass spectrometry for the analysis of presence and quantity of halogenated trace gases in air. Anthropogenic release of substances from this species class to the atmosphere and the ensuing chemical and physical interaction of these substances (and their degradation products) with stratospheric ozone and the radiative budget of the atmosphere demand monitoring and regulation. The consequential need for atmospheric observations was recently summarised very well by Stephen A. Montzka: "Understanding the effectiveness of policies controlling GHGs and ODSs requires atmospheric observations of a suite of trace gases such as those provided by global sampling networks.", Montzka et al. (2015), p. 4447. To keep up with the introduction of new compounds to the atmosphere and at the same time cover small trends of persistent compounds reliably, sophisticated instrumental analytics are required. Moreover, considering the vast amount of species found in a sample of tropospheric air, the conventional method of quadrupole mass spectrometry seems outdated as it cannot monitor the full mass spectrum and be sensitive enough to quantify species in the ppt to ppq concentration range at the same time. In most applications it is therefore tuned to monitor specific molecule signals; thus making it unresponsive towards other signals at that time. In contrast, the inherent full mass range data acquisition of a time-of-flight mass spectrometer (TOFMS) would make it ideally suited for this task, provided that sensitivity, precision, accuracy and dynamic range are sufficient. Consequently, the task of this work was to set up a GC-TOFMS that fulfils these requirements and to demonstrate the general suitability of the technique through the application to air sample analysis.

A new analytical instrument was set up; comprised of sample stream selection, sample preconcentration and state-of-the-art gas chromatograph (GC) and TOFMS. For possible remote-site monitoring application in the future, the setup should be fully automated and field deployable. While GC and TOFMS could be acquired on the market after thorough survey, the sample preconcentration unit could not and was therefore self-built, based on the experience from the Master's thesis of the author (Obersteiner, 2012). The experience gained in the comparison of TOFMS and the "classical" detection technique quadrupole MS (QPMS) which was also J. Hoker's dissertation topic (Hoker, 2015), delivered im-

portant insights for the selection of a suitable TOFMS and its implementation in the analytical system. Results obtained in the course of this work were presented in three publications, treating (i) the preconcentration method, (ii) the comparison of QPMS and TOFMS and (iii) the performance of the newly assembled GC-TOFMS instrument. Chronologically, they were published in the order (ii), (iii), (i); the performance of the preconcentration method could thereby be assessed over a longer period of time and on different instruments.

In the first publication, the design, characterisation and application of a single stage, direct injecting preconcentration - thermodesorption unit is presented (Obersteiner et al., 2016b). The setup is unique in terms of the used cooling technique, a Stirling cooler, which allows a purely electrical operation. The independence from the supply of a liquid cryogen without having to compromise preconcentration temperatures of $< -80\,°C$ in combination with a compact and light-weight design makes the setup ideally suited for remote field application wherever electrical power is available. The reliability of operation is best assured by thousands of measurements conducted with the unit installed in the aircraft instrument GhOST-MS. Characterisation results furthermore attest the applicability to high-precision analysis of halogenated trace gases by absent or insignificant blank residues of analytes. While sample preconcentration is essential for the analysis of very low-concentrated species like many halogenated trace gases, the method is in principal also applicable to other compound classes like volatile hydrocarbons as well as upstream of other detection methods than a mass spectrometer (e.g. a flame ionisation detector). Furthermore, the substance range could likely be extended to more volatile species (e.g. CF_4 or C_2F_6) by the introduction of a CO_2-removal technique before preconcentration.

The first laboratory setup of the preconcentration unit was used in the second publication for the comparison of a TOFMS, the Almsco BenchTOF-dx (model E24; now distributed by Markes), with a state-of-the-art QPMS as reference (Hoker et al., 2015). Both detectors ran in parallel, connected to a split downstream of the GC. This makes the comparison independent from the influence of e.g. sample preconcentration or gas chromatography on investigated quantities like measurement precision. The BenchTOF-dx turned out to be outstandingly sensitive, comparable to a QPMS monitoring the signal of only one specific molecule fragment. The improvement compared to QPMS is of course the

full mass range data. In theory, mass resolving power of the MS also allows to gain additional selectivity by the separation of neighbouring signals from ions of equal nominal but differing exact mass. This was however not possible with the BenchTOF-dx due to limited mass resolution ($m/\Delta m < 1000$) and restricted data access, unsuited for a scientific application. The BenchTOF-dx delivered reproducible results over time, comparable to that of the QPMS, let aside some down-time due to technical difficulties. A big disadvantage of this TOFMS was found in significant non-linear response, rendering it unsuited for a straight-forward, quantitative analysis in the described application, which however might be negligible in another field of application. Unsatisfyingly, up to now no reliable method for their correction was found.

Both downsides of the BenchTOF-dx could by conquered with the GC-TOFMS setup *FASTOF* (fully automated in-situ GC-TOFMS), which became operational end 2014 (Obersteiner et al., 2016a). The TOFMS from Tofwerk AG, Switzerland, inherits a significantly higher mass resolving power of $m/\Delta m$ ~4000, completely accessible data and neither significant non-linearity after data processing nor detector saturation up to a pre-concentration volume of 10 L for the investigated species. Although a non-linear response was found under certain circumstances, its source was identified and the signal disturbance causing non-linear response is corrected by a straight-forward approach. At the same time, the instrument shows measurement precision comparable to the QPMS used as a benchmark for the BenchTOF-dx as well as high sensitivity that is significantly enhanced by the selectivity gained from mass resolution. The higher price of the Tofwerk TOFMS compared to the Almsco instrument is therefore justified from this perspective. In addition, full automation and reliable operation significantly reduce efforts needed to conduct measurement series – the time saved can be invested in data evaluation where it is actually needed. The design of the overall setup allows possible ground-based field application in the future.

Overall, TOFMS has proven to be a very valuable new tool in the field of atmospheric halocarbon research. The large substance range due to the full mass range spectra and the possibility to identify unknown chromatographic signals with ease thanks to the good mass resolving power are very valuable features of this technique. Despite some new limitations that were indiscernible with the QPMS like the sensitivity towards CO_2 and H_2O, the advantageous features are backed up by high precision and sensitivity as well

as, in case of the Tofwerk instrument, large dynamic range and linear response presuming dedicated data processing. Measurement accuracy was verified by cross-comparison experiments to both in-house and external instruments.

The working group of Prof. A. Engel has so far been the only one worldwide that published the application of TOFMS in this field of research, i.e. the quantitative analysis of halogenated trace gases in ambient air. To further promote this analytical technology, the next step would be field deployment for in-situ monitoring of halogenated trace gases in air masses, e.g. ground-based observations at Taunus Observatory, Kleiner Feldberg, Germany. As there is no monitoring station equipped for this task in Germany yet, this could be a big step forward for the surveillance of halogenated greenhouse gases as well as ozone depleting substances. A combination of site measurement data with inverse modelling (e.g. Keller et al., 2011; Lunt et al., 2015; Stohl et al., 2009) would in this case be desirable. The vast amount of traceable species in each GC-TOFMS measurement call for a higher degree of automation in data processing. IAU_Chrom, the self-written software used to integrate chromatographic signals, has been applied and improved over the last years and can now be considered out of "beta" stage. However, a programmatic solution to go from peak area to mixing ratio will be needed in the future, especially if a database of in-situ measurement data should be created. In addition to the analysis of known species, TOFMS data offers the possibility to analyse signals that were unknown at the time of measurement in retrospect. Provided that the signal is chromatographically resolved, present in the calibration gas and detector response is linear, an approximate calibration could be achieved, making the TOFMS data a "digital air archive" (see also Hoker, 2015). Although this cannot replace "real" air sample archives like e.g. the Cape Grim Archive (cryogenically collected, high pressure samples of atmospheric background air; e.g. Fraser et al., 1999; Laube et al., 2014; Oram et al., 1995), it is much cheaper in maintenance and requires only the space of a few hard drives. Future applications of GC-TOFMS could also include aircraft operation, where the large substance range would be a key improvement and time resolution could benefit from the high spectra rates possible with the TOFMS.

References

Andreae, M. O., Atlas, E., Harris, G. W., Helas, G., de Kock, A., Koppmann, R., Maenhaut, W., Manø, S., Pollock, W. H., Rudolph, J., Scharffe, D., Schebeske, G., and Welling, M.: Methyl halide emissions from savanna fires in Southern Africa, J. Geophys. Res., 101, 23603, doi: 10.1029/95jd01733, 1996.

Bais, A. F., Lubin, D. (Lead Authors), Arola, A., Bernhard, G., Blumthaler, M., Chubarova, N., Erlick, C., Gies, H. P., Krotkov, N., Lantz, K., Mayer, B., McKenzie, R. L., Piacentini, R. D., Seckmeyer, G., Slusser, J. R., and Zerefos, C. S. (Coauthors): Surface ultraviolet radiation: Past, present, and future. Chapter 7 in: Scientific Assessment of Ozone Depletion: 2006, Global Ozone Research and Monitoring Pproject Report No. 50., World Meteorological Organization (WMO), Geneva, Switzerland, 58 pp., 2007.

Bassford, M. R., Simmonds, P. G., and Nickless, G.: An automated system for near-real-time monitoring of trace atmospheric halocarbons, Anal. Chem., 70, 958-965, doi: 10.1021/ac970861z, 1998.

Bekki, S., Bodeker, G. E. (Coordinating Lead Autorhs), Bais, A. F., Butchart, N., Eyring, V., Fahey, D. W., Kinnison, D. E., Langematz, U., Mayer, B., Portmann, R. W., Rozanov, E. (Lead Authors), Braesicke, A. J., Charlton-Perez, N. E., Chubarova, I., B., C. S., Diaz, N. P., Gillett, M. A., Giorgetta, P., Komala, N., Lefèvre, F., McLandress, (Coauthors), Perlwitz, J., Peter, T., and Shibata, K. C.: Future ozone and its impact on surface UV. Chapter 3 in: Scientific Assessment of Ozone Depletion: 2010, Global Ozone Research and Monitoring Pproject Report No. 52, World Meteorological Organization (WMO), Geneva, Switzerland, 2011.

Bönisch, H.: Untersuchung des Transports in der Untersten Stratosphäre anhand von in-situ Messungen langlebiger Spurengase, Dissertation, Goethe Universität Frankfurt am Main, Frankfurt am Main, 188 pp., 2005.

Bönisch, H., Engel, A., Curtius, J., Birner, T., and Hoor, P.: Quantifying transport into the lowermost stratosphere using simultaneous in-situ measurements of SF_6 and CO_2, Atmos. Chem. Phys., 9, 5905-5919, doi: 10.5194/acp-9-5905-2009, 2009.

Bonk, T. and Humeny, A.: Maldi-TOF-MS analysis of protein and DNA, The Neuroscientist, 7, 6-12, 2001.

Brewer, A. W.: Evidence for a world circulation provided by the measurements of helium and water vapour distributions in the stratosphere, Q. J. Roy. Meteor. Soc., 75, 351-363, doi: 10.1002/qj.49707532603, 1949.

Brinckmann, S.: Short-lived brominated gases: Observations from source regions to the stratosphere, Dissertation, Goethe Universität Frankfurt am Main, Frankfurt am Main, 2011.

Bruner, F., Crescentini, G., Mangani, F., Brancaleoni, E., Cappiello, A., and Ciccioli, P.: Determination of halocarbons in air by gas chromatography-high resolution mass spectrometry, Anal. Chem., 53, 798-801, doi: 10.1021/ac00229a013, 1981.

Bujok, O., Tan, V., Klein, E., Nopper, R., Bauer, R., Engel, A., Gerhards, M.-T., Afchine, A., McKenna, D. S., Schmidt, U., Wienhold, F. G., and Fischer, H.: GHOST – a novel airborne gas chromatograph for in situ measurements of long-lived tracers in the lower stratosphere: Method and applications, J. Atmos. Chem., 39, 37-64, doi: 10.1023/A:1010789715871, 2001.

Burkholder, J. B., Cox, R. A., and Ravishankara, A. R.: Atmospheric degradation of ozone depleting substances, their substitutes, and related species, Chem. Rev. (Washington, DC, U. S.), 115, 3704-3759, doi: 10.1021/cr5006759, 2015.

Butler, J. H., Battle, M., Bender, M. L., Montzka, S. A., Clarke, A. D., Saltzman, E. S., Sucher, C. M., Severinghaus, J. P., and Elkins, J. W.: A record of atmospheric halocarbons during the twentieth century, Nature, 399, 749-755, doi: 10.1038/21586, 1999.

Cameron, A. E. and Eggers, D. F.: An ion "velocitron", Rev. Sci. Instrum., 19, 605, doi: 10.1063/1.1741336, 1948.

References

Carpenter, L. J., Reimann, S. (Lead Authors), Burkholder, J. B., Clerbaux, C., Hall, B. D., Hossaini, R., Laube, J. C., and Yvon-Lewis, S. A. (Coauthors): Ozone-depleting substances (ODSs) and other gases of interest to the montreal protocol. Chapter 1 in: Scientific Assessment of Ozone Depletion: 2014, Global Ozone Research and Monitoring Pproject Report No. 55., World Meteorological Organization (WMO), Geneva, Switzerland, 105 pp., 2014.

Chapman, S.: A theory of upper-atmospheric ozone, Mem. Roy. Meteor. Soc., 3, 1930.

Chernushevich, I. V., Loboda, A. V., and Thomson, B. A.: An introduction to quadrupole-time-of-flight mass spectrometry, J. Mass Spectrom., 36, 849-865, doi: 10.1002/jms.207, 2001.

Clemons, C. A. and Altshuller, A. P.: Responses of electron-capture detector to halogenated substances, Anal. Chem., 38, 133-136, doi: 10.1021/ac60233a039, 1966.

Clerbaux, C., Cunnold, D. M. (Lead Authors), Anderson, J., Engel, A., Fraser, P. J., Mahieu, E., Manning, A., Miller, J., Montzka, S. A., Nassar, R., Prinn, R., Reimann, S., Rinsland, C. P., Simmonds, P., Verdonik, D., Weiss, R., Wuebbles, D., and Yokouchi, Y. (Coauthors): Long-lived compounds. Chapter 1 in: Scientific Assessment of Ozone Depletion: 2006, Global Ozone Research and Monitoring Pproject Report No. 50., World Meteorological Organization (WMO), Geneva, Switzerland., 63 pp., 2007.

Crescentini, G., Mangani, F., Mastrogiacomo, A. R., and Bruner, F.: Calibration method for the gas chromatographic analysis of halocarbons in atmospheric samples using permeation tubes and an electron-capture detector, J. Chromatogr. A, 204, 445-451, doi: 10.1016/s0021-9673(00)81691-x, 1981.

Cronn, D. R. and Harsch, D. E.: Determination of atmospheric halocarbon concentrations by gas chromatography-mass spectrometry, Anal. Lett., 12, 1489-1496, doi: 10.1080/00032717908082548, 1979.

Crutzen, P. J.: The influence of nitrogen oxides on the atmospheric ozone content, Q. J. Roy. Meteor. Soc., 96, 320-325, doi: 10.1002/qj.49709640815, 1970.

Djozan, D. and Assadi, Y.: Optimization of the gas stripping and cryogenic trapping method for capillary gas-chromatographic analysis of traces of volatile halogenated compounds in drinking-water, J. Chromatogr. A, 697, 525-532, doi: Doi 10.1016/0021-9673(94)00980-N, 1995.

Douglass, A., Fioletov, V. (Lead Authors), Godin-Beekmann, S., Müller, R., Stolarski, R. S., Webb, A. L. A., Arola, A., Burkholder, J. B., Burrows, J. P., Chipperfield, M. P., Cordero, R., David, C., den Outer, P. N., Diaz, S. B., Flynn, L. E., Hegglin, M., Herman, J. R., Huck, P., Janjai, S., Jánosi, I. M., Krzy´scin, J. W., Liu, Y., Logan, J., Matthes, K., McKenzie, R. L., Muthama, N. J., Petropavlovskikh, I., Pitts, M., Ramachandran, S., Rex, M., Salawitch, R. J., Sinnhuber, B.-M., Staehelin, J., Strahan, S., Tourpali, K., Valverde-Canossa, J., and Vigouroux, C. (Coauthors): Stratospheric ozone and surface ultraviolet radiation. Chapter 2 in: Scientific Assessment of Ozone Depletion: 2010, Global Ozone Research and Monitoring Pproject Report No. 52, World Meteorological Organization (WMO), Geneva, Switzerland, 80 pp., 2011.

Drewnick, F., Hings, S. S., DeCarlo, P. F., Jayne, J. T., Gonin, M., Fuhrer, K., Weimer, S., Jimenez, J. L., Demerjian, K. L., Borrmann, S., and Worsnop, D. R.: A new time-of-flight aerosol mass spectrometer (TOF-AMS) - instrument description and first field deployment, Aerosol Sci. Technol., 39, 637-658, doi: 10.1080/02786820500182040, 2005.

Elkins, J., Moore, F., and Kline, E.: Update: New airborne gas chromatograph for NASA airborne platforms, NASA Earth Science Technology Conference 2001, University of Maryland, 2002.

Elkins, J. W., Fahey, D. W., Gilligan, J. M., Dutton, G. S., Baring, T. J., Volk, C. M., Dunn, R. E., Myers, R. C., Montzka, S. A., Wamsley, P. R., Hayden, A. H., Butler, J. H., Thompson, T. M., Swanson, T. H., Dlugokencky, E. J., Novelli, P. C., Hurst, D. F., Lobert, J. M., Ciciora, S. J., McLaughlin, R. J., Thompson, T. L., Winkler, R. H., Fraser, P. J., Steele, L. P., and Lucarelli, M. P.: Airborne gas chromatograph for in situ measurements of long-lived species in the upper troposphere and lower stratosphere, Geophys. Res. Lett., 23, 347-350, doi: 10.1029/96gl00244, 1996.

References

Engel, A., Mobius, T., Bonisch, H., Schmidt, U., Heinz, R., Levin, I., Atlas, E., Aoki, S., Nakazawa, T., Sugawara, S., Moore, F., Hurst, D., Elkins, J., Schauffler, S., Andrews, A., and Boering, K.: Age of stratospheric air unchanged within uncertainties over the past 30 years, Nature Geoscience, 2, 28-31, doi: 10.1038/ngeo388, 2009.

Engel, A., Strunk, M., Muller, M., Haase, H. P., Poss, C., Levin, I., and Schmidt, U.: Temporal development of total chlorine in the high-latitude stratosphere based on reference distributions of mean age derived from CO_2 and SF_6, J. Geophys. Res.-Atmos., 107, doi: 10.1029/2001jd000584, 2002.

Eyer, S., Tuzson, B., Popa, M. E., van der Veen, C., Röckmann, T., Rothe, M., Brand, W. A., Fisher, R., Lowry, D., Nisbet, E. G., Brennwald, M. S., Harris, E., Zellweger, C., Emmenegger, L., Fischer, H., and Mohn, J.: Real-time analysis of $\delta^{13}C$- and δD-CH_4 in ambient air with laser spectroscopy: Method development and first intercomparison results, Atmos. Meas. Tech., 9, 263-280, doi: 10.5194/amt-9-263-2016, 2016.

Fabian, P., Borchers, R., Penkett, S. A., and Prosser, N. J. D.: Halocarbons in the stratosphere, Nature, 294, 733-735, doi: 10.1038/294733a0, 1981.

Fahey, D. W. and Hegglin, M. I.: Twenty questions and answers about the ozone layer: 2010 update. In: Scientific Assessment of Ozone Depletion: 2010, Global Ozone Research and Monitoring Pproject Report No. 52, World Meteorological Organization (WMO), Geneva, Switzerland, 68 pp., 2011.

Farman, J. C., Gardiner, B. G., and Shanklin, J. D.: Large losses of total ozone in Antarctica reveal seasonal ClO_x/NO_x interaction, Nature, 315, 207-210, doi: 10.1038/315207a0, 1985.

Finnigan, R. E.: Quadrupole mass spectrometers, Anal. Chem., 66, 969A-975A, doi: 10.1021/ac00091a002, 1994.

Forster, P. M., Thompson, D. W. J. (Coordinating Lead Authors), Baldwin, M. P., Chipperfield, M. P., Dameris, M., Haigh, J. D., Karoly, D. J., Kushner, P. J., Randel, W. J., Rosenhof, K. H., Seidel, D. J., Solomon, S. (Lead Authors), Beig, G., Braesicke, P., Butchart, N., Gillett, N. P., Grise, K. M., Marsh, D. R., McLandress, C., Rao, T. N., Son, S.-W., Stechikov, G. L., and Yoden, S. (Coauthors): Stratospheric changes and climate. Chapter 4 in: Scientific Assessment of Ozone Depletion: 2010, Global Ozone Research and Monitoring Pproject Report No. 52, World Meteorological Organization (WMO), Geneva, Switzerland, 2011.

Fraser, P. J., Oram, D. E., Reeves, C. E., Penkett, S. A., and McCulloch, A.: Southern hemispheric halon trends (1978–1998) and global halon emissions, J. Geophys. Res., 104, 15985, doi: 10.1029/1999jd900113, 1999.

Gohlke, R. S.: Time-of-flight mass spectrometry. Application to capillary column gas chromatography, Anal. Chem., 34, 1332-1333, doi: 10.1021/ac60190a002, 1962.

Goldan, P. D., Kuster, W. C., Albritton, D. L., and Schmeltekopf, A. L.: Stratospheric $CFCl_3$, CF_2Cl_2, and N_2O height profile measurements at several latitudes, J. Geophys. Res., 85, 413, doi: 10.1029/JC085iC01p00413, 1980.

Gostlow, B., Robinson, A. D., Harris, N. R. P., O'Brien, L. M., Oram, D. E., Mills, G. P., Newton, H. M., Yong, S. E., and A Pyle, J.: µDIRAC: An autonomous instrument for halocarbon measurements, Atmos. Meas. Tech., 3, 507-521, doi: 10.5194/amt-3-507-2010, 2010.

Gribble, G. W.: Naturally occurring organohalogen compounds--a survey, J. Nat. Prod., 55, 1353-1395, doi: 10.1021/np50088a001, 1992.

Grimsrud, E. P. and Rasmussen, R. A.: The analysis of chlorofluorocarbons in the troposphere by gas chromatography-mass spectrometry, Atmos. Environ., 9, 1010-1013, doi: 10.1016/0004-6981(75)90021-9, 1975.

Guilhaus, M.: Special feature: Tutorial. Principles and instrumentation in time-of-flight mass spectrometry, J. Mass Spectrom., 30, 1519-1532, doi: 10.1002/jms.1190301102, 1995.

References

Guilhaus, M., Selby, D., and Mlynski, V.: Orthogonal acceleration time-of-flight mass spectrometry, Mass Spectrom. Rev., 19, 65-107, doi: 10.1002/(SICI)1098-2787(2000)19:2<65::AID-MAS1>3.0.CO;2-E, 2000.

Hartmann, D. L., Klein-Tank, A. M. G., Rusticucci, M., Alexander, L. V., Brönnimann, S., Charabi, Y., Dentener, F. J., Dlugokencky, E. J., Easterling, D. R., Kaplan, A., Soden, B. J., Thorne, P. W., Wild, M., and Zhai, P. M.: Observations: Atmosphere and surface. In: Climate Change 2013: The Physical Science Basis. Contribution of Working Group I to the fifth Assessment Report of the Intergovernmental Panel on Climate Change, Cambridge, United Kingdom and New York, NY, USA, 2013.

Helmig, D.: Air analysis by gas chromatography, J. Chromatogr. A, 843, 129-146, doi: 10.1016/s0021-9673(99)00173-9, 1999.

Highwood, E. J. and Shine, K. P.: Radiative forcing and global warming potentials of 11 halogenated compounds, J. Quant. Spectorsc. Ra., 66, 169-183, doi: 10.1016/s0022-4073(99)00215-0, 2000.

Hodnebrog, Ø., Etminan, M., Fuglestvedt, J. S., Marston, G., Myhre, G., Nielsen, C. J., Shine, K. P., and Wallington, T. J.: Global warming potentials and radiative efficiencies of halocarbons and related compounds: A comprehensive review, Rev. Geophys., 51, 300-378, doi: 10.1002/rog.20013, 2013.

Hoker, J.: Charakterisierung eines GC-TOF-MS-systems zur Messung halogenierter Kohlenwasserstoffe, Dissertation, Goethe Universität Frankfurt am Main, Frankfurt am Main, 196 pp., 2015.

Hoker, J., Obersteiner, F., Bönisch, H., and Engel, A.: Comparison of GC/time-of-flight MS with GC/quadrupole ms for halocarbon trace gas analysis, Atmos. Meas. Tech., 8, 2195-2206, doi: 10.5194/amt-8-2195-2015, 2015.

Hu, Q., Noll, R. J., Li, H., Makarov, A., Hardman, M., and Graham Cooks, R.: The orbitrap: A new mass spectrometer, J. Mass Spectrom., 40, 430-443, doi: 10.1002/jms.856, 2005.

IPCC: In: Climate Change 2013: The Physical Science Basis. Contribution of Working Group I to the fifth Assessment Report of the Intergovernmental Panel on Climate Change, Cambridge, United Kingdom and New York, NY, USA, 2013.

Isidorov, V. A., Zenkevich, I. G., and Ioffe, B. V.: Volatile organic compounds in solfataric gases, J. Atmos. Chem., 10, 329-340, doi: 10.1007/bf00053867, 1990.

Keller, C. A., Hill, M., Vollmer, M. K., Henne, S., Brunner, D., Reimann, S., O'Doherty, S., Arduini, J., Maione, M., Ferenczi, Z., Haszpra, L., Manning, A. J., and Peter, T.: European emissions of halogenated greenhouse gases inferred from atmospheric measurements, Environ. Sci. Technol., 46, 217-225, doi: 10.1021/es202453j, 2011.

Keppler, F., Eiden, R., Niedan, V., Pracht, J., and Scholer, H. F.: Halocarbons produced by natural oxidation processes during degradation of organic matter, Nature, 403, 298-301, doi: 10.1038/35002055, 2000.

Kloss, C., Newland, M., Oram, D., Fraser, P., Brenninkmeijer, C., Röckmann, T., and Laube, J.: Atmospheric abundances, trends and emissions of CFC-216ba, CFC-216ca and HCFC-225ca, Atmosphere, 5, 420-434, doi: 10.3390/atmos5020420, 2014.

Lary, D. J.: Catalytic destruction of stratospheric ozone, J. Geophys. Res., 102, 21515, doi: 10.1029/97jd00912, 1997.

Laube, J. C.: Determination of the distribution of halocarbons in the tropical upper troposphere and stratosphere, Dissertation, Goethe Universität Frankfurt am Main, Frankfurt am Main, 2008.

Laube, J. C. and Engel, A.: First atmospheric observations of three chlorofluorocarbons, Atmos. Chem. Phys., 8, doi: 10.5194/acp-8-5143-2008, 2008.

Laube, J. C., Hogan, C., Newland, M. J., Mani, F. S., Fraser, P. J., Brenninkmeijer, C. A. M., Martinerie, P., Oram, D. E., Röckmann, T., Schwander, J., Witrant, E., Mills, G. P., Reeves, C. E., and Sturges, W. T.: Distributions, long term trends and emissions of four perfluorocarbons in remote parts of the atmosphere and firn air, Atmos. Chem. Phys., 12, 4081-4090, doi: 10.5194/acp-12-4081-2012, 2012.

References

Laube, J. C., Newland, M. J., Hogan, C., Brenninkmeijer, C. A. M., Fraser, P. J., Martinerie, P., Oram, D. E., Reeves, C. E., Röckmann, T., Schwander, J., Witrant, E., and Sturges, W. T.: Newly detected ozone-depleting substances in the atmosphere, Nature Geoscience, doi: 10.1038/ngeo2109, 2014. doi: 10.1038/ngeo2109, 2014.

Lee, J. M., Sturges, W. T., Penkett, S. A., Oram, D. E., Schmidt, U., Engel, A., and Bauer, R.: Observed stratospheric profiles and stratospheric lifetimes of HCFC-141b and HCFC-142b, Geophys. Res. Lett., 22, 1369-1372, doi: 10.1029/95gl01313, 1995.

Lovelock, J. E.: Electron absorption detectors and technique for use in quantitative and qualitative analysis by gas chromatography, Anal. Chem., 35, 474-481, doi: 10.1021/ac60197a038, 1963.

Lovelock, J. E. and Lipsky, S. R.: Electron affinity spectroscopy—a new method for the identification of functional groups in chemical compounds separated by gas chromatography1, J. Am. Chem. Soc., 82, 431-433, doi: 10.1021/ja01487a045, 1960.

Lovelock, J. E. and Watson, A. J.: Electron-capture detector, J. Chromatogr. A, 158, 123-138, doi: 10.1016/s0021-9673(00)89961-6, 1978.

Lunt, M. F., Rigby, M., Ganesan, A. L., Manning, A. J., Prinn, R. G., O'Doherty, S., Muhle, J., Harth, C. M., Salameh, P. K., Arnold, T., Weiss, R. F., Saito, T., Yokouchi, Y., Krummel, P. B., Steele, L. P., Fraser, P. J., Li, S., Park, S., Reimann, S., Vollmer, M. K., Lunder, C., Hermansen, O., Schmidbauer, N., Maione, M., Arduini, J., Young, D., and Simmonds, P. G.: Reconciling reported and unreported HFC emissions with atmospheric observations, Proc. Natl. Acad. Sci. U. S. A., 112, 5927-5931, doi: 10.1073/pnas.1420247112, 2015.

Mamyrin, B. A.: Time-of-flight mass spectrometry (concepts, achievements, and prospects), Int. J. Mass Spectrom., 206, 251-266, doi: 10.1016/S1387-3806(00)00392-4, 2001.

Mamyrin, B. A., Karataev, V. I., Shmikk, D. V., and Zagulin, V. A.: The mass-reflectron, a new nonmagnetic time-of-flight mass spectrometer with high resolution, Journal of Experimental and Theoretical Physics, 64, 1973.

Manney, G. L., Santee, M. L., Rex, M., Livesey, N. J., Pitts, M. C., Veefkind, P., Nash, E. R., Wohltmann, I., Lehmann, R., Froidevaux, L., Poole, L. R., Schoeberl, M. R., Haffner, D. P., Davies, J., Dorokhov, V., Gernandt, H., Johnson, B., Kivi, R., Kyro, E., Larsen, N., Levelt, P. F., Makshtas, A., McElroy, C. T., Nakajima, H., Parrondo, M. C., Tarasick, D. W., von der Gathen, P., Walker, K. A., and Zinoviev, N. S.: Unprecedented arctic ozone loss in 2011, Nature, 478, 469-475, doi: 10.1038/nature10556, 2011.

McDaniel, A. H., Cantrell, C. A., Davidson, J. A., Shetter, R. E., and Calvert, J. G.: The temperature dependent, infrared absorption cross-sections for the chlorofluorocarbons: CFC-11, CFC -12, CFC -13, CFC -14, CFC -22, CFC -113, CFC -114, and CFC -115, J. Atmos. Chem., 12, 211-227, doi: 10.1007/bf00048074, 1991.

Midgley, T.: From the periodic table to production, Ind. Eng. Chem., 29, 241-244, doi: 10.1021/ie50326a032, 1937.

Midgley, T. and Henne, A. L.: Organic fluorides as refrigerants, Ind. Eng. Chem., 22, 542-545, doi: 10.1021/ie50245a031, 1930.

Miller, B. R., Weiss, R. F., Salameh, P. K., Tanhua, T., Greally, B. R., Mühle, J., and Simmonds, P. G.: Medusa: A sample preconcentration and GC/MS detector system for in situ measurements of atmospheric trace halocarbons, hydrocarbons, and sulfur compounds, Anal. Chem., 80, 1536-1545, doi: 10.1021/ac702084k, 2008.

Molina, M. J. and Rowland, F. S.: Stratospheric sink for chlorofluoromethanes: Chlorine atom catalysed destruction of ozone, Nature, 249, 810-812, doi: 10.1038/249810a0, 1974.

References

Montzka, S. A., McFarland, M., Andersen, S. O., Miller, B. R., Fahey, D. W., Hall, B. D., Hu, L., Siso, C., and Elkins, J. W.: Recent trends in global emissions of hydrochlorofluorocarbons and hydrofluorocarbons: Reflecting on the 2007 adjustments to the montreal protocol, J. Phys. Chem. A, 119, 4439-4449, doi: 10.1021/jp5097376, 2015.

Montzka, S. A., Reimann, S. (Coordinating Lead Authors), Engel, A., Krüger, K., O'Doherty, S., Sturges, W. T. (Lead Authors), Blake, D., Dorf, M., Fraser, P., Froidevaux, L., Jucks, K., Kreher, K., Kurylo, M. J., Mellouki, A., Miller, J., Nielsen, O.-J., Orkin, V. L., Prinn, R. G., Rhew, R., Santee, M. L., Stohl, A., and Verdonik, D. (Coauthors): Ozone-depleting substances (ODSs) and related chemicals. Chapter 1 in: Scientific Assessment of Ozone Depletion: 2010, Global Ozone Research and Monitoring Pproject Report No. 52, World Meteorological Organization (WMO), Geneva, Switzerland, 108 pp., 2011.

Moore, F. L.: Balloonborne in situ gas chromatograph for measurements in the troposphere and stratosphere, J. Geophys. Res., 108, doi: 10.1029/2001jd000891, 2003.

Mühle, J., Huang, J., Weiss, R. F., Prinn, R. G., Miller, B. R., Salameh, P. K., Harth, C. M., Fraser, P. J., Porter, L. W., Greally, B. R., O'Doherty, S., and Simmonds, P. G.: Sulfuryl fluoride in the global atmosphere, J. Geophys. Res., 114, doi: 10.1029/2008jd011162, 2009.

Myhre, G., Shindell,. D. (Coordinating Lead Authors), Bréon, F.-M., Collins, W., Fuglestvedt, J., Huang, J., Koch, D., Lamarque, J.-F., Lee, D., Mendoza, B., Nakajima, T., Robock, A., Stephens, G., Takemura, T., and Zhang, H. (Lead Authors): Anthropogenig and natural radiadive forcing. In: Climate Change 2013: The Physical Science Basis. Contribution of Working Group I to the fifth Assessment Report of the Intergovernmental Panel on Climate Change, Cambridge, United Kingdom and New York, NY, USA, 2013.

NASA: Ozone hole watch, http://ozonewatch.gsfc.nasa.gov/monthly/SH.html, last access: Dec 16 2015.

NOAA-ESRL: Trends in atmospheric carbon dioxide, http://www.esrl.noaa.gov/gmd/ccgg/trends/#mlo, last access: Dec 14 2015.

Nowack, P. J., Abraham, N. L., Braesicke, P., and Pyle, J. A.: Stratospheric ozone changes under solar geoengineering: Implications for UV exposure and air quality, Atmos. Chem. Phys., 16, 4191-4203, doi: 10.5194/acp-16-4191-2016, 2016.

Obersteiner, F.: Development of a cryogenic sample enrichment system for the quantification of airborne halocarbons, Thesis (M.Sc.), Goethe Universität Frankfurt am Main, Frankfurt am Main, 108 pp., 2012.

Obersteiner, F., Bönisch, H., and Engel, A.: An automated gas chromatography time-of-flight mass spectrometry instrument for the quantitative analysis of halocarbons in air, Atmos. Meas. Tech., 9, 179-194, doi: 10.5194/amt-9-179-2016, 2016a.

Obersteiner, F., Bönisch, H., Keber, T., Doherty, S., and Engel, A.: A versatile, refrigerant-free cryofocusing-thermodesorption unit for preconcentration of traces gases in air, Atmospheric Measurement Techniques Discussions, doi: 10.5194/amt-2016-196, 2016b. 1-36, doi: 10.5194/amt-2016-196, 2016b.

Oram, D. E., Reeves, C. E., Penkett, S. A., and Fraser, P. J.: Measurements of HCFC-142b and HCFC -141b in the cape grim air archive: 1978–1993, Geophys. Res. Lett., 22, 2741-2744, doi: 10.1029/95GL02849, 1995.

Paul, W. and Steinwedel, H.: Notizen: Ein neues Massenspektrometer ohne Magnetfeld, Zeitschrift für Naturforschung A, 8, doi: 10.1515/zna-1953-0710, 1953.

Pawson, S., Steinbrecht, W. L. A., Charlton-Perez, A. J., Fujiwara, M., Karpechko, A. Y., Petropavlovskikh, I., Urban, J., and Weber, M. C.: Update on global ozone: Past, present, and future. Chapter 2 in: Scientific Assessment of Ozone Depletion: 2014, Global Ozone Research and Monitoring Project – Report No. 55, World Meteorological Organization (WMO), Geneva, Switzerland, 2014.

Ramanathan, V.: Greenhouse effect due to chlorofluorocarbons - climatic implications, Science, 190, 50-51, doi: 10.1126/science.190.4209.50, 1975.

References

Ramaswamy, V. (Coordinating Lead Author), Boucher, O., Haigh, D., Hauglustaine, D., Haywood, J., Myhre, G., Nakajima, T., Shi, G. Y., and Solomon, S. (Lead Authors): Radiative forcing of climate change. Chapter 6 in: Climate Change 2001: The Scientific Basis. Contribution of Working Group I to the third Assessment Report of the Intergovernmental Panel on Climate Change, Intergovernmental Panel on Climate Change, Cambridge, United Kingdom and New York, NY, USA, 68 pp., 2001.

Ravishankara, A. R., Turnipseed, A. A., Jensen, N. R., Barone, S., Mills, M., Howard, C. J., and Solomon, S.: Do hydrofluorocarbons destroy stratospheric ozone?, Science, 263, 71-75, doi: 10.1126/science.263.5143.71, 1994.

Riediger, O.: Entwicklung und Einsatz eines flugzeuggetragenen Instrumentes zur in situ-Messung langlebiger Spurengase in der Stratosphäre, Dissertation, Goethe Universität Frankfurt am Main, Frankfurt am Main, 294 pp., 2000.

Romashkin, P., Hurst, D., Elkins, J., Dutton, G., Fahey, D., Dunn, R., Moore, F., Myers, R., and Hall, B.: In situ measurements of long-lived trace gases in the lower stratosphere by gas chromatography, J. Atmos. Oc. Tech., 18, 1195-1204, 2001

Sala, S., Bönisch, H., Keber, T., Oram, D. E., Mills, G., and Engel, A.: Deriving an atmospheric budget of total organic bromine using airborne in situ measurements from the Western Pacific area during SHIVA, Atmos. Chem. Phys., 14, 6903-6923, doi: 10.5194/acp-14-6903-2014, 2014.

Schoenenberger, F., Vollmer, M. K., Rigby, M., Hill, M., Fraser, P. J., Krummel, P. B., Langenfelds, R. L., Rhee, T. S., Peter, T., and Reimann, S.: First observations, trends, and emissions of HCFC -31 (CH_2ClF) in the global atmosphere, Geophys. Res. Lett., 42, 7817-7824, doi: 10.1002/2015gl064709, 2015.

Simpson, W. R., Brown, S. S., Saiz-Lopez, A., Thornton, J. A., and Glasow, R.: Tropospheric halogen chemistry: Sources, cycling, and impacts, Chem Rev, 115, 4035-4062, doi: 10.1021/cr5006638, 2015.

Solomon, S.: Stratospheric ozone depletion: A review of concepts and history, Rev. Geophys., 37, 275, doi: 10.1029/1999rg900008, 1999.

Stohl, A., Seibert, P., Arduini, J., Eckhardt, S., Fraser, P., Greally, B. R., Lunder, C., Maione, M., Mühle, J., O'Doherty, S., Prinn, R. G., Reimann, S., Saito, T., Schmidbauer, N., Simmonds, P. G., Vollmer, M. K., Weiss, R. F., and Yokouchi, Y.: An analytical inversion method for determining regional and global emissions of greenhouse gases: Sensitivity studies and application to halocarbons, Atmos. Chem. Phys., 9, 1597-1620, doi: 10.5194/acp-9-1597-2009, 2009.

Stolarski, R. S. and Rundel, R. D.: Fluorine photochemistry in the stratosphere, Geophys. Res. Lett., 2, 443-444, doi: 10.1029/GL002i010p00443, 1975.

Sturges, W. T., Oram, D. E., Carpenter, L. J., Penkett, S. A., and Engel, A.: Bromoform as a source of stratospheric bromine, Geophys. Res. Lett., 27, 2081-2084, doi: 10.1029/2000gl011444, 2000.

Sturrock, G. A., Etheridge, D. M., Trudinger, C. M., Fraser, P. J., and Smith, A. M.: Atmospheric histories of halocarbons from analysis of antarctic firn air: Major Montreal Protocol species, J. Geophys. Res., 107, doi: 10.1029/2002jd002548, 2002.

Sulbaek Andersen, M. P., Nielsen, O. J., Wallington, T. J., Karpichev, B., and Sander, S. P.: Assessing the impact on global climate from general anesthetic gases, Anesth. Analg., 114, 1081-1085, doi: 10.1213/ANE.0b013e31824d6150, 2012.

Totterdill, A., Kovacs, T., Gomez Martin, J. C., Feng, W., and Plane, J. M.: Mesospheric removal of very long-lived greenhouse gases SF_6 and CFC-115 by metal reactions, lyman-alpha photolysis, and electron attachment, J. Phys. Chem. A, 119, 2016-2025, doi: 10.1021/jp5123344, 2015.

UNEP: Handbook for the montreal protocol on substances that deplete the ozone layer. United Nations Environment Programme (UNEP), Ozone Secretariat, Nairobi, Kenya, 2012a.

References

UNEP: Handbook for the vienna convention for the protection of the ozone layer. United
Nations Environment Programme (UNEP), Ozone Secretariat, Nairobi, Kenya,
2012b.

Velders, G. J., Andersen, S. O., Daniel, J. S., Fahey, D. W., and McFarland, M.: The
importance of the Montreal Protocol in protecting climate, Proc. Natl. Acad. Sci.
U. S. A., 104, 4814-4819, doi: 10.1073/pnas.0610328104, 2007.

Velders, G. J., Fahey, D. W., Daniel, J. S., McFarland, M., and Andersen, S. O.: The
large contribution of projected HFC emissions to future climate forcing, Proc.
Natl. Acad. Sci. U. S. A., 106, 10949-10954, doi: 10.1073/pnas.0902817106,
2009.

Vollmer, M. K., Reimann, S., Hill, M., and Brunner, D.: First observations of the fourth
generation synthetic halocarbons HFC-1234yf, HFC-1234ze(e), and HCFC-
1233zd(e) in the atmosphere, Environ. Sci. Technol., 49, 2703-2708, doi:
10.1021/es505123x, 2015.

Volz, A., Ehhalt, D. H., and Cosatto, H.: The vertical distribution of cfm and related
species in the stratosphere, Pure Appl. Geophys., 116, 545-553, doi:
10.1007/BF01636907, 1978.

Wallington, T. J., Sulbaek Andersen, M. P., and Nielsen, O. J.: Atmospheric chemistry of
short-chain haloolefins: Photochemical ozone creation potentials (POCPs), global
warming potentials (GWPs), and ozone depletion potentials (ODPs),
Chemosphere, 129, 135-141, doi: 10.1016/j.chemosphere.2014.06.092, 2015.

Wang, J.-L., Chang, C.-J., Chang, W.-D., Chew, C., and Chen, S.-W.: Construction and
evaluation of automated gas chromatography for the measurement of
anthropogenic halocarbons in the atmosphere, J. Chromatogr. A, 844, 259-269,
doi: 10.1016/s0021-9673(99)00395-7, 1999.

Weiss, R. F., Mühle, J., Salameh, P. K., and Harth, C. M.: Nitrogen trifluoride in the
global atmosphere, Geophys. Res. Lett., 35, doi: 10.1029/2008gl035913, 2008.

Wiley, W. C. and McLaren, I. H.: Time-of-flight mass spectrometer with improved resolution, Rev. Sci. Instrum., 26, 1150, doi: 10.1063/1.1715212, 1955.

WMO: Scientific Assessment of Ozone Depletion: 2010, Global Ozone Research and Monitoring Pproject Report No. 52, World Meteorological Organization (WMO), Geneva, Switzerland, 2011.

Wofsy, S. C., McElroy, M. B., and Yung, Y. L.: The chemistry of atmospheric bromine, Geophys. Res. Lett., 2, 215-218, doi: 10.1029/GL002i006p00215, 1975.

Wolff, M. M. and Stephens, W. E.: A pulsed mass spectrometer with time dispersion, Rev. Sci. Instrum., 24, 616-617, 1953.

Wollnik, H., Becker, R., Götz, H., Kraft, A., Jung, H., Chen, C. C., Van Ysacker, P. G., Janssen, H. G., Snijders, H. M. J., Leclercq, P. A., and Cramers, C. A.: A high-speed gas chromatograph coupled to a time-of-flight mass analyzer, Int. J. Mass Spectrom. Ion Processes, 130, L7-L11, doi: 10.1016/0168-1176(93)03938-i, 1994.

Woolfenden, E.: Sorbent-based sampling methods for volatile and semi-volatile organic compounds in air part 1: Sorbent-based air monitoring options, J Chromatogr A, 1217, 2674-2684, doi: 10.1016/j.chroma.2009.12.042, 2010.

Worton, D. R., Mills, G. P., Oram, D. E., and Sturges, W. T.: Gas chromatography negative ion chemical ionization mass spectrometry: Application to the detection of alkyl nitrates and halocarbons in the atmosphere, J Chromatogr A, 1201, 112-119, doi: 10.1016/j.chroma.2008.06.019, 2008.

Zubarev, R. A. and Makarov, A.: Orbitrap mass spectrometry, Anal. Chem., 85, 5288-5296, doi: 10.1021/ac4001223, 2013.

Section II: Publications

i. "A versatile, refrigerant-free cryofocusing – thermodesorption unit for the preconcentration of trace gases in air"

Own Contribution

Wrote the manuscript, which was proof-read by A. Engel, H. Bönisch, T. Keber and S. O'Doherty.

Developed the experimental design (characterisation), partly together with H. Bönisch, conducted the experiments and evaluated and prepared the results for the publication.

Designed the setup (excluding GhOST instrument) partly together with L. Merkel, and assembled the preconcentration unit.

Mechanical construction of individual parts was done by the workshop of the institute (F. Malkemper and L. Merkel).

1 **A versatile, refrigerant-free cryofocusing-thermodesorption**

2 **unit for preconcentration of traces gases in air**

3 F. Obersteiner[1], H. Bönisch[2], T. Keber[1], S. O'Doherty[3] and A. Engel[1]

4 [1] Institute for Atmospheric and Environmental Science, Goethe University Frankfurt,

5 Frankfurt, Germany

6 [2] Institute of Meteorology and Climate Research, KIT, Karlsruhe, Germany

7 [3] School of Chemistry, University of Bristol, Bristol, United Kingdom

8 *Correspondence to*: F. Obersteiner, obersteiner@iau.uni-frankfurt.de

9 **Abstract.** We present a compact and versatile cryofocusing-thermodesorption unit, which we

10 developed for quantitative analysis of halogenated trace gases in ambient air. Possible appli-

11 cations include aircraft-based in-situ measurements, in-situ monitoring and laboratory opera-

12 tion for the preconcentration of analytes from flask samples. Analytes are trapped on adsorp-

13 tive material cooled by a Stirling cooler to low temperatures (e.g. −80 °C) and desorbed sub-

14 sequently by rapid heating of the adsorptive material (e.g. +200 °C). The setup neither in-

15 volves exchange of adsorption tubes nor any further condensation or refocusation steps. No

16 moving parts are used that would require vacuum insulation. This allows a simple and robust

17 single-stage design. Reliable operation is ensured by the Stirling cooler, which does not re-

18 quire refilling of a liquid refrigerant while allowing significantly lower adsorption tempera-

19 tures compared to commonly used Peltier elements. We use gas chromatography - mass spec-

20 trometry for separation and detection of the preconcentrated analytes after splitless injection.

21 A substance boiling point range of approximately −80 °C to +150 °C and a substance mixing

22 ratio range of less than 1 ppt (pmol mol^{-1}) to more than 500 ppt in preconcentrated sample

23 volumes of 0.1 to 10 L of ambient air is covered, depending on the application and its analyti-

24 cal demands. We present the instrumental design of the preconcentration unit and demonstrate

25 capabilities and performance through the examination of injection quality, analyte break-

26 through and analyte residues in blank tests. Application examples are given by the analysis of

27 flask samples collected at Mace Head Atmospheric Research Station in Ireland using our la-

28 boratory GC-TOFMS instrument and by data obtained during a research flight with our in-situ

29 aircraft instrument GhOST-MS.

1   Introduction

Atmospheric trace gases introduced to or elevated in concentration in the environment by human activities often show adverse environmental impacts. Prominent examples are chlorofluorocarbons (CFCs) and their intermediate replacements, hydrochlorofluorocarbons (HCFCs), which deplete stratospheric ozone (Farman et al., 1985; Molina and Rowland, 1974; Montzka et al., 2011; Solomon, 1999). Present-day CFC-replacements, namely hydrofluorocarbons (HFCs), have zero ozone depletion potentials (ODPs) but are still potent greenhouse gases like CFCs and HCFCs (Hodnebrog et al., 2013; Velders et al., 2009). Another example are non-methane hydrocarbons (NMHCs), which produce harmful tropospheric ozone in the presence of nitrogen oxides (Haagen-Smit and Fox, 1956; Marenco et al., 1994; Monks et al., 2015).

Many of the species found in the compound classes named above show atmospheric concentrations too low for direct detection and quantification by means of instrumental analytics. Therefore, a preconcentration step is required. The method of cryofocusing-thermodesorption is a common technique for that purpose (e.g. Aragón et al., 2000; Demeestere et al., 2007; Dettmer and Engewald, 2003; Eyer et al., 2016; Hou et al., 2006). In principal, an ambient air sample from either a sample flask or continuous flow for online measurement is preconcentrated on adsorptive material at a specific adsorption temperature, T_A. If T_A is significantly below ambient temperature, this step is referred to as "cryofocusing" or "cryotrapping". Trapped analytes are re-mobilized subsequently by heating the adsorptive material to a desorption temperature T_D and flushed e.g. onto a gas chromatographic column with a carrier gas and detected with a suitable detector.

The primary motivation for the development of the instrumentation described in this manuscript was halocarbon analysis in ambient air. More specifically, there were no commercial instruments available which met the requirements of remote in-situ and aircraft operation: compact (as small as possible), lightweight (<5 kg), safe containment of working fluids and preferentially cryogen-free, pure electrical operation. Liquid cooling agents like liquid nitrogen (LN_2) or argon (LAr) (e.g. Apel et al., 2003; Farwell et al., 1979; Helmig and Greenberg, 1994) offer large cooling capacity but are difficult to operate on board of an aircraft due to safety restrictions and supply demand, e.g. when operating the aircraft from remote airports. Compression coolers (e.g. Miller et al., 2008; O'Doherty et al., 1993; Saito et al., 2010) offer less cooling capacity in terms of heat lift compared to liquid cooling agents and are relatively

Atmospheric
Measurement
Techniques
Discussions

1   large in size and weight compared to widespread Peltier type cooling options (Peltier ele-

2   ments; e.g. de Blas et al., 2011; Simmonds et al., 1995; commercial thermodesorbers available

3   from e.g. Markes or PerkinElmer). Peltier elements have the advantage of being very small

4   and requiring only electrical power for cooling. However, their cooling capacity and mini-

5   mum temperature cannot compete with compression- and refrigerant-based coolers. Stirling

6   coolers pose an in-between solution, well-suited for maintenance-free remote operation: like

7   Peltier coolers, they only require electrical power, do not contain any potentially dangerous

8   working fluids (only helium) or cryogens but have a significantly higher cooling capacity.

9   While not being as powerful as refrigerant-based coolers (LN_2, LAr), they still have compara-

10 ble minimum temperatures. To our knowledge, the use of Stirling coolers for similar purposes

11 like the one described here is rare with few published exceptions like the preconcentration of

12 methane by Eyer et al. (2016) or the trapping of CO_2 as a carbon capture technology by Song

13 et al. (2012).

14 The principal design of the cryofocusing-thermodesorption unit in description was developed

15 for the airborne in-situ instrument GhOST-MS (Gas chromatograph for the Observation of

16 Tracers – coupled with a Mass Spectrometer, Sala et al., 2014) and successfully used during

17 three research campaigns up to now – 2011: SHIVA (carrier aircraft: DLR FALCON), 2013:

18 TACTS (carrier aircraft: DLR HALO), 2015/2016: PGS (carrier aircraft: DLR HALO). To

19 extend the substance range, we then developed similar cryofocusing-thermodesorption units

20 for our other GC-MS instruments (Hoker et al., 2015; Obersteiner et al., 2016), which are

21 currently operated in the laboratory. Both detailed description and characterisation of the pre-

22 concentration unit were not discussed in the publications Hoker et al. (2015), Obersteiner et

23 al. (2016) (laboratory setups) and Sala et al. (2014) (aircraft instrument). Within this manu-

24 script, a general instrumental description is given in section 2, which is applicable for all the

25 named setups. Characterisation results discussed in section 3 are based on the latest version of

26 the laboratory setup (Obersteiner et al., 2016). To demonstrate the versatility and reliability of

27 the setup, application examples are given in section 4 for sample analysis in the laboratory as

28 well as in-situ aircraft operation. Results are summarized and conclusions are drawn in sec-

29 tion 5.

1   **2   Instrumentation**

2   This section gives a description of principal components of the sample preconcentration unit

3   and is valid for all our analytical setups presented in Sala et al. (2014), Hoker et al. (2015) and

4   Obersteiner et al. (2016). The following section 2.1 outlines the general measurement proce-

5   dure and gas flow as well as its integration into a chromatographic detection system. Sections

6   2.2 and 2.3 describe the implementation of the main operations of the unit; cooling ("trap-

7   ping", i.e. preconcentration of analytes) and heating (desorption of analytes). A preconcentra-

8   tion system can always only be as good as the analytical set-up behind it. The pre-

9   concentration system described here has been designed for the coupling with a chromato-

10   graphic system but in principle could also be adapted for coupling with other techniques. Spe-

11   cific technical components of the instrumentation used in this work to characterise the pre-

12   concentration unit will be listed in section 3.

13   **2.1   Measurement procedure and gas flow in GC application**

14   For the preconcentration of analytes, the sample is flushed through a micro packed column of

15   cooled adsorptive material. Analytes are "trapped" on the adsorptive material as the steady

16   state of adsorption and desorption is strongly shifted towards adsorption by the low tempera-

17   ture of the adsorptive material. By subsequent rapid heating of the adsorptive material, the

18   steady state is instantaneously shifted towards desorption ("thermodesorption"). Formerly

19   trapped analytes are flushed backwards onto the warm chromatographic column with a carrier

20   gas. There is no further refocusing or separation step, except for higher-boiling compounds on

21   the GC column itself. **Figure 1** shows a flow scheme of the setup. The outflow of the sample

22   loop during preconcentration ("stripped air"; mainly nitrogen and oxygen) is collected in a

23   previously evacuated reference volume for analyte quantification (2 L electro-polished stain-

24   less steel flask; volume determination by pressure difference). A mass flow controller (MFC)

25   is mounted between sample loop and reference volume for sample flow control. The MFC can

26   also be used for sample volume determination e.g. for sample volumes larger than the refer-

27   ence volume. Hardware control is implemented with a LabVIEW cRIO assembly (compact,

28   reconfigurable input output; National Instruments Inc., USA) using self-written control soft-

29   ware. It operates the preconcentration unit automatically, i.e. controls system parameters like

30   sample loop temperature by cooling and heating concomitant with system states like precon-

31   centration, desorption etc.

Atmospheric
Measurement
Techniques
Discussions

Open Access

2.2 Cryofocusing: sample loop and cooling technique

A stainless steel tube with 1/16" outer diameter (OD) and 1 mm inner diameter (ID) is used as sample loop. The tube is packed with adsorptive material and placed inside an aluminium cuboid ("coldhead") which is cooled continuously to maintain a specific adsorption temperature. **Figure 2** shows a technical drawing of sample loop and coldhead. The coldhead can contain two sample loops; in this case one of them is an empty stainless steel tube with 1/16 inch OD and 1 mm ID to characterize the sample loop heater. For that purpose, a thin temperature sensor is inserted into the empty tube. To save space and avoid mechanical, moving parts, the sample loop is not removed from the coldhead during desorption. It is insulated and thereby isolated electrically by two layers of glass silk and four layers of Teflon shrinking hose. The insulation is a variable parameter which determines the rate at which heat is exchanged between sample loop and coldhead. Consequently, it determines coldhead warm-up rate during desorption and sample loop cool-down rate after desorption. More insulation would result in longer cool-down time after desorption but also to less heat flowing into the cold head, thus to lower possible temperature of the cold head. The insulation used represents a compromise that works well for the application presented here but could potentially be improved by e.g. using a ceramic insulator. The coldhead itself is insulated towards surrounding air with 45 mm of Aeroflex HF material (Aeroflex Europe GmbH, Germany).

The Stirling cooler used for cooling offers the advantage of requiring only electrical power while providing a relatively large cooling capacity at very low minimum temperatures. The latter are comparable to liquid nitrogen in case of Sunpower CryoTel MT, CT and GT Stirling coolers, with maximum heat lifts of 5 W to 16 W at −196 °C according to the manufacturer. Heat that is removed from the coldhead by the Stirling cooler has to be released to the surrounding air; either directly by an air-fin heat rejection or indirectly by a water coolant system mounted to the cooler's warm side. The cooler should maintain a defined adsorption temperature T_A of the sample loop over the series of measurements. However, during thermodesorption, a certain amount of heat is transferred to the coldhead as the sample loop is kept directly inside with only a small amount of insulation. Excess heat has to be removed by the Stirling cooler to regain T_A for the preconcentration of the next sample. The preconcentration unit is attached to a gas chromatograph; therefore, the gas chromatographic runtime allows coldhead and sample loop to cool down after thermodesorption and return to T_A before preconcentrating the next sample.

1 Besides chromatographic runtime, various factors determine the minimum cycle time (i.e.

2 sample measurement frequency) including:

- targeted adsorption temperature T_A
- Stirling cooler's cooling capacity (i.e. heat lift around T_A) and coldhead insulation as well as ambient temperature
- thermodesorption duration and T_D as well as insulation of the sample loop
- volume of the sample to preconcentrate and preconcentration flow

3 To give a practical example, **Table 1** shows cycle times derived from routine operation data.

4 With the laboratory setup, a total time per measurement of 18.6 minutes is necessary if

5 $T_A = -120\ °C$ and $T_D \approx 200\ °C$ is desired – mainly determined by the time needed to compen-

6 sate the warm-up of the coldhead during desorption. This minimum time interval significantly

7 shortens to 8.5 minutes if T_A is increased to $-80\ °C$ (same T_D). Data from the in-situ setup

8 shown in **Table 1** demonstrates that even shorter cycle times of 4.1 minutes are possible with

9 a decreased preconcentration volume (100 mL instead of 500 mL; requiring a detector that is

10 sensitive enough) and a slightly higher T_A. General measures to increase the number of meas-

11 urements per time would be to increase the preconcentration flow, reduce the sample size (see

12 in-situ setup), improve the coldhead and sample loop insulation and increase the cooling ca-

13 pacity.

14 After desorption, sample loop temperature drops in an exponential decay shaped curve due to

15 the decreasing temperature difference between coldhead and sample loop. After a desorption

16 at $T_D \approx 200\ °C$, sample loop and coldhead temperature reached similar temperatures after ap-

17 proximately 30 s cool-down time ($T_A = -80\ °C$). The cool-down time increases to about 90 s

18 at $-120\ °C$ cold head temperature. Considering the total run times shown in (**Table 1**), sample

19 loop cool-down time is not a limiting factor to the overall cycle time. Consequently, thermal

20 insulation of the sample loop could still be increased, thereby decreasing coldhead warm-up

21 during desorption.

Atmospheric
Measurement
Techniques

Open Access

EGU

Discussions

1 **2.3 Thermodesorption: sample loop heater**

2 Depending on the targeted substance class to analyse and the analytical technique, the re-

3 quirements for thermodesorption will differ. In case of a gas chromatographic system for

4 analysis of volatile compounds, these requirements are:

5 • a fast initial increase in temperature to yield a sharp injection of highly volatile

6 analytes onto the GC column,

7 • no overshooting of a maximum temperature in case of thermally unstable sample

8 compounds or adsorptive material (e.g. HayeSep D, $T_D < 290 \,°C$)

9 • preservation of the desorption temperature over a time period for desorption of

10 analytes with higher boiling points

11 • good overall repeatability, especially of the injection of highly volatile analytes

12 Desorption heating is implemented by pulsing a direct current (max. 12 V / 40 A, relay:

13 Celduk Okpac; spec. switching frequency 1 kHz, Celduk Relays, France) directly through the

14 sample loop tubing which has a resistance of ~0.5 Ω. A temperature sensor (Pt100, 1.5 mm

15 OD) was welded to the outside of the sample loop tubing (see also **Figure 2**), for feedback

16 control of the heater temperature. However, mainly due to the thermal mass of the sensor and

17 its proximity to the coldhead (despite the insulation), it was found to give no representative

18 values for temperature inside the sample loop during desorption. Differences of around

19 100 °C were found in comparison to temperature measured within the sample loop (equilibri-

20 um state; after 2-3 minutes of continuous heating). Nevertheless, the temperature sensor can

21 be (after being characterised) used for feedback control as the indicated values are reproduci-

22 ble. As an alternative to feedback control, a deterministic heater with prescribed output set-

23 tings can be used. For security reason, measured coldhead and sample loop temperature have

24 to be used as heater shutdown triggers in this case.

25 **Figure 3** shows a comparison of temperature sensor data from in- and outside the empty sam-

26 ple loop as well as the coldhead. Very good results were achieved with a two-stage, determin-

27 istic heater setup with a fast heat-up, a small overshoot between stage 1 and 2 of the heating

28 phase and preservation of T_D with only a small drift and fluctuation. With the described heater

29 setup, T_D can be reached within a very short time of approximately 3 seconds. Initial heating

30 rates (first second of heat pulse) were calculated to be more than 200 °C s^{-1} depending on the

31 power output setting. As the sample loop is getting warmer, heating rate drops resulting in a

32 mean heating rate of about 80 °C s^{-1} during stage 1.

1   If a deterministic heater is used instead of a feedback controlled heater, sample loop tempera-

2   ture becomes directly dependent on coldhead temperature (more precisely: heat flow from the

3   sample loop into the coldhead). Consequently, higher output settings are necessary at lower

4   coldhead temperatures to achieve comparable temperatures. On the other hand, if the cold-

5   head gets warmer, sample loop temperature increases as well. This effect can be observed in

6   **Figure 3** as a slight upward drift of the sample loop temperature (red curve, temperature

7   measured within the sample loop) during stage 2. The absolute temperature differences caused

8   by this drift as well as the oscillation amplitude are small (approximately 20 °C min. to max.

9   and 4 °C standard deviation without trend correction) compared to the temperature difference

10   between coldhead and sample loop during heating (about 300 °C).

11   Besides the problem of differing inner and outer temperature of the sample loop during heat-

12   ing, temperature was not found to be distributed homogeneously alongside the empty sample

13   loop inside the coldhead. Temperature differences of up to ±30 °C at 200 °C mean tempera-

14   ture were observed with the current setup if measuring temperature at different points within

15   the sample loop, potentially due to (a) difficulties in accurately measuring the inner tempera-

16   ture (wall contact of sensor) and (b) inhomogeneity in sample loop insulation as well as varia-

17   tions in tubing wall width or carbon content leading to an inhomogeneous electrical resistance

18   and thus an inhomogeneous distribution of heat. These temperature variations might be differ-

19   ent or ideally negligible in the sample loop packed with adsorptive material. However, the

20   finding underlines the importance of an insulation as homogeneous as possible and suggests

21   that "cold points" (possibility of insufficient desorption) as well as "hot points" (possibility of

22   adsorptive material or analyte decomposition) are possible along the sample loop, which has

23   to be taken into consideration when setting up and testing the preconcentration setup, i.e. to

24   not exceed the temperature limit of the adsorptive material.

Atmospheric
Measurement
Techniques
Discussions

3 Characterisation

This section discusses characterisation results (section 3.2 and 3.3) obtained with the
GC-TOFMS instrument described in Obersteiner et al. (2016) as it covers the widest sub-
stances range (see supplementary information) and therefore allows the most differentiated
analysis. A brief description of this analytical instrument is given in the following section 3.1;
see Obersteiner et al. (2016) for details on GC and MS. We consider these results to be valid
in principle also for our other GC-MS setup discussed by Hoker et al. (2015) and the GhOST-
MS described by Sala et al. (2014) as all preconcentration setups rely on the same principal
setup and similar components are used.

3.1 Analytical instrument

A Sunpower CryoTel CT free piston Stirling cooler (Ametek Inc., USA) is used for cooling of
the coldhead. In the described setup, a water coolant system (Alphacool, Germany) originally
intended for cooling of a personal computer's processing units removes heat from the Stirling
cooler's heat rejection. Sunpower Stirling coolers are optionally also available with an air-fin
heat rejection that requires a continuous air stream during operation. For sample loop heater
control, a pulse-width modulation (PWM; 20 ms period, 1 µs minimum width) with a pre-
scribed output is used (deterministic heater; see section 2.3). Heater operation during desorp-
tion is separated into a short initial "heat-up" stage with a high output of the PWM and a
longer "hold" stage with lower heater output to maintain desorption temperature. The sample
loop is packed with adsorptive material over a length of approximately 100 mm (~20 mg).
Two different adsorptive materials were used in different sample loops installed in the course
of this work; HayeSep D, 80/100 mesh (VICI International AG, Switzerland) and
Unibeads 1S, 60/80 mesh (Grace, USA).

A Bronkhorst EL-FLOW F-201CM (Bronkhorst, the Netherlands) is used for sample flow
control (downstream of the sample loop in order to avoid contamination) in combination with
a Baratron 626 pressure sensor (0-1000 mbar, accuracy incl. non-linearity 0.25 % of reading,
MKS Instruments, Germany) for analyte quantification by pressure difference measurement.
An Agilent 7890 B gas chromatograph (GC) with a GS GasPro PLOT column (Agilent Tech-
nologies, Inc. USA; 0.32 mm inner diameter) using a ramped temperature program (45 °C to
200 °C with 25 °C min^{-1}) and backflush option is used for analyte separation. Purified helium
6.0 is used as carrier gas (Praxair Technologies Inc., German supplier; purification system:

Atmospheric
Measurement
Techniques
Open Access
Discussions

EGU

1   Vici Valco HP2). For analyte detection, a Tofwerk EI-TOF (model EI-003, Tofwerk AG,

2   Switzerland) mass spectrometer (MS) is attached to the GC. All samples are dried using mag-

3   nesium perchlorate kept at 80 °C prior to preconcentration. Artificial additions of analytes to

4   the sample from the dryer were excluded by comparing measurements of dried and undried

5   blank gas. All tubing upstream of the sample loop was heated to >100 °C to avoid substance

6   loss to tubing walls.

7   **Figure 4** shows a typical chromatogram from an ambient air sample for three selected

8   mass-to-charge ratios (m/Q). Two different adsorptive materials were used in the course of

9   this work (HayeSep D, Unibeads 1S) which showed partly differing adsorption and desorption

10   properties; results are discussed separately if appropriate. To achieve high measurement pre-

11   cision and minimum uncertainties introduced by the preconcentration unit, both the analyte

12   adsorption (preconcentration) and analyte desorption (injection) into the chromatographic

13   system have to be quantitative and repeatable. The following section describes tests and re-

14   sults for the characterisation of both aspects.

3.2 Adsorption

16   The sample loop essentially is a micro packed chromatographic column with a limited surface

17   area where sorption can take place. The low temperature during sample preconcentration

18   shifts the steady state of analyte partitioning between mobile and solid phase mostly to the

19   solid phase. This preconcentration technique "strips" the air of its most abundant constituents;

20   nitrogen, oxygen and argon. Other, less volatile but still very abundant constituents like CO_2

21   are however trapped, depending on adsorption temperature. Elution of such species from the

22   GC column after thermodesorption and injection can cause problems with regard to chroma-

23   tography as well as detection, depending on GC configuration and detection technique. With

24   the setup described here, the elution of CO_2 limits the analysable substance range as the detec-

25   tor shows saturation during the elution of CO_2. Regarding preconcentration of targeted ana-

26   lytes, the concept of an adsorption-desorption steady state suggests that at a certain point a

27   breakthrough of analytes occurs, depending on a combination of loading of the solid phase

28   with sample molecules and time to achieve steady state, in turn influenced by sample flow

29   rate and pressure. Consequently, the maximum possible sample volume and/or minimum du-

30   ration of preconcentration are dependent on the adsorptive material used, volatility (and con-

31   centration) of the targeted analytes as well as sample flow rate and pressure. For typical sam-

32   ple volumes of 0.5 L and 1.0 L (at standard temperature and pressure) and a constant sample

1   back pressure of 2.5 bar abs., no significant impact of sample preconcentration flow was

2   found within the tested range of 50 mL·min^{-1} to 150 mL·min^{-1} for any of the analysed sub-

3   stances. Higher or lower flow rates and pressure were not possible or suitable for practical

4   reasons like flow restriction and valve operating pressure.

5   Substance breakthrough (i.e. substance-specific adsorption capacity) was analysed in volume

6   variation experiments, comprising measurements of the same reference air with preconcentra-

7   tion volumes of up to 10 L and referencing the volume-corrected detector response against

8   default preconcentration volumes of e.g. 1 L ("relative response"). Quantitative trapping is

9   then indicated by a relative response of 1; a relative response <1 would indicate an underesti-

10   mation (i.e. loss by breakthrough), a relative response of >1 would indicate an overestimation

11   (i.e. increase by a memory effect from the preceding sample). To structure the following dis-

12   cussion, two classes of substances are formed and treated separately: "medium volatile sub-

13   stances" with boiling points > -30 °C (e.g. CFC-12, CCl_2F_2) and "highly volatile substances"

14   with boiling points < -30 °C (e.g. HFC-23, CHF_3). The substances discussed are selected

15   based on the criteria volatility and (preferably high) concentration. The adsorption of sub-

16   stances with lower volatility (BP > 30 °C) was assumed to be quantitative. Results discussed

17   in the following are displayed in **Table 2**.

18   ***Medium volatile substances.*** As a reference for halocarbon analysis, CFC-12 (CCl_2F_2) and

19   CFC-11 (CCl_3F) were chosen due to their high mixing ratios of about 525 and

20   235 pmol·mol^{-1} (ppt, parts per trillion) in present-day, ambient air and moderate volatility

21   with boiling points of -29.8 °C and $+23.8$ °C. For a volume of 10 L preconcentrated air on the

22   Unibeads 1S sample loop, both substances showed a deviation from linear response of

23   +0.6 % ± 0.42 % for CFC-12 and +0.6 % ± 0.22 % respectively for CFC-11. The positive

24   deviation from linearity is still found within the 3-fold measurement precision determined for

25   the experiment and could potentially be an artefact of the detector used which tends to slightly

26   overestimate strong signals and underestimate weak signals; see section 3.4 in

27   Obersteiner et al. (2016). Hence, no significant breakthrough or detector saturation was ob-

28   served for both substances CFC-12 and CFC-11.

29   ***Highly volatile substances.*** More volatile compared to CFC-12 and CFC-11 but similar in

30   mixing ratio is carbonyl sulfide (COS) with a boiling point of -50.2 °C and an ambient air

31   mixing ratio of typically around 500 ppt. Against 1 L reference sample volume (sample

32   mixing ratio: 525 ppt), COS showed a quantitative adsorption up to 5 L on the Unibeads 1S

1   sample loop with a deviation from linear response of +0.9 % ± 0.80 %. At 10 L sample

2   volume, a breakthrough occurred giving a deviation from linear response of

3   −35.2 % ± 0.52 %. The substance analysed with highest volatility was HFC-23 with a boiling

4   point of −82.1 °C and a current background air mixing ratio of ~40 ppt. Referenced against a

5   sample volume of 0.5 L, significant breakthrough occurred at a sample volume of 2.5 L with a

6   deviation from linear response of −39.2 % ± 2.75 %. The highest sample volume quantitative-

7   ly adsorbed in the experiment was 1.0 L with a relative response of −0.3 % ± 2.75 %

8   (HayeSep D sample loop). A similar behaviour was observed for ethyne (C_2H_2), with a subli-

9   mation point of −80.2 °C, a mixing ratio of approximately 610 ppt in the sample and a devia-

10   tion from linear response of −20.2 % ± 1.22 % at 2.5 L sample volume (HayeSep D sample

11   loop). However, ethyne was also analysed on the Unibeads 1S sample loop which gave a quite

12   different result with a deviation from linear response of +10.1 % ± 0.51 %, thus breakthrough

13   did not occur. The positive, non-linear response is caused potentially by a system blank (see

14   also section 3.3). Unfortunately, HFC-23 could not be analysed in ambient air samples for

15   comparison on the Unibeads 1S sample loop as its ion signals are masked by large amounts of

16   CO_2 still eluting from the GC column at the retention time of HFC-23.

17   Concluding, the adsorption process was found to be substance specific as both HFC-23 and

18   ethyne are comparably volatile but significantly less ethyne broke through despite its 15-fold

19   elevated mixing ratio (Unibeads 1S sample loop). The comparison of ethyne breakthrough on

20   the HayeSep D and Unibeads 1S sample loop suggests that the adsorption process is depend-

21   ent on the chosen adsorptive material. A comparison of adsorptive materials is however not

22   the focus of this work; such a comparative adsorption study was e.g. conducted for methane

23   (CH_4) preconcentration by Eyer et al. (2014). From the comparison of the breakthrough ob-

24   served for COS and the quantitative adsorption of CFC-12 and CFC-11, it can be concluded

25   that volatility is the primary factor that determines breakthrough. Quantitative adsorption is

26   not limited by principal adsorption capacity (i.e. the absolute number of molecules adsorbed)

27   of the adsorptive material and material amount for a sample volume of up to 10 L and an ad-

28   sorption temperature of −80 °C.

29

3.3 Desorption

While adsorption is characterised by the quantitative trapping of highly volatile substances, desorption is characterised by sharpness and repeatability of the injection represented by chromatographic peak shape and retention time variance (qualitative aspect; section 3.3.1) as well as the amount of blank residues (quantitative aspect; section 3.3.2). Blank residues ("memory effect") have to be divided into residues that remain on the adsorptive material after desorption ("preconcentration residues" or "preconcentration memory effect") and residues that remain in the analytical setup (tubing etc.) upstream of the sample loop, thus had not reached the sample loop ("system residues" or "system memory effect").

3.3.1 Peak shape and retention time stability

To demonstrate injection sharpness, **Figure 5 A** shows the chromatographic signal of CFC-11 eluted from the GC column kept isothermal at 150 °C and **Figure 5 B** the chromatographic signal as observed with the ramped GC program. Both signals generally show a Gaussian peak shape with a slight tailing of the right flank. In comparison, the "unfocused" signal from the isothermal column reflecting the sharpness of the direct injection is wider by a factor of ~3 but still narrow enough to allow for good peak separation in most standard GC methods with runtimes between 10 to 30 minutes; the full peak width at half maximum (FWHM) was calculated to be 6.3 s (0.10 min) for the isothermal peak and 2.0 s (0.03 min) for the focused peak.

Injection quality can further be judged by the stability of retention times of the first chromatographic signals obtained with the ramped GC program, as these are only very little influenced by the chromatographic system (in particular there is nearly no refocusing on the chromatographic column). **Table 3** shows retention times and their variability expressed as relative standard deviation and variance as well as the chromatographic signal width (FWHM) of the respective substance. Variances are less than 0.02 s on average. Together with signal width, they decrease reversely proportional to retention time, which shows the increasing influence of chromatographic separation (from HFC-23 to CFC-11 in **Table 3**). Even at incomplete refocusation by gas chromatography, the desorption procedure of the preconcentration unit gives close to Gaussian peak shapes except a slight tailing of the right flank. The tailing effect could potentially be reduced by refocusing the high-volatile analyte fraction on a second sample loop. The high repeatability of the injection is shown by the low variability in retention time of the first signals in the chromatogram (**Table 3**).

3.3.2 Analyte residues

Analyte residues can originate from inherent system *contamination* or constitute a remainder from the previous sample (*memory effect*). Analyte residues were investigated with (a) an unloaded injection after multiple 1 L ambient air sample injections, i.e. subsequent thermode-sorption of the sample loop without switching to load-position between runs (see **Figure 1**) and (b) the preconcentration of 1 L helium from the carrier gas supply using the same path as the sample, including dryer etc. after multiple 1 L ambient air sample measurements. Analyte residues on the sample loop (*sample loop memory*) as well as carrier gas contaminations are investigated by (a) while (b) includes analyte residues within the tubing upstream of the sample loop, i.e. stream selection, sample dryer etc. (*system memory*). To get the most complete picture possible, 65 substances were analysed, most of them halo- and hydrocarbons (see supplementary information for a detailed list) on both a HayeSep D as well as a Unibeads 1S sample loop. Substances with low measurement precision ($> 10 \%$) were excluded from the investigation.

In general, most of the detected analyte residues are most probably caused by system contaminations (HFCs from fittings, solenoid valve membranes etc.) or carrier gas contaminations (hydrocarbons) as they show a constant background. In principal, the amount of a residue is dependent on volatility and concentration, so extremely elevated concentrations of low-volatile substances might lead to a memory effect that was not detected in the current investigation with 1 L preconcentration volume of unpolluted ambient air. Detailed results for the two different adsorptive materials tested are discussed in the following.

Unibeads 1S adsorptive material. 13 of 65 substances (20%) did show detectable residues on the sample loop which did not represent a system memory but a system contamination, e.g. from the carrier gas, sealing materials etc. as they were always present and did not disappear in subsequent unloaded injections. Respective residues were generally larger with increasing boiling point (e.g. n-propane < benzene). Most of them were hydrocarbons and the halocarbons chloro- and iodomethane (CH_3Cl, CH_3I) and chloroethane (C_2H_5Cl) as well as HFC-134 (CHF_2CHF_2). No further CFCs, HCFCs, PFCs or HFCs were detected in the unloaded sample loop injection (see Obersteiner et al. (2016) for a discussion of detection limits). Of the remaining 52 substances, 36 also did not show any detectable residues in the helium blank. Of the 17 substances that did show residues (contamination and memory effect combined), 7 had residues below 0.5 % of the signal area determined in the preceding ambient air measurement. Again, residues were found mostly for hydrocarbons but not CFCs or HCFCs. Concluding,

1   the Unibeads 1S sample loop seems to be a good choice for halocarbon monitoring measure-

2   ments (one measurement per sample) as there were nearly no halocarbon residues in subse-

3   quent helium blank measurements.

4   ***HayeSep D adsorptive material.*** The HayeSep D sample loop showed a considerably higher

5   amount of sample loop residues with 22 detectable substances from the selected 65 (34 %).

6   Again, most of these substances were hydrocarbons but also some halogenated compounds

7   like Tetrachloromethane (CCl_4) and Bromoform ($CHBr_3$). Of the remaining 43 substances, 28

8   were undetectable in the helium blank (system free of contamination and memory effect). 13

9   of the detectable substances showed responses of < 0.5 % relative to the preceding ambient air

10   sample, also including CFC-11 with 0.05 % and CFC-113 with 0.2 %. While the named halo-

11   genated compounds CCl_4 and $CHBr_3$ as well as CFC-113 and CFC-11 were undetectable in

12   subsequent blank gas measurements, residues of many hydrocarbons were persistent, suggest-

13   ing a system contamination. In summary, the HayeSep D sample loop showed an overall

14   higher number of residues which is likely caused by a higher desorption temperature of the

15   Unibeads 1S sample loop which can be heated faster and to a higher temperature without de-

16   grading the material. Nevertheless, the residues on both adsorptive materials were on a tolera-

17   ble level (below average measurement precision) for flask measurements with multiple meas-

18   urements per sample.

Atmospheric
Measurement
Techniques
Discussions

4 Application

4.1 Laboratory operation: flask sample measurements

For quality assurance of the laboratory instrumentation, five air samples were analysed and compared to our reference GC-QPMS (gas chromatograph coupled to a quadrupole mass spectrometer) which uses a similar preconcentration setup (Hoker et al., 2015). Consistent results with the NOAA network (National Oceanic and Atmospheric Administration) were demonstrated for the GC-QPMS in the past during the IHALACE intercomparison (Hall et al., 2014), however with a different sample preconcentration using liquid nitrogen (Brinckmann et al., 2012; Laube and Engel, 2008; Laube et al., 2010). The current laboratory setup using the Stirling cooler-based preconcentration has been described by Hoker et al. (2015) and has shown very consistent results with previous measurements. The samples for the application and intercomparison discussed here were collected between July 7th and September 11th 2015 at Mace Head Atmospheric Research Station in Ireland (53°20′ °N, 9°54′ °W, 30 m above sea level). Samples were filled "moist" (no sample drying) into 2 L electro-polished stainless steel flasks (two flasks in parallel per sampling date). The comparison is extended to include in-situ measurement data from the online monitoring Medusa GC-MS (Miller et al., 2008) operated by the AGAGE (Advanced Global Atmospheric Gases Experiment) network at Mace Head Station. Medusa GC-MS data points were chosen within ±1 hour of the flask samples' sampling time. **Figure 6** shows a comparison of absolute quantification results for CFC-12 (CCl_2F_2). Very good agreement within the 1-fold measurement error is achieved in comparison to the Medusa GC-MS and within the 2-fold measurement error in comparison to the reference GC-QPMS. While the Medusa GC-MS is calibrated with secondary calibration gases (AGAGE flasks H-265 and H-266; CFC-12 scale: SIO-05), both our instruments were calibrated with different ternary calibration gasses, referenced to the same secondary calibration gas (AGAGE flask H-218; CFC-12 scale: SIO-05). Taking into account that all three instruments were calibrated with different calibration gases which rely on the same calibration scale but are based on a chain of intercalibrations, this result stands proof for highly accurate measurement results, excluding the absolute scale error.

4.2 Aircraft in-situ operation: GhOST-MS

Reliability of operation is best demonstrated with the in-situ GC-MS GhOST-MS[1]. **Figure 7** shows a chromatogram obtained from the injection of a preconcentrated sample volume of 100 mL of ambient air. With a chromatographic runtime of 2.9 minutes and a total cycle time of 4.1 minutes (see also **Table 1**), a data frequency is achieved that is very high for a GC-MS system with a total of 27 identified and simultaneously measured species on m/Q of bromine, chlorine and iodine in negative chemical ionisation mode using argon as reagent gas. The cycle time is limited by cooldown of the adsorptive material (HayeSep D) to −70 °C needed to quantitatively trap the earliest eluting analyte, Halon 1301 ($CBrF_3$). The very good overall performance of the GhOST-MS including the preconcentration unit used in this in-situ application can be inferred from actual measurement data obtained during a research flight of the recent PGS campaign (POLSTRACC/GW-LCycle/SALSA) of the HALO aircraft on flight 160226a (PGS-14). **Figure 8** shows a tracer-tracer correlation between Halon 1301 and Halon 1211 ($CBrClF_2$). The measurements are colour-coded to show potential temperature θ. As expected, the lowest mixing ratios are observed at the highest potential temperature. Both tracers have relatively long steady-state lifetimes of 72 years for Halon 1301 (58-97, derived from model data and observations) and 16 years for Halon 1211 (10-39, model data) (SPARC, 2013) so that a compact correlation of mixing ratios of these two traces gases is expected in the stratosphere (Plumb and Ko, 1992). Due to its relatively low boiling point (−57.8 °C), Halon 1301 is the first species eluting from the chromatographic column. The shape of the chromatographic peak is thus strongly influenced by the injection, as refocusing on the chromatographic column is expected to play a negligible role. As a correlation derived from measurement data can only be as compact as the measurement precision allows, the compactness of the correlation shown in **Figure 8** gives an indication of the high measurement precision achieved with the GhOST-MS. The fact that this compact correlation includes a substance whose precision is strongly influenced by its thermodesorption shows that the sample preconcentration system on GhOST-MS is able to reproducibly trap and desorb even low boiling compounds like Halon 1301.

GhOST-MS has been deployed during a total of more than 200 flight hours on the HALO aircraft without a single failure of the preconcentration unit. In addition, measurements with GhOST-MS were performed as part of the SHIVA campaign in Borneo, providing a complete bromine budget for the upper tropical troposphere up to about 13 km (Sala et al., 2014). The

---

[1] Manuscript on the current GhOST setup and characterisation in preparation by Keber et al.

Atmospheric
Measurement
Techniques
Discussions

Open Access

EGU

1   preconcentration unit presented here therefore is not only able to provide high precision but is

2   also able to operate reliably under difficult conditions like aircraft operation with varying hu-

3   midity and temperatures, including operation during humid and hot conditions in the tropics.

Atmospheric
Measurement
Techniques
Discussions

Open Access

EGU

5 Summary and conclusion

A single-stage, refrigerant-free sample preconcentration unit for ambient air analysis is presented and characterised. The setup has proven to be applicable for both in-situ and laboratory operation and can quantitatively trap and desorb a wide range of halo- and hydrocarbons (see supplementary information). The use of different adsorptive materials is possible with the setup; two of which were used during this work, HayeSep D and Unibeads 1S. Both materials are well suited for analysis of halogenated trace gases in general. While HayeSep D is an established material for this task, Unibeads 1S potentially is a good alternative that has better heat tolerance and showed fewer sample loop blanks in the presented characterisation.

The preconcentration unit is positioned between more sophisticated but also more expensive and complicated solutions like e.g. the Medusa preconcentration unit described by Miller et al. (2008) and setups that use less powerful, Peltier-based cooling options that sacrifice adsorption temperature and therefore reduce the trappable substance range. The described setup is unique in terms of the used cooling technique, a Stirling cooler. The latter allows very low temperatures of -120 °C tested in this work and -173 °C reported by Eyer et al. (2016) for the preconcentration of methane with a comparable Stirling cooler without having to rely on a cooling agent like liquid nitrogen or liquid argon. The Stirling cooler as a cooling option is ideally suited for in-situ, remote-site operation, where refrigerant-based cooling options are very difficult to operate and space is limited – like the aircraft-based in-situ GC-MS instrument GhOST-MS. Moreover, the absence of mechanical/moving parts as well as the lack of necessity of vacuum insulation of cooled parts facilitates installation and maintenance. No exchange of adsorption tubes is necessary. Overall, the setup is relatively cheap with the Stirling cooler being the most expensive part by far.

The simplicity of the single-stage design also has a downside; a major problem is the trapping of large amounts of CO_2 and injection into the detection system (see also section 3.2), especially when using trapping temperatures below -80 °C. Due to this limitation, the current configuration is not applicable to highly volatile compounds like CF_4, C_2F_6 or C_2H_6. Cooling capacity should however be sufficient to ensure quantitative trapping of such compounds on a suitable adsorptive material. Therefore, a starting point for future improvement is removal of CO_2 to extend the already large substance range by compounds of higher volatility. Regarding desorption, no blank residues were found for halocarbons that would cause concern or render the setup unsuited for halocarbon analysis (see "Appendix B: Blank Residues"). However,

1   relatively large amounts of hydrocarbons remained in blank measurements. These blanks are

2   not an inherent problem of the preconcentration setup but more likely due to the adsorptive

3   materials used. Additional experiments are needed to reduce those uncertainties and extend

4   the applicability of the preconcentration unit to quantitative hydrocarbon analysis.

1 **Acknowledgements**

Atmospheric
Measurement
Techniques
Discussions

References

Apel, E. C., Hills, A. J., Lueb, R. A., Zindel, S., Eisele, S., and Riemer, D. D.: A fast-GC/MS system to measure C_2 to C_4 carbonyls and methanol aboard aircraft, J. Geophys. Res., 108, doi: 10.1029/2002jd003199, 2003.

Aragón, P., Atienza, J., and Climent, M. D.: Analysis of organic compounds in air: A review, Crit. Rev. Anal. Chem., 30, 121-151, doi: 10.1080/10408340091164207, 2000.

Brinckmann, S., Engel, A., Bönisch, H., Quack, B., and Atlas, E.: Short-lived brominated hydrocarbons – observations in the source regions and the tropical tropopause layer, Atmos. Chem. Phys., 12, 1213-1228, doi: 10.5194/acp-12-1213-2012, 2012.

de Blas, M., Navazo, M., Alonso, L., Durana, N., and Iza, J.: Automatic on-line monitoring of atmospheric volatile organic compounds: Gas chromatography-mass spectrometry and gas chromatography-flame ionization detection as complementary systems, Sci. Total Environ., 409, 5459-5469, doi: 10.1016/j.scitotenv.2011.08.072, 2011.

Demeestere, K., Dewulf, J., De Witte, B., and Van Langenhove, H.: Sample preparation for the analysis of volatile organic compounds in air and water matrices, J Chromatogr A, 1153, 130-144, doi: 10.1016/j.chroma.2007.01.012, 2007.

Dettmer, K. and Engewald, W.: Ambient air analysis of volatile organic compounds using adsorptive enrichment, Chromatographia, 57, S339-S347, doi: 10.1007/BF02492126, 2003.

Eyer, S., Stadie, N. P., Borgschulte, A., Emmenegger, L., and Mohn, J.: Methane preconcentration by adsorption: A methodology for materials and conditions selection, Adsorption, 20, 657-666, doi: 10.1007/s10450-014-9609-9, 2014.

Eyer, S., Tuzson, B., Popa, M. E., van der Veen, C., Röckmann, T., Rothe, M., Brand, W. A., Fisher, R., Lowry, D., Nisbet, E. G., Brennwald, M. S., Harris, E., Zellweger, C., Emmenegger, L., Fischer, H., and Mohn, J.: Real-time analysis of δ^{13}C- and δD-CH$_4$ in ambient air with laser spectroscopy: Method development and first intercomparison results, Atmos. Meas. Tech., 9, 263-280, doi: 10.5194/amt-9-263-2016, 2016.

Farman, J. C., Gardiner, B. G., and Shanklin, J. D.: Large losses of total ozone in Antarctica reveal seasonal ClO$_x$/NO$_x$ interaction, Nature, 315, 207-210, doi: 10.1038/315207a0, 1985.

Atmospheric
Measurement
Techniques
Discussions

1   Farwell, S. O., Gluck, S. J., Bamesberger, W. L., Schutte, T. M., and Adams, D. F.:

2   Determination of sulfur-containing gases by a deactivated cryogenic enrichment and capillary

3   gas chromatographic system, Anal. Chem., 51, 609-615, doi: 10.1021/ac50042a007, 1979.

4   Haagen-Smit, A. J. and Fox, M. M.: Ozone formation in photochemical oxidation of organic

5   substances, Ind. Eng. Chem., 48, 1484-1487, doi: 10.1021ie51400a033, 1956.

6   Hall, B. D., Engel, A., Mühle, J., Elkins, J. W., Artuso, F., Atlas, E., Aydin, M., Blake, D.,

7   Brunke, E. G., Chiavarini, S., Fraser, P. J., Happell, J., Krummel, P. B., Levin, I.,

8   Loewenstein, M., Maione, M., Montzka, S. A., O'Doherty, S., Reimann, S., Rhoderick, G.,

9   Saltzman, E. S., Scheel, H. E., Steele, L. P., Vollmer, M. K., Weiss, R. F., Worthy, D., and

10 Yokouchi, Y.: Results from the international halocarbons in air comparison experiment

11 (IHALACE), Atmos. Meas. Tech., 7, 469-490, doi: 10.5194/amt-7-469-2014, 2014.

12 Helmig, D. and Greenberg, J. P.: Automated in situ gas chromatographic-mass spectrometric

13 analysis of ppt level volatile organic trace gases using multistage solid-adsorbent trapping, J.

14 Chromatogr. A, 677, 123-132, doi: 10.1016/0021-9673(94)80551-2, 1994.

15 Hodnebrog, Ø., Etminan, M., Fuglestvedt, J. S., Marston, G., Myhre, G., Nielsen, C. J., Shine,

16 K. P., and Wallington, T. J.: Global warming potentials and radiative efficiencies of

17 halocarbons and related compounds: A comprehensive review, Rev. Geophys., 51, 300-378,

18 doi: 10.1002/rog.20013, 2013.

19 Hoker, J., Obersteiner, F., Bönisch, H., and Engel, A.: Comparison of GC/time-of-flight MS

20 with GC/quadrupole MS for halocarbon trace gas analysis, Atmos. Meas. Tech., 8, 2195-

21 2206, doi: 10.5194/amt-8-2195-2015, 2015.

22 Hou, Y., Yang, L., Wang, B., Xu, J., Yang, Y., Yang, Y., Cao, Q., and Xie, X.: Analysis of

23 chemical components in tobacco flavors using stir bar sorptive extraction and thermal

24 desorption coupled with gas chromatography-mass spectrometry, Chinese Journal of

25 Chromatography, 24, 601-605, doi: 10.1016/S1872-2059(06)60026-6, 2006.

26 Laube, J. C. and Engel, A.: First atmospheric observations of three chlorofluorocarbons,

27 Atmos. Chem. Phys., 8, 2008.

28 Laube, J. C., Kaiser, J., Sturges, W. T., Bönisch, H., and Engel, A.: Chlorine isotope

29 fractionation in the stratosphere, Science, 329, 1167, doi: 10.1126/science.1191809, 2010.

Atmospheric
Measurement
Techniques
Discussions

1 Marenco, A., Gouget, H., Nédélec, P., Pagés, J.-P., and Karcher, F.: Evidence of a long-term

2 increase in tropospheric ozone from Pic Du Midi data series: Consequences: Positive radiative

3 forcing, J. Geophys. Res.-Atmos., 99, 16617-16632, doi: 10.1029/94JD00021, 1994.

4 Miller, B. R., Weiss, R. F., Salameh, P. K., Tanhua, T., Greally, B. R., Mühle, J., and

5 Simmonds, P. G.: Medusa: A sample preconcentration and GC/MS detector system for in situ

6 measurements of atmospheric trace halocarbons, hydrocarbons, and sulfur compounds, Anal.

7 Chem., 80, 1536-1545, doi: 10.1021/ac702084k, 2008.

8 Molina, M. J. and Rowland, F. S.: Stratospheric sink for chlorofluoromethanes: Chlorine atom

9 catalysed destruction of ozone, Nature, 249, 810-812, doi: 10.1038/249810a0, 1974.

10 Monks, P. S., Archibald, A. T., Colette, A., Cooper, O., Coyle, M., Derwent, R., Fowler, D.,

11 Granier, C., Law, K. S., Mills, G. E., Stevenson, D. S., Tarasova, O., Thouret, V., von

12 Schneidemesser, E., Sommariva, R., Wild, O., and Williams, M. L.: Tropospheric ozone and

13 its precursors from the urban to the global scale from air quality to short-lived climate forcer,

14 Atmos. Chem. Phys., 15, 8889-8973, doi: 10.5194/acp-15-8889-2015, 2015.

15 Montzka, S. A., Reimann, S. (Coordinating Lead Authors), Engel, A., Krüger, K., O'Doherty,

16 S., Sturges, W. T. L. A., Blake, D., Dorf, M., Fraser, P., Froidevaux, L., Jucks, K., Kreher, K.,

17 Kurylo, M. J., Mellouki, A., Miller, J., Nielsen, O.-J., Orkin, V. L., Prinn, R. G., Rhew, R.,

18 Santee, M. L., Stohl, A., and Verdonik, D. C.: Ozone-depleting substances (ODSs) and related

19 chemicals. Chapter 1 in: Scientific assessment of ozone depletion: 2010, global ozone

20 research and monitoring project report no. 52., World Meteorological Organization (WMO),

21 Geneva, Switzerland, 108 pp., 2011.

22 O'Doherty, S. J., Simmonds, P. G., and Nickless, G.: Analysis of replacement

23 chlorofluorocarbons using carboxen microtraps for isolation and preconcentration in gas

24 chromatography-mass spectrometry, J. Chromatogr. A, 657, 123-129, doi: 10.1016/0021-

25 9673(93)83043-r, 1993.

26 Obersteiner, F., Bönisch, H., and Engel, A.: An automated gas chromatography time-of-flight

27 mass spectrometry instrument for the quantitative analysis of halocarbons in air, Atmos.

28 Meas. Tech., 9, 179-194, doi: 10.5194/amt-9-179-2016, 2016.

1   Plumb, R. A. and Ko, M. K. W.: Interrelationships between mixing ratios of long-lived

2   stratospheric constituents, Journal of Geophysical Research: Atmospheres, 97, 10145-10156,

3   doi: 10.1029/92jd00450, 1992.

4   Saito, T., Yokouchi, Y., Stohl, A., Taguchi, S., and Mukai, H.: Large emissions of

5   perfluorocarbons in east asia deduced from continuous atmospheric measurements, Environ.

6   Sci. Technol., 44, 4089-4095, doi: 10.1021/es1001488, 2010.

7   Sala, S., Bönisch, H., Keber, T., Oram, D. E., Mills, G., and Engel, A.: Deriving an

8   atmospheric budget of total organic bromine using airborne in situ measurements from the

9   western pacific area during SHIVA, Atmos. Chem. Phys., 14, 6903-6923, doi: 10.5194/acp-

10 14-6903-2014, 2014.

11 Simmonds, P. G., O'Doherty, S., Nickless, G., Sturrock, G. A., Swaby, R., Knight, P.,

12 Ricketts, J., Woffendin, G., and Smith, R.: Automated gas chromatograph/mass spectrometer

13 for routine atmospheric field measurements of the CFC replacement compounds, the

14 hydrofluorocarbons and hydrochlorofluorocarbons, Anal. Chem., 67, 717-723, doi:

15 10.1021/ac00100a005, 1995.

16 Solomon, S.: Stratospheric ozone depletion: A review of concepts and history, Rev. Geophys.,

17 37, 275, doi: 10.1029/1999rg900008, 1999.

18 Song, C.-F., Kitamura, Y., Li, S.-H., and Ogasawara, K.: Design of a cryogenic CO_2 capture

19 system based on stirling coolers, International Journal of Greenhouse Gas Control, 7, 107-

20 114, doi: 10.1016/j.ijggc.2012.01.004, 2012.

21 SPARC: Sparc report on the lifetimes of stratospheric ozone-depleting substances, their

22 replacements, and related species, M. Ko, P. Newman, S. Reimann, S. Strahan (Eds.), SPARC

23 Report No. 6, WCRP-15/2013, 2013.

24 Velders, G. J., Fahey, D. W., Daniel, J. S., McFarland, M., and Andersen, S. O.: The large

25 contribution of projected HFC emissions to future climate forcing, Proc. Natl. Acad. Sci. U. S.

26 A., 106, 10949-10954, doi: 10.1073/pnas.0902817106, 2009.

27

Atmospheric
Measurement
Techniques

Open Access

Discussions

1 **Tables**

2 **Table 1.** Cycle times at T_A of -80 °C / -120 °C (laboratory setup) and -70 °C (in-situ setup), based on
3 operational data. Laboratory setup configuration: Sunpower CryoTel CT Stirling cooler, preconcentra-
4 tion volume: 500 mL at 100 mL·min^{-1}, $T_D \approx 200$ °C for 3 min. In-situ setup configuration: Twinbird
5 SC-TD08 Stirling cooler, preconcentration volume: 100 mL at 100 mL·min^{-1}, $T_D \approx 200$ °C for 1 min.
6 Adsorptive material, both setups: HayeSep D. Due to a smaller coldhead, cooling rate and warm-up
7 during desorption are considerably larger with the in-situ setup, despite the shorter desorption time.

T_A [°C]	cooling rate at T_A [°C·min^{-1}]	warm-up during desorption [°C]	minimum cycle time including preconcentration after T_A is reached [min]
Laboratory instrument (GC-TOFMS)			
−80	−2.2	7.7	8.5
−120	−1.2	16.3	18.6
In-situ instrument (GhOST-MS)			
−70	−4.1	13.5	4.1

8

Atmospheric
Measurement
Techniques

Open Access

Discussions

1   **Table 2**. Results from a volume variation experiment, comprising measurements of the same reference
2   air with preconcentration volumes (PrcVol) of up to 2, 5 and 10 L. Laboratory setup, adsorptive mate-
3   rial Unibeads 1S. Volume-corrected detector response is referenced against calibration preconcentra-
4   tion volumes of 1 L (rR). rR <100% indicates underestimation (e.g. loss by breakthrough); rR >100%
5   indicates overestimation (e.g. increase by a memory effect from the preceding sample or contamina-
6   tion). Breakthrough is observed for COS at a preconcentration volume of 10 L while ethyne shows
7   signs of a system contamination (rR >100% despite a higher volatility compared to COS). CFC-12 and
8   CFC-11 show no indication of breakthrough, with all deviations from 100% rR below 3 σ.

Substance	PrcVol [L]	rR	rR: 1 σ	PrcVol [L]	rR	rR: 1 σ	PrcVol [L]	rR	rR: 1 σ
Ethyne (C_2H_2)		102.0%	0.66%		108.9%	0.70%		109.2%	0.70%
Carbonyl sulfide (COS)	2	102.2%	0.82%	5	100.9%	0.81%	10	64.8%	0.52%
CFC-12 (CCl_2F_2)		99.9%	0.41%		100.7%	0.42%		100.6%	0.42%
CFC-11 (CCl_3F)		100.2%	0.21%		100.5%	0.22%		100.6%	0.22%

9

Atmospheric
Measurement
Techniques
Discussions

1 **Table 3.** Retention times t_R with relative standard deviations rSD and variances in [s] for selected sub-
2 stances (same as **Table 2**) as well as their respective average signal width expressed as FWHM in [s].
3 Values derived from 112 individual measurements of different ambient air samples using the ramped
4 GC program. Sample loop adsorptive material: HayeSep D. HFC-23 is the first detectable substance,
5 least separated by chromatography. CFC-11 can be considered a reference for optimal chromatograph-
6 ic performance of the given setup.

Substance	t_R [min]	t_R rSD	Variance [s]	Avg. Peak Width [s]
HFC-23 (CHF_3)	3.01	0.105%	0.0386	4.09
Ethyne (C_2H_2)	3.74	0.047%	0.0118	2.77
Carbonyl sulfide (COS)	3.86	0.040%	0.0092	2.29
CFC-12 (CCl_2F_2)	5.01	0.014%	0.0018	2.26
CFC-11 (CCl_3F)	7.25	0.006%	0.0008	2.24

7

Atmospheric
Measurement
Techniques

Open Access

Discussions

EGU
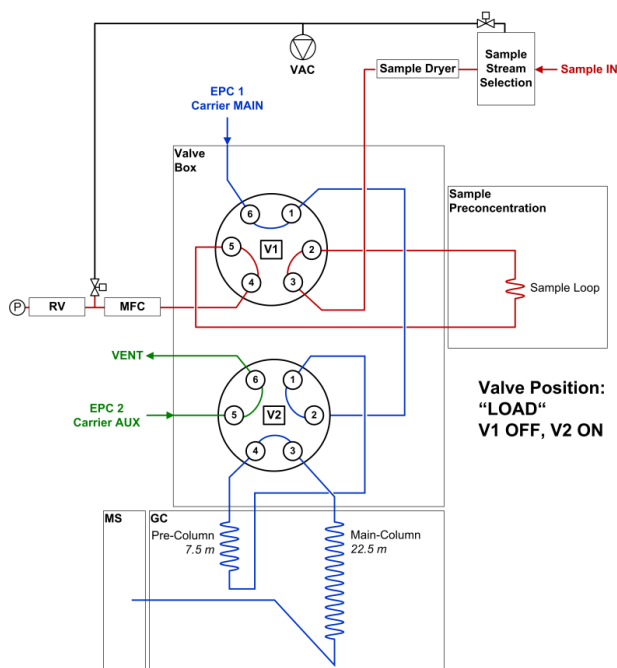
1   **Figures**

2

3   **Figure 1.** Flow scheme showing the gas flow during preconcentration. Two electronic pressure
4   controllers, EPC 1 and EPC 2, control the carrier gas flow. The two 6-port 2-position rotary
5   valves V1 and V2 are set to OFF/ON position. A sample is preconcentrated (red flow path);
6   sample components not trapped in the sample loop flow through the mass flow controller
7   (MFC) into the reference volume (RV). By switching V1 to ON position (for desorption), the
8   sample loop is injected onto the GC column. Sample loop as well as reference volume and
9   stream selection valves are evacuated prior to the preconcentration of the next sample. By
10 switching V2 to OFF, it separates pre- and main-column; the pre-column is flushed backwards.
11 This prevents high-boiling, non-targeted species from reaching the main-column.
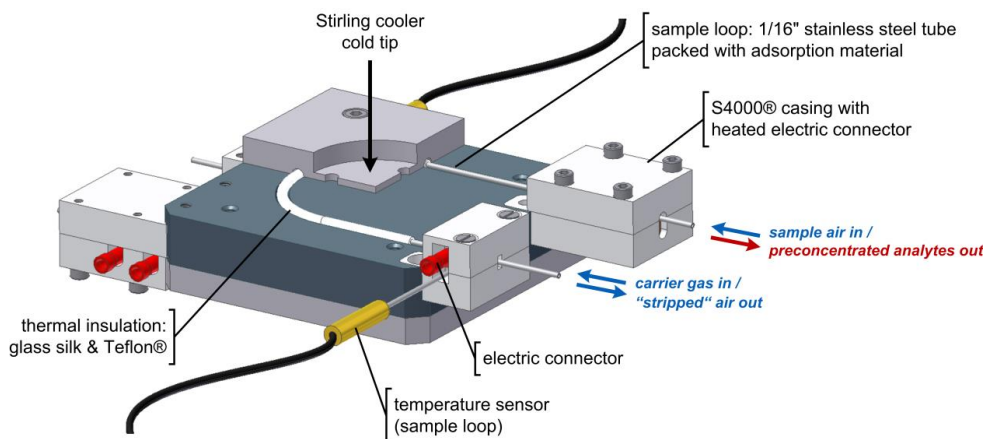
1

2 **Figure 2.** Technical drawing of the coldhead and sample loop placed inside. Three plates of
3 anodized aluminium can hold two sample loops. The Stirling cooler's cold tip screwed to the
4 coldhead removes heat for cooling. Heat for sample desorption is generated by a current directly
5 applied to the sample loop. The electric connector in the direction of sample flow (upper right
6 side of the drawing) is heated constantly to 150 °C to avoid a cold point due to the mass of the
7 electric connector and its proximity to the coldhead (S4000® insulation material:
8 Brandenburger, Germany).

Atmospheric
Measurement
Techniques

Open Access

Discussions

EGU

1
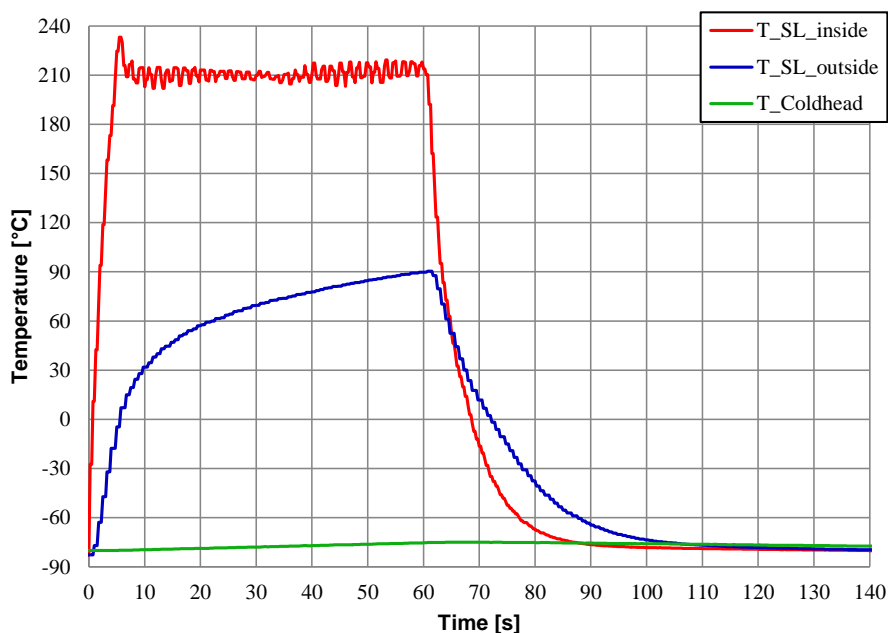
Figure 3. Desorption temperature curve inside the sample loop with a preceding adsorption
temperature of −80 °C and a subsequent cool-down from desorption to adsorption temperature.
Red curve, "T_SL_inside": signal from temperature sensor shifted inside the sample loop. Blue
curve, "T_SL_outside": temperature sensor signal from the sensor welded to the outer sample
loop tubing wall. Green curve, "T_Coldhead": temperature of the coldhead. Deterministic
heater, output in this example: 50 % in stage 1, held 5 s, and 30 % in stage 2, held 55 s. The
periodic oscillation of T_D observed is a result of a very slow pulse width modulation used in the
testing setup: 100 ms period with 10 ms minimum increment.

Atmospheric
Measurement
Techniques
Discussions
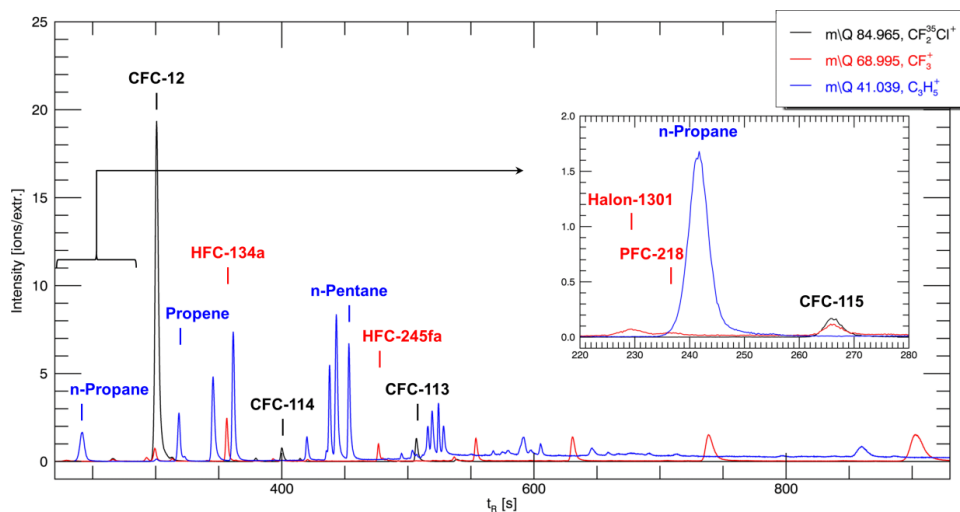
Figure 4. Chromatogram from a 1 L ambient air sample obtained with the GC-MS setup described in Obersteiner et al., 2016. X-axis: retention time t_R in seconds. Y-axis: signal intensity expressed as ions per extraction which are derived from a 22.7 kHz TOFMS extraction rate, averaged to yield a mass spectra rate of 4 Hz. X- and Y-axis description also valid for the magnified section. Black graph: mass-to-charge ratio (m/Q) = 84.965 signal from a typical CFC fragment ion $CF_2{}^{35}Cl^+$. Red graph: m/Q = 68.995 signal from a typical PFC or HFC fragment ion $CF_3{}^+$. Blue graph: m/Q = 41.039 signal from a typical hydrocarbon fragment ion $C_3H_5{}^+$. The magnified section shows the chromatographic peak of n-propane and three other compounds to demonstrate injection quality of substances least re-focused by chromatography.

Atmospheric
Measurement
Techniques

Open Access

Discussions

1
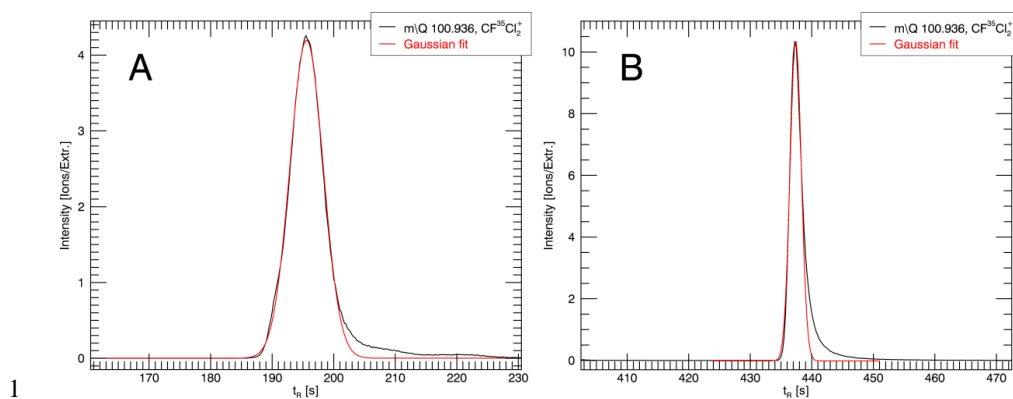
Figure 5. Comparison of chromatographic peak shapes of the $CF^{35}Cl_2^+$ fragment ion signal of
CFC-11 ($CFCl_3$), from an injection of 1 L preconcentrated ambient air onto the GC column kept
isothermal at 150 °C (A) and onto the GC column kept at 45 °C and ramped to 200 °C
subsequently (B) (see section 3.1). X-axis: retention time t_R in seconds; t_R interval shown is 70 s
in both plots. Y-axis: signal intensity expressed as ions per extraction (see **Figure 4**). The red
curve shows a Gaussian fit for comparison of actual peak shape and a peak shape that is
considered ideal. FWHM of fit: (A) 6.3 s (0.10 min) and (B) 2.0 s (0.03 min). Adsorptive
material: Unibeads 1S.

1
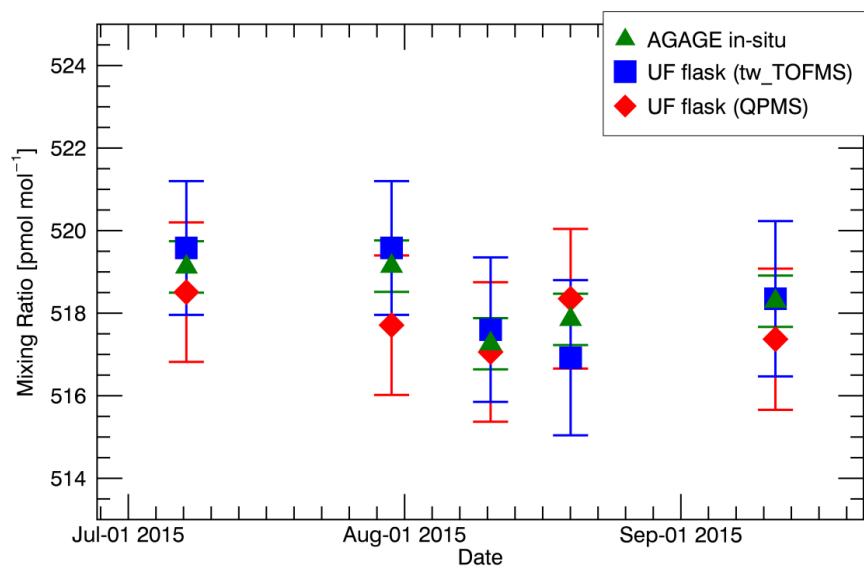
Figure 6. CFC-12 (CCl$_2$F$_2$) mixing ratios at Mace Head Atmospheric Research Station, Ireland
(53°20′ °N, 9°54′ °W, 30 m above sea level) derived from 2 L stainless steel flask samples
measured with the instrument in description (GC-TOFMS, blue squares), our reference
instrument (GC-QPMS, red diamonds) and values taken from the online measurement data of
the in-situ Medusa GC-MS (green triangles). Error bars: 1-fold measurement precision of each
instrument (Medusa system: typical precision taken from Miller et al. (2008)). Calibration scale,
all instruments: SIO-05.

1
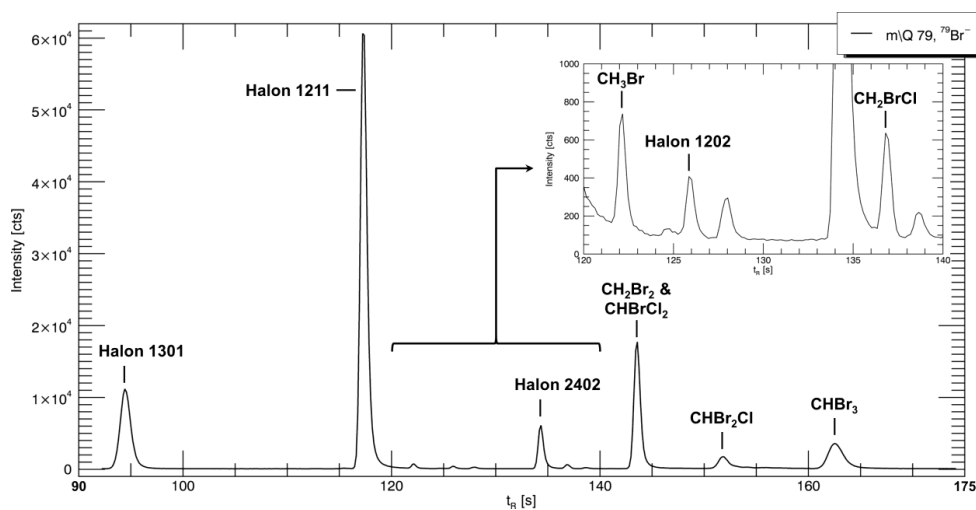
Figure 7. Chromatogram from a preconcentration of 0.1 L ambient air obtained with the in-situ
GC-MS setup GhOST-MS. X-axis: retention time t_R in seconds. Y-axis: signal intensity in
counts, arbitrary unit. MS: Agilent 5975C in negative chemical ionization mode (reagent:
argon). Black graph: mass-to-charge ratio $m/Q = 79$ signal of $^{79}Br^-$ ions from brominated trace
gases.

Atmospheric
Measurement
Techniques
Discussions
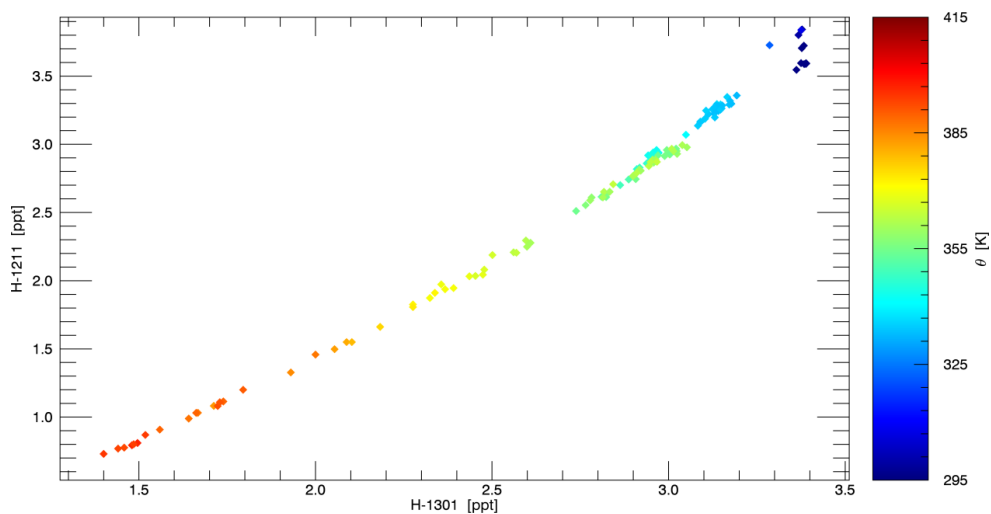
Figure 8. Tracer-tracer correlation of Halon 1301 (CBrF$_3$, x-axis) vs. Halon 1211 (CBrClF$_2$, y-axis). Color code indicates potential temperature θ in [K]. Data was obtained during the POLSTRACC mission with the HALO aircraft, flight 160226a (PGS-14). Preliminary data; calibration scale of Halon 1301 and 1211: SIO-05.

ii. "Comparison of GC/time-of-flight MS with GC/quadrupole MS for halocarbon trace gas analysis"

Citation

Hoker, J., Obersteiner, F., Bönisch, H., and Engel, A.: Comparison of GC/time-of-flight MS with GC/quadrupole MS for halocarbon trace gas analysis, Atmospheric Measurement Techniques, 8, 2195-2206, DOI: 10.5194/amt-8-2195-2015, 2015.

Own Contribution

Wrote parts of the manuscript, which was proofread by A. Engel and H. Bönisch. Wrote parts of the answers-to-the-reviewers during the review process.

Provided technical support for the preconcentration unit and assisted in data evaluation by providing IDL code and software support for IAU_Chrom.

Experimental design and data evaluation as well as preparation of results for the manuscript and figures were done by J. Hoker.

Mechanical construction work conducted by the workshop of the institute (L. Merkel).

Atmospheric
Measurement
Techniques

Open Access

Comparison of GC/time-of-flight MS with GC/quadrupole MS for halocarbon trace gas analysis

J. Hoker, F. Obersteiner, H. Bönisch, and A. Engel

Institute for Atmospheric and Environmental Science, Goethe University Frankfurt,
Frankfurt, Germany

Correspondence to: A. Engel (an.engel@iau.uni-frankfurt.de)

Abstract. We present the application of time-of-flight mass spectrometry (TOF MS) for the analysis of halocarbons in the atmosphere after cryogenic sample preconcentration and gas chromatographic separation. For the described field of application, the quadrupole mass spectrometer (QP MS) is a state-of-the-art detector. This work aims at comparing two commercially available instruments, a QP MS and a TOF MS, with respect to mass resolution, mass accuracy, stability of the mass axis and instrument sensitivity, detector sensitivity, measurement precision and detector linearity. Both mass spectrometers are operated on the same gas chromatographic system by splitting the column effluent to both detectors. The QP MS had to be operated in optimised single ion monitoring (SIM) mode to achieve a sensitivity which could compete with the TOF MS. The TOF MS provided full mass range information in any acquired mass spectrum without losing sensitivity. Whilst the QP MS showed the performance already achieved in earlier tests, the sensitivity of the TOF MS was on average higher than that of the QP MS in the "operational" SIM mode by a factor of up to 3, reaching detection limits of less than 0.2 pg. Measurement precision determined for the whole analytical system was up to 0.2 % depending on substance and sampled volume. The TOF MS instrument used for this study displayed significant non-linearities of up to 10 % for two-thirds of all analysed substances.

1 Introduction

With increasing evidence that anthropogenic chlorinated and brominated hydrocarbons can be transported into the stratosphere and release chlorine and bromine atoms that can de-

plete ozone in catalytic cycles (Molina and Rowland, 1974; Farman et al., 1985; Solomon, 1990), the production and use of such species were regulated under the Montreal Protocol in 1987. Most of these fully halogenated compounds are declining in the atmosphere (Montzka and Reimann, 2011). However, many partially halogenated compounds are still increasing in the atmosphere (Montzka and Reimann, 2011), as are some newly detected fully halogenated species (Laube et al., 2014). Also, many fluorocarbons which do not destroy stratospheric ozone and are thus not regulated under the protocol show increasing trends in the atmosphere (Laube et al., 2012; Ivy et al., 2012; Vollmer et al., 2011). Although these fluorocarbons do not destroy ozone, many of them are strong greenhouse gases with long atmospheric lifetimes, resulting in increased radiative forcing of the troposphere. Therefore, the need persists for continuous measurements to identify new compounds in the atmosphere and monitor and document their atmospheric trends. The mass spectrometric instrument commonly used for halocarbon analysis is the quadrupole mass spectrometer (QP MS) (Cooke et al., 2001; Aydin et al., 2002; Miller et al., 2008; Sala et al., 2014). Besides the QP MS, the use of high mass resolving and extremely sensitive sector field MS has also been reported (Lee et al., 1995; Laube et al., 2014). Time-of-flight mass spectrometry (TOF MS) has only been applied sporadically for measurements of atmospheric trace gases (Kim and Kim, 2012; Kundel et al., 2012; Watson et al., 2011; Jordan et al., 2009) and in particular not with focus on halocarbons. The main advantage of coupling a TOF MS to a gas chromatograph (GC) over using the QP MS is the intrinsic full mass range acquisition and the better mass resolution and accuracy. The identification of unknown peaks is signif-

icantly facilitated by these advantages and the use of more narrow mass intervals is expected to reduce interferences and background noise. In addition, much higher data acquisition rates are possible using TOF MS, which is an advantage for fast chromatography. A TOF MS instrument can measure more than 10000 mass spectra per second. They are added up and averaged over a certain time period to yield the desired time resolution. The possibility of operating the TOF MS at high data rates is also of high interest for fast chromatography and narrow peaks, for which the operating frequency of quadrupole instruments (especially when measuring several ions) can be a limiting factor. The maximum time resolution for the TOF MS used in this study is 50 Hz. An increase in the data frequency will lead to decreased signal-to-noise levels. The data frequency must therefore be optimised to provide a sufficient number of data points per chromatographic peak while keeping the signal-to-noise level as high as possible. In contrast, a QP MS is a mass filter and will only measure one mass at a time. It needs to scan many individual masses sequentially to register a full mass spectrum. To achieve high sensitivity, QP MS are therefore often operated in single ion monitoring (SIM) mode in which the instrument is tuned to only one or a few selected ion masses and all other ions do not pass the quadrupole mass filter. Regardless of these limitations of the QP MS, it is widely used in analytical chemistry due to its stability, ease of operation, high degree of linearity, good reproducibility as well as sensitivity. Especially for atmospheric monitoring the advantage of obtaining the full mass information from the TOF instrument might allow retrospective quantifications of species which were not target at the time of the measurement. For this purpose the TOF MS must be well characterised (in particular with respect to linearity) and the calibration gas used during the measurements must contain measurable amounts of the retrospective substances and be traceable to an absolute scale.

In this paper, a comparison of a state-of-the-art QP MS and a TOF MS is presented, with both mass spectrometers being coupled to the same gas chromatographic system. The instrumental setup is described in Sect. 2. The GC QP MS system was characterised and used before for studies by Laube and Engel (2008); Brinckmann et al. (2012) and showed consistent results in the international comparison IHALACE (International Halocarbons in Air Comparison Experiment) with the NOAA (National Oceanic and Atmospheric Administration) network (Hall et al., 2013). We discuss the use of TOF MS in atmospheric trace gas measurements, in particular for the detection and quantification of halocarbons, focusing on four substances: CFC-11, CFC-12, Halon-1211 and Iodomethane. These four substances cover the boiling point and typical concentration range of a total of 35 substances analysed. The six key parameters for atmospheric trace gas measurements discussed in this paper are (1) mass resolution and (2) mass accuracy of the detectors, (3) stability of the mass axis and instrument sensitivity, (4) detector sensitivity represented by the limits of detection (LOD), (5) repro-
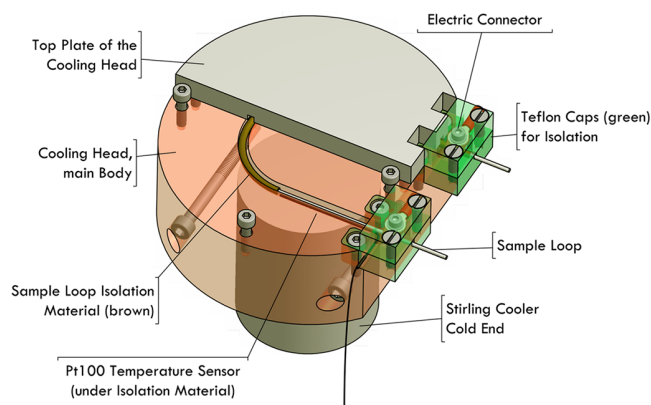
Figure 1. Schematic of the cooling head. The aluminium cylinder which contains the sample loop is placed on top of the Stirling cooler's cold end. Electric connectors are located at each end of the sample loop for resistive heating.

ducibility of the measurement procedure and (6) the linearity of the detectors for varying amounts of analyte. The underlying experiments are described in Sect. 3 and their results are discussed in Sect. 4. Section 5 summarises the results of this work.

2 Instrumental

2.1 Preconcentration unit

Atmospheric mixing ratios (mole fractions) of halocarbons are very low, i.e. in the parts per trillion (ppt) to parts per quadrillion range (ppq). To achieve signals clearly distinguished from noise in GC MS analysis, a sample preconcentration procedure is required. In this work, the method of sample preconcentration on adsorptive material followed by thermodesorption prior to gas chromatographic separation was used. Figure 1 shows a schematic of the preconcentration unit; an explanation follows. A similar setup was described by (Sala et al., 2014). A 1/16 inch stainless steel tube (sample loop, ID = 1 mm, length = 15 cm) packed with HayeSep D (10 mg) adsorption material was cooled to a temperature of −80 °C for sample preconcentration. The sample flow during preconcentration was adjusted to 50 mL min^{-1} controlled by a needle valve. For cooling, a Stirling cooler was used (Global Cooling, Inc., model M150). The sample loop was placed inside a cooled aluminium cylinder (cooling head) and was thermally and electrically isolated with two layers of glass silk and one layer of Teflon shrinking hose. The cooling head was thermally isolated towards ambient air with two layers of Aeroflex-HF material. All sample components which were not trapped on the adsorption material were collected in a 2 L stainless steel flask equipped with a pressure sensor. The pressure difference between beginning and end of the preconcentration phase was recorded to calcu-

late the preconcentration volume. After the preconcentration phase, the sample loop was heated resistively to $+180\,°C$ in a few seconds for instantaneous injection of the trapped analyte fraction onto the GC column. Desorption temperature was maintained for 4 min to clean the sample loop from all remaining compounds. All tubing (stainless steel) used for sample transfer between sample flask and preconcentration unit as well as preconcentration unit and GC was heated to $80\,°C$ to avoid loss of analytes to the tubing wall.

2.2 Gas chromatograph

An Agilent Technologies 7890A GC with a Gas Pro PLOT column (0.32 mm inner diameter) was used for separation of analytes according to their boiling points. The column had a total length of 30 m, divided inside the GC oven into 7.5 m pre-column (backwards flushable) and 22.5 m main column. Purified helium 5.0 (Alphagaz 1, Air Liquide, Inc.) was used as carrier gas. The GC was operated with constant carrier gas pressure on both pre- and main column. The temperature program of the GC consisted of five phases. (1) For the first 2 min, the temperature was kept at $50\,°C$. (2) Then the oven was heated at a rate of $15\,°C\,min^{-1}$ up to $95\,°C$, (3) from thereon at $10\,°C\,min^{-1}$ up to $135\,°C$ and (4) then at a rate of $22\,°C\,min^{-1}$ up to $200\,°C$. (5) The final temperature of $200\,°C$ was kept for 2.95 min. The resulting runtime was 17.95 min. The pre-column was flushed backwards with carrier gas after 12.6 min to avoid contamination with high-boiling substances. The gas chromatographic column was connected to the QP MS and the TOF MS using a Valco three-port union and two fused silica transfer lines. The transfer line to the QP MS had a total length of 0.70 m with an inner diameter of 0.1 mm, and the transfer line to the TOF MS had a total length of 2.10 m with an inner diameter of 0.15 mm. Based on the length, temperatures and inner diameters of the transfer lines, a split ratio of 63 : 37 (TOF MS : QP MS) was calculated. Using the ratios of the peak areas of the quadrupole when receiving the entire sample (TOF transfer line plugged) to those obtained in the split mode, a spilt ratio of 66 : 34 was calculated. We have adapted this latter value as it is based on actual measurements rather than calculations. All parts of the transfer lines outside the GC oven were heated to $200\,°C$.

2.3 Mass spectrometer

The two mass spectrometers in comparison were (1) an Agilent Technologies 5975C QP MS and (2) a Markes International (former ALMSCO) Bench TOF-dx E-24 MS. Both MS were operated in electron ionisation mode with an ionisation energy of 70 eV and ioniser temperatures of $230\,°C$. The QP MS was operated in SIM and SCAN mode (see Table 2 for more information). As the GC was operated in constant pressure mode, i.e. the head pressure of the columns were kept constant, the carrier gas flow into the two MS therefore
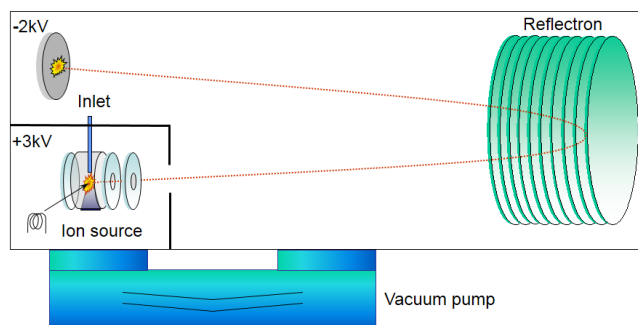
Figure 2. Scheme for the direct ion extraction of the Bench TOF-dx direct extraction (five technologies GmbH, G. Horner and P. Schanen, personal communication, 2014). The red dotted line represents a typical ion path.

varied according to the temperature ramp during each gas chromatographic run. Pressures inside the ion flight tubes of the MS therefore also varied; the TOF MS had a pressure range from 1.8×10^{-6} to 1.6×10^{-6} hPa and the QP MS had a pressure range from 2.1×10^{-5} to 1.8×10^{-5} hPa. The Bench TOF-dx uses a direct ion extraction technique with an acceleration voltage of 5 kV. In contrast to many other TOF instruments, the ions are accelerated directly from the ion source into the drift tube instead of extracting them from the ion source and then accelerating them orthogonally to the extraction direction (orthogonal extraction). The direct extraction method in combination with the high acceleration energy orients the instrument towards a high sensitivity, especially for heavier ions (five technologies GmbH, G. Horner and P. Schanen, personal communication, 2014). The TOF MS was set up to detect mass ranges from 45 to $500\,m/z$; higher and lower m/z were discarded. The reason to discard ions with m/z ratio below 45 was to eliminate a large part of the CO_2 which is trapped by our preconcentration method and can lead to saturation of the detector. A schematic of the Bench TOF-dx is given in Fig. 2. The spectra extraction rate was adjusted to 4 Hz to get a data acquisition rate comparable to that of the QP MS.

3 Experimental

All characterisation experiments were conducted using a high-pressure air sample (50 L Aluminium flask, 70 bar) filled in 2007 at Jungfraujoch, Switzerland. Prior to preconcentration, the air sample was dried using a heated ($70\,°C$) $Mg(ClO_4)_2$ water trap. Halocarbon mixing ratios were assigned to this reference gas by calibration against an AGAGE (Advanced Global Atmospheric Gas Experiment) gas standard (H-218). Table 1 shows reference gas mixing ratios of specific substances discussed in this paper.

Table 1. Mixing ratios in ppt in the reference gas used in this work for the discussed substances.

Substance	Formula	MR [ppt]	Scale
CFC-12	CCl_2F_2	544.42	SIO-05
CFC-11	CCl_3F	250.79	Prinn et al. (2000)
Halon 1211	$CBrClF_2$	4.41	Cunnold et al. (1997)
Iodomethane	CH_3I	0.88	NOAA-Dec09 Cohan et al. (2003)

3.1 Measurement procedure and data evaluation

To ensure measurement quality, both MS were tuned in regular intervals (autotune by operating software) at least every 2 months but especially before sample measurements and/or characterisation experiments. Autotune options of both mass spectrometers were used without further manual adjustments. To increase the sensitivity and linearity of the TOF MS, its detector voltage was increased by 30 V, as described in Sect. 4.6. Additionally, a zero measurement (evacuated sample loop), a blank measurement (preconcentration of purified Helium 5.0) and two calibration gas measurements were conducted to condition the system before every measurement series. At the end of every measurement series, another blank measurement was added. Every measurement series itself consisted of a calibration measurement followed by two sample measurements (same sample). This sequence of three measurements was repeated n times depending on the type of experiment and then terminated by a calibration measurement. For characterisation experiments both calibration and sample measurements were taken from the same gas cylinder (reference gas, see description above) but treated differently in data evaluation, e.g. as a calibration or sample measurement. Chromatographic peaks were integrated with a custom designed software written in the programming language IDL. The peak integration is based not on a standard baseline integration method commonly used in chromatographic applications but on a peak fitting algorithm. For the results shown here Gaussian fits were used for peak integration. This software was also used for data processing by Sala et al. (2014) and described there. Noise calculation was performed on baseline sections of the ion mass traces of interest. The noise level was determined as the 3-fold standard deviation of the residuals between data points and a second degree polynomial fit through these data points. This approach accounts for a drifting non-linear baseline. Otherwise, a non-linear baseline would cause an overestimation of the noise level. The integrated detector signal was divided by the preconcentration volume to get the detector response per sample volume. To account for detector drift during measurement series, the calibration measurements bracketing the sample pairs were interpolated linearly. Thereby, interpolated calibration points are generated for each sample measure-

ment. The response for each sample was then derived by calculating the quotient between sample and corresponding interpolated calibration point. Experiments were conducted to analyse six key parameters (Sect. 3.2 to 3.7) important for measurements of halogenated trace gases in the atmosphere: mass resolution, mass accuracy, limits of detection, stability of the mass axis and instrument sensitivity, measurement precision and reproducibility as well as detector linearity.

3.2 Mass resolution

The mass resolution (R) is defined as follows:

$$R = \frac{m}{\Delta m}, \tag{1}$$

with Δm being the full width at half maximum (FWHM) of the exact mass m of the ion signal.

The mass resolution determines whether two neighbouring mass peaks can be separated from each other. It is considered an instrument property, i.e. influenced only by internal factors like instrument geometry, ion optics, etc. The mass resolution of the TOF MS was calculated with its operating software ProtoTOF in a mass calibration tune. The QP MS was operated with MS Chemstation (Agilent Technologies, Inc.) which only processes unit mass resolution, independent of mass range.

3.3 Mass accuracy

The mass accuracy (δa) defined as

$$\delta a \text{ [ppm]} = \frac{m - m_m}{m_m \times 10^{-6}} \tag{2}$$

and quantifies the deviation between a measured ion mass m_m and the according expected exact mass m of each fragment. Like mass resolution, it is considered an instrument property. In this work, so called 1 amu centroid mass spectra are used to calculate mass accuracy. The exact mass is thus taken as the maximum intensity of the mass spectrum within a certain window (± 0.5 u) around the nominal mass. Mass accuracy was calculated for four different ion masses of four different substances: HFC-134a (CF_3^+, 68.995 u), CFC-12 ($CF_2^{35}Cl^+$, 84.866 u), CFC-11 ($CF^{35}Cl_2^+$, 100.936 u,) and methyl iodide (CH_3I^+, 141.928 u), which cover most of the mass range of the substance peaks in our chromatogram. Individual values for the mass accuracy were taken at the maximum of each chromatographic peak. Data from reproducibility experiments (see Sect. 3.6) as well as regular sample measurements were analysed to gain information about mass accuracy for the four exemplary ion masses. Only measurements taken under well-equilibrated conditions were used for this analysis. As the first two measurements of a measurement day often show enhanced variability they were excluded from the analysis of the mass accuracy.

Table 2. Dwell time settings for given substance fragments in QP MS modes with a data frequency of ≈ 3 Hz. SCAN mode (1): QP scanned from 50 to 500 u with 1.66 scans per second and a dwell time of 3.7 ms. Optimised (opti.) SIM mode (2): settings used for measurements on which LOD calculation was based, with 310 ms dwell time per ion and a scan rate of 3 scans per second. Operational SIM mode (3): default settings, used for reproducibility and linearity experiments with 3 scans per second.

Substance	Fragment	m/z [u]	QP SCAN mode for LOD calculation (1)	Optimised (opti.) SIM mode dwell time [ms] for LOD calculation (2)	Operational (oper.) SIM mode dwell time [ms] for LOD calculation (3)
			1.66 scans per second	3 scans per second	3 scans per second
CFC-12	$CCl^{35}F_2^+$	85	50 to 500 u		50
CFC-11	$CCl_2^{35}F^+$	101		310 ms dwell time	70
Halon 1211	$CCl^{35}F_2^+$	85	3.7 ms dwell time		100
Iodomethane	CH_3I^+	142			70

Table 3. Three exemplary halocarbon/hydrocarbon fragment pairs with equal unit mass but differing exact mass. The qualitative separating resolution (qual. R_{sep}) with $n_\sigma = 2$ and the quantitative separating resolution (quan. R_{sep}) with $n_\sigma = 8$.

Fragment	Exact mass m [u]	Δm [u]	Qual. R_{sep} $(n_\sigma = 2)$	Quant. R_{sep} $(n_\sigma = 8)$
$CClF_2^+$	84.966	0.136	> 600	> 2500
$C_6H_{13}^+$	85.102			
CF_3^+	68.995	0.075	> 900	> 3700
$C_5H_9^+$	69.070			
$C_2H_3^{35}Cl^{37}Cl^+$	98.958	0.159	> 600	> 2500
$C_7H_{15}^+$	99.117			

Table 4. The difference of the minimal (Min) and maximal (Max) values in % in one reproducibility experiment for the relative response is shown with a 1σ relative standard deviation (RSD) over all measurements (20) on this day. In the comment line the trend of the calibration gas over the day is given.

Mass spectrometer	Substance	Max−Min [%]	RSD [%]	Comment
TOF MS	CFC-12	4	1.41	linear
QP MS	CFC-12	4	1.28	linear
TOF MS	CFC-11	5	1.32	linear
QP MS	CFC-11	5	1.38	linear
TOF MS	Halon-1211	7	1.97	linear
QP MS	Halon-1211	1	0.63	linear
TOF MS	Iodomethane	10	3.73	scatter
QP MS	Iodomethane	5	1.92	scatter

3.4 Stability of the mass axis and instrument sensitivity

To evaluate the stability of the two mass spectrometers with respect to sensitivity and accuracy of the mass axis, a reproducibility experiment was used. The relative difference between the minimum and maximum detector response of the day and the 1σ standard deviation of all measurements over this day were taken as measures of the drift. For drift in mass accuracy over the day, the mean value and the 1σ standard deviation are given for the main masses for the following four compounds: HFC-134a (CF_3^+, 68.995 u), CFC-12 ($CF_2^{35}Cl^+$, 84.866 u), CFC-11 ($CF^{35}Cl_2^+$, 100.936 u,) and Iodomethane (CH_3I^+, 141.928 u). To evaluate the stability of the mass accuracy over a longer time period, the mass accuracy was calculated on measurement days with different time differences since the last mass calibration tune.

3.5 Limits of detection

The lowest amount of a substance that can reliably be proven is considered to be its LOD and serves as a measure for the sensitivity of the analytical system. Based on the assumption that a molecule fragment (f) can be detected when its detec-

tor signal height (H_{f_i}) is equal to or higher than 3 times the signal noise (N_{f_i}) on the adjacent baseline (signal-to-noise level (S / N) > 3), a limit of detection for a fragment (f_i) from an analyte substance (S_i) with a mass (m_{S_i}) in the injected sample can be calculated as

$$\text{LOD}_{S_i} = \frac{3 \cdot N_{f_i} \cdot m_{S_i}}{H_{f_i}}. \tag{3}$$

For comparison with the QP MS, the LOD of both instruments were calculated from calibration gas measurements by linear downscaling. Possible detector non-linearities were omitted in this case. The LOD error was considered to be the standard deviation of 10 calculated limits of detection. Different settings of the QP MS (SCAN mode (1), optimised (opti.) SIM mode (2) and operational (oper.) SIM mode (3)) were applied. In the SCAN mode (1), the quadrupole MS scanned from 50 to 500 u (comparable to the mass range of the TOF MS) with a dwell time of ≈ 3.7 ms ion^{-1} and a scan rate of 1.66 scans per second. In the optimised SIM mode (2), the quadrupole MS measured only one ion with a dwell time of 310 ms with ≈ 3 scans per second. In the operational SIM mode (3) the quadrupole MS measured several masses
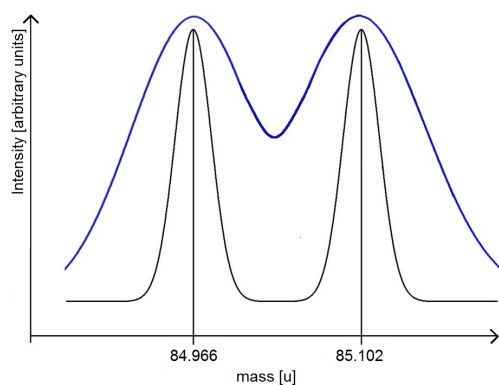
Figure 3. Schematic display of two different mass resolutions (blue and black curves). Two signals on masses 84.966 and 85.102 u with equal intensities demonstrate the mass separation with $R = 600$ (blue curve) and $R = 3700$ (black curve). Assuming Gaussian peak shapes for the signals, $R = 3700$ separates both peak by 8σ (quantitative separation) and $R = 600$ separates them by only 2σ (qualitative separation).

(up to six) in one scan with individual dwell times given in Table 2 and ≈ 3 scans per second.

The LOD in pg and ppq were calculated for 0.28 L sample volume with respect to the split ratio (see Sect. 2.2) and then extrapolated to 1 L of ambient air.

3.6   Reproducibility and measurement precision

The measurement precision describes the repeatability of a measurement. We determine the precision from the reproducibility (i.e. the standard deviation) of the measurements. The mean reproducibility is derived from dedicated multiple experiments designed to assess measurement precision (reproducibility experiment). Reproducibility was analysed over five measurement series, conducted on 5 different days, to give the mean measurement precision. Every experiment followed the procedure described in Sect. 3.1, with a total of 19 evaluated measurements of the same ambient air sample. A subset of the samples was treated as standard, the other part as unknown samples (two samples bracketed by two standards). Every individual measurement of these five series was conducted with a preconcentration volume of 0.28 L of the reference gas. Two additional reproducibility experiments were conducted with a higher preconcentration volume of 1 L to assess the possible dependence of the reproducibility on the preconcentrated sample volume. For each sample pair, the standard deviation of the relative response was calculated, summed up over all pairs and divided by the number of pairs to form the sample pair measurement reproducibility of that measurement series. The described procedure was applied to all analysed substances and reproducibility experiments. The mean value of measurement reproducibilities is considered to be the measurement precision of the system for the respective substance and volume.

3.7   Detector linearity

Detector linearity was analysed in two linearity experiments by varying the default preconcentration volume of 0.28 L by factors of 0.33, 0.66, 1.25 and 2 (sample positions in the measurement sequence, see Sect. 3.1). As calibration measurements, the default preconcentration volume was used. For comparison, detector responses were calculated as the ratio of the area of a chromatographic peak (A) to the preconcentration volume (V). All detector responses were normalised to 1 (relative detector response) by dividing them by the mean A/V of the calibration measurements. An ideally linear detector would show a relative response of 1 for any preconcentration volume used. The errors for the linearity measurements were derived as the 3-fold standard deviation given from reproducibility experiments.

4   Results and discussion

4.1   Mass resolution

If mass resolution is sufficiently high, it is possible to separate mass peaks of equal unit mass but differing exact mass. This separation drastically enhances the possibility to identify specific molecule fragments and to reduce cross-sensitivity. For halocarbon analysis, it is interesting to separate halogenated molecule fragments with exact masses typically below unit mass from other fragments with exact masses typically at or slightly above unit mass (e.g. hydrocarbon fragments). It could then be possible to reduce background noise generated by interfering ion signals or even compensate co-elution of non-target species from the GC column. For quantitative analysis the separation of adjacent mass signals implicates a possible loss of signal area when both mass peaks are not fully separated. The imposed error, i.e. the peak area lost due to separation, should not decrease measurement precision and should therefore be lower than the targeted measurement precision, in our case 0.1 %.

For this purpose, the definition of a qualitative and a quantitative separating resolution R_{Sep} is introduced (see Fig. 3 for an illustration). Assuming a Gaussian peak shape (normal distribution) of the ion signal on the mass axis, a separation of two neighbouring signals m_1 and m_2 (with $m_2 > m_1$) by 8σ (SD, 4σ per peak) is considered a quantitative separation (less than 0.01 % loss of peak area) while a separation by less than 8σ is considered to be only a qualitative separation. Further assuming that 1σ is approximately 1/2 FWHM (or 1/2 Δm respectively) and that Δm_1 is not significantly different from Δm_2, one can estimate R_{Sep} (at m_1 or m_2) for a known $(m_2 - m_1)$ difference:

$$R_{\text{sep}} = \frac{m_1}{\Delta m_1} = \frac{m_1}{\frac{2 \cdot (m_2 - m_1)}{n_\sigma}}. \tag{4}$$

For a value of $n_\sigma = 8$, Eq. (4) gives the quantitative separating resolution, while for a value of $n_\sigma = 2$ it gives a

Table 5. The limit of detection (LOD) in ppq and pg of the substances CFC-12, CFC-11, Halon-1211 and Iodomethane in 1 L of air sample per detector. The dwell times and settings for the QP MS are given in Table 2. The given errors are 1σ standard deviation.

Substance	LOD TOF [ppq]	LOD TOF [pg]	LOD QP [ppq] SCAN (1)	LOD QP [pg] SCAN (1)	LOD QP [ppq] opti. SIM (2)	LOD QP [pg] opti. SIM (2)	LOD QP [ppq] oper. SIM (3)	LOD QP [pg] oper. SIM (3)
CFC-12	25 ± 2	0.12 ± 0.02	241 ± 19	1.18 ± 0.09	21 ± 3	0.10 ± 0.01	48 ± 6	0.23 ± 0.30
CFC-11	31 ± 2	0.17 ± 0.02	370 ± 19	2.05 ± 0.29	36 ± 1	0.20 ± 0.01	64 ± 9	0.35 ± 0.05
Halon-1211	27 ± 2	0.182 ± 0.004	276 ± 53	1.84 ± 0.13	36.0 ± 0.3	0.240 ± 0.002	43 ± 5	0.29 ± 0.02
Iodomethane	12.00 ± 0.01	0.069 ± 0.001	Not a Number	Not a Number	16 ± 1	0.090 ± 0.003	42 ± 2	0.24 ± 0.05

Table 6. The reproducibility (REP) for the QP MS and the TOF MS as a mean value of five measurement series with 20 measurements each and a preconcentration volume of 0.28 L. The given errors are 1σ standard deviation over five reproducibility experiments.
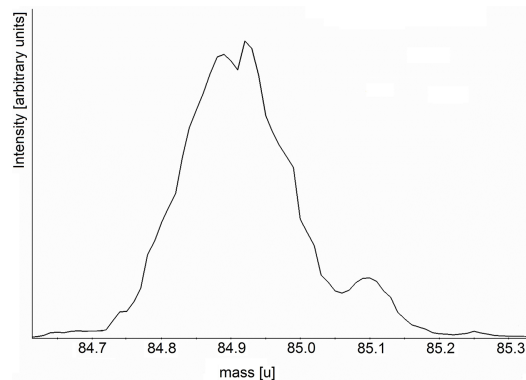
Substance	Formula	REP QP [%]	REP TOF [%]
CFC-12	CCl_2F_2	0.56 ± 0.31	0.56 ± 0.18
CFC-11	CCl_3F	0.45 ± 0.26	0.54 ± 0.23
Halon-1211	$CBrClF_2$	1.56 ± 0.52	0.94 ± 0.39
Iodomethane	CH_3I	3.96 ± 0.72	3.44 ± 1.61

Table 7. The reproducibility (REP) for the QP MS and the TOF MS as a mean value of two measurement series with 20 measurements each and a preconcentration volume of 1.00 L. The given errors are 1σ standard deviation over two reproducibility experiments.

Substance	Formula	REP QP [%]	REP TOF [%]
CFC-12	CCl_2F_2	0.22 ± 0.10	0.23 ± 0.09
CFC-11	CCl_3F	0.14 ± 0.03	0.16 ± 0.00
Halon-1211	$CBrClF_2$	0.60 ± 0.05	0.55 ± 0.21
Iodomethane	CH_3I	1.31 ± 0.23	0.99 ± 0.30

Figure 4. So-called 0.01 u mass spectrum of the substance Trichloromethane. Two mass peaks are shown. The higher one by mass 84.9 u is identified as the molecule fragment ($CH^{35}Cl^{37}Cl^+$) and the other one by mass 85.1 u is an unidentified hydrocarbon peak.

qualitative separating resolution. Table 3 shows some examples for qualitative and quantitative separating resolutions required for separation of halogenated mass fragments from hydrocarbon molecule fragments with slightly different masses.

To separate e.g. the $CClF_2^+$ ion signal from the $C_6H_{13}^+$ ion signal qualitatively, a resolution of 600 is necessary. For a quantitative separation, the mass resolution has to be $R = 3700$ according to the definition of 8σ separation (see above). For the Bench TOF-dx, the calculated mass resolution was $R = 1000$ at mass 218.985 u for the fragment $C_4F_9^+$ in a mass calibration tune by the software ProtoTOF. This allows a qualitative separation of two neighbouring mass peaks like the ones listed in Table 3, e.g. the separation of mass 84.966 u to mass 85.102 u. An example of a mass spectrum centred around 85 u is shown in Fig. 4 for a chromatogram of a typical ambient air sample at a retention time of 11.35 minutes. Two mass peaks, one centred at 84.943 u ($CH^{35}Cl^{37}Cl^+$), a fragment of the Trichloromethane ($CHCl_3$) molecule and one with a mass

slightly above unit mass, can be clearly distinguished. The higher mass is the result of an unidentified hydrocarbon peak eluting shortly before the Trichloromethane peak.

The resulting chromatogram centred at 11.3 minutes is shown in Fig. 5. Three different mass ranges were extracted from the raw data, the nominal mass range from 84.5 u to 85.5 u, the lower mass range from 84.7 u to 85.0 u and the higher mass range from 85.0 u to 85.3 u. When extracting the information centred around the unit mass range, a double peak is observed. An extraction of the lower mass range of the 85 u signal yields a much lower signal in the earlier eluting peak yet the signal cannot be reduced to baseline level. An extraction of the higher mass range of the signal gives a larger signal for the earlier eluting peak, but again the signal does not drop to baseline level.

This shows that the mass resolution of the Bench TOF-dx is sufficient to qualitatively show that two different fragments are present but that the resolution does not allow the separatation of these fragments in a way sufficient for quantifications. For a quantitative separation as defined above, the mass resolution of the Bench TOF-dx is not sufficient without further data processing steps like a peak deconvolution.

4.2 Mass accuracy

While sufficient mass resolution is necessary for an unambiguous separation of two mass peaks, mass accuracy is in addition needed for chemical identification of the detected ion. The better the mass accuracy, the lower the number of possible fragments that might be the source of the mass signal. The mass accuracy for the Bench TOF-dx was found to be in a range of 50 to 170 ppm for a mass range from 69 u to 142 u. Mass accuracies for the analysed target masses were determined as follows: (100 ± 60) ppm for mass 68.995 u, (80 ± 50) ppm for 84.966 u, (120 ± 50) ppm for 100.936 u and (130 ± 40) ppm for 141.928 u. A correlation between the displayed masses is observed: when the accuracy of one mass is decreased, the others are, too. There is no correlation given by the proximity of target masses to tuning compound (PFTBA, e.g. 68.995 u) masses. A suspected reason for the instability of the mass axis is the instrument temperature and resulting changes in material elongation. This is, however, speculation. At a mass resolution of $R = 1000$ at ion mass 85 u and an accuracy of 100 ppm, the mass difference between measured and exact mass would be 10 % of the FWHM of this mass peak (or 5 % at 50 ppm). The stability and absolute accuracy in the determination of the exact mass is thus not a significant additional limitation in the ability of the Bench TOF-dx to separate different ions (see Sect. 4.1).

4.3 Stability of the mass axis and instrument sensitivity

A reproducibility experiment was used to evaluate the stability of two detectors over a measurement series (typically 10 h). For that purpose, the minimum and maximum value of the detector response relative to all recorded responses and the 1-fold relative standard deviation of all recorded responses were used (see Table 4).

For the substances CFC-11 and CFC-12 the drift of the sensitivity of the TOF MS and QP MS are on the same level. For the low concentrated substances, the drift of the TOF MS is higher than that of the QP MS.

For evaluating the stability of the mass axis, the drift over a day was calculated as mean accuracy and standard deviation (1σ). The stability over a long time period was observed over different days away from a mass accuracy tune. As shown in Sect. 4.2 the mass accuracy of the Bench TOF-dx was observed to be on the order of 50–170 ppm. Within this uncertainty no drift of the mass axis with time could be observed for periods of up to 19 days after the mass axis calibration. The stability and absolute accuracy in the determination of the exact mass is thus not a significant additional limitation in the ability of the Bench TOF-dx to separate different ions (see Sect. 4.1).
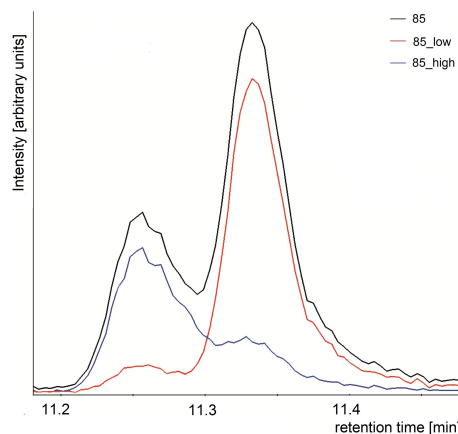
Figure 5. A chromatogram of an unidentified hydrocarbon peak (smaller one) eluting slightly earlier than the higher Trichloromethane peak. The nominal mass 85 u (black) shows a double peak. By choosing the lower mass range (84.7 u to 85.0 u; red) a lower signal for the unidentified hydrocarbon peak is observed, and by choosing the higher mass range (85.0 u to 85.3 u, blue) a lower signal for the Trichloromethane peak is observed.

4.4 Limits of detection

For halocarbon measurement, sensitivity is an important issue as atmospheric concentrations can be below $1\,\mathrm{pg\,L^{-1}}$ of ambient air, especially for newly released anthropogenic species. Table 5 shows the calculated LOD for the QP and the TOF MS for the four selected species with different measurement settings of the quadrupole MS detector.

For the QP MS, the signal-to-noise level of a certain m/z depends on the concentration and dwell time. The dwell time represents the time interval in which the quadrupole mass filter is tuned to the specific mass-to-charge ratio m/z before switching to the next mass setting. Lower dwell times will decrease sensitivity but allow for more different mass filter settings per scan, resulting in more different m/z monitored per time. Higher dwell times increase the detector sensitivity towards specified m/z ratios but reduce the number of m/z monitored per time. For this work, data based on three different instrument settings were used for LOD calculation (see Table 2). The SCAN mode of the QP MS was chosen for a direct comparison with the TOF MS (scan range from 45 u to 500 u) and is shown in Table 2 (1). Higher and lower m/z ratios were discarded. Reducing the scan range will result in better detection limits for the QP MS and theoretically also for the TOF MS as long as no significant amounts of ions heavier than the chosen upper scan limit are produced in the ion source. Remaining ions in the TOF MS flight tube from a preceding extraction would result in unambiguous detector signals. The optimised SIM mode monitors only one m/z of the respective substance, Table 2 (2). In measurements of ambient air, several m/z are usually monitored simultaneously (operational SIM mode (3)). The dwell times are optimised

for the different substances. For substances with high concentration shorter dwell times are chosen, while the dwell time is increased for substances with low concentrations in order to increase the sensitivity. Only one ion is measured for most species in order to reach optimum sensitivity. As a consequence, limits of detection are higher in such measurements as in the optimised SIM mode. Respective LOD for the discussed dwell time settings are shown in Table 5.

In comparison to the QP MS, the TOF MS is up to 12 times more sensitive than the QP MS in the SCAN mode. In the optimised SIM mode with increased dwell times (2) for specific ion masses, limits of detection in quadrupole MS and time-of-flight MS are similar. During routine measurements (operational SIM mode (3)), the limits of detection of the TOF MS were up to a factor of 3 lower than those of the QP MS.

4.5 Reproducibility

A high measurement precision is required as it is of great importance to detect very small variability of halocarbons in the atmosphere, e.g. to characterise trends of highly persistent substances (Montzka and Reimann, 2011; Montzka et al., 2009; Vollmer et al., 2006). Table 6 shows exemplary reproducibilities for both instruments based on a preconcentration volume of 0.28 L. The reproducibility is rather similar for both MS, with values below 1 % for the species with high ambient air concentrations and therefore high signal-to-noise levels (CFC-12 and CFC-11). For the species with lower concentration and lower signal-to-noise levels the reproducibility of the TOF seems to be slightly but not significantly better (see Table 6).

The reproducibilities shown in Table 6 are based on measurements with a relatively small sample volume. Larger preconcentration volumes should result in better reproducibilities as signal-to-noise levels are increased and error sources during sample preparation should become smaller relative to the sample volume. Therefore, two reproducibility experiments with a larger preconcentration volume of 1 L were performed. The results are shown in Table 7.

The increase of the preconcentration volume to 1 L yields a significant improvement of the measurement precision. The high signal-to-noise species CFC-12 and CFC-11 now show reproducibilities below 0.3 % for the QP and for the TOF. For the low signal-to-noise species Halon-1211 and CH_3I the reproducibilities are improved by a factor of up to 4 for the TOF MS and by a factor of up to 3 for the QP MS, with the TOF instrument showing better reproducibilities. As for the TOF MS, the detector itself was found to be a limitation to higher preconcentration volumes as it showed saturation effects for some analysed ions already at 0.5 L preconcentrated sample. For example, CFC-12 had to be evaluated on mass 87 u (relative abundance: 32.6 %) and CFC-11 on mass 103 u (relative abundance: 65.7 %) (NIST, 2014) as both main quantifier ion masses (85 and 101 u) showed satu-

ration in the respective retention time windows. This saturation reflects the limited dynamic range of the analog to digital converter (memory of 8 bits) used in the Bench TOF-dx.

4.6 Linearity

For the calculation of the mixing ratio of a measured substance, its detector signal has to be correlated with the signal of the same substance in a calibration measurement with known mixing ratio. If the detector behaves linearly, this correlation is linear and the calculation of the mixing ratio is straight forward. As mixing ratios in different air samples might vary to a great extent (e.g. diurnal variations of short-lived substances) (Sala et al., 2014; Derwent et al., 2012; Law and Sturges, 2011), a linear detector simplifies data evaluation to a great extent. Furthermore, retrospective analysis of substances that were not identified at the time of measurement is possible without an unknown error due to detector non-linearity. Figures 6 and 7 show linearity plots for the QP MS for the CFC-11 and CFC-12 based on two linearity experiments. The QP MS showed a linear behaviour within the measurement errors (3-fold measurement reproducibility for the respective substance). This linearity test includes possible effects of the preconcentration unit (quantitative adsorption and desorption) as well as the determination of the preconcentration volume, the GC and data processing (signal integration). Figures 6 and 7 illustrate results from the two linearity experiments for the TOF MS. For CFC-11 (Fig. 6) a deviation from linearity for small preconcentration volumes of nearly 10 % is observed, while detector behaviour is close to the ideal value for high preconcentration volumes. The red curve was derived based on the standard detector voltage of -2244.8 V. An decrease of the detector voltage by -30 V brought slight improvements but did not solve the issue. Figure 7 shows a linearity plot for the substance CFC-12. For CFC-12 the detector is considered to be linear within the error bars. Both detectors compared in this work depend on the same sample preparation and separation steps before detection. As measurement reproducibilities of QP MS and TOF MS were not significantly different, the direct comparison is possible without limitations. The examples displayed for the QP MS and the TOF MS are two of 35 substances measured and analysed. The QP MS showed linear behaviour for all substances within the uncertainty range. The non-linearity of the TOF-MS was highest for the low preconcentration volume (33 %, 0.09 L) with deviations of -10 to $+20$ % compared to a standard preconcentration volume of 100 % (0.28 L). For most substances the instrument showed a similar behaviour as observed for CFC-11 (decreased sensitivity for low amounts of analyte) while some species showed the opposite behaviour (increased sensitivity with decreasing amount of analyte). Reasons for this conflicting behaviour are still subject to further investigations. Proportionality of detector signal against the amount of analyte in the sample over the given concentration range was thus
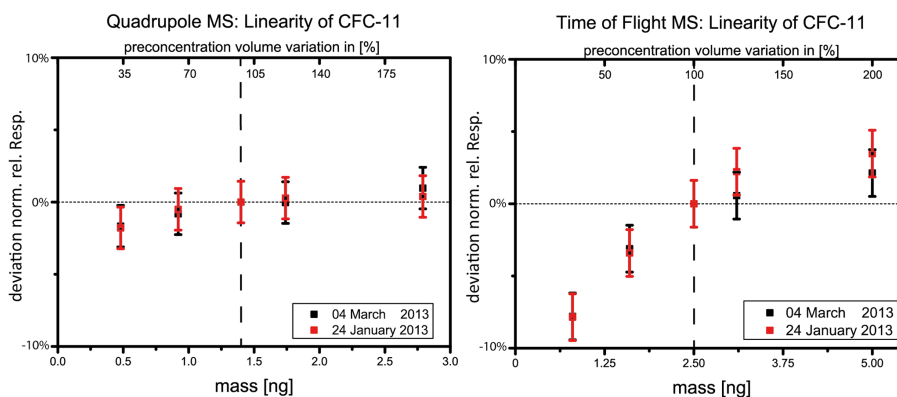
Figure 6. Linearity graphs of CFC-11 ($CFCl_2^+$ fragment) based on two different linearity experiments (red and black plots in each graph). Primary x axis (lower): mass on column in ng. Secondary x axis (upper): preconcentration volume variation in % versus a default preconcentration volume of 0.28 L (dashed line). Y axis: deviation from the normalised relative detector response versus the detector response of the default preconcentration volume). For every preconcentration volume, the relative response should be one in case of a linear detector behaviour (dashed line). The error bars show the three-fold measurement precision, on the left-hand side for the QP MS and on the right-hand side for the TOF MS. The second linearity experiment (black) of the TOF MS was conducted with an decreased detector voltage (-2274.8 V instead of -2244.8 V).
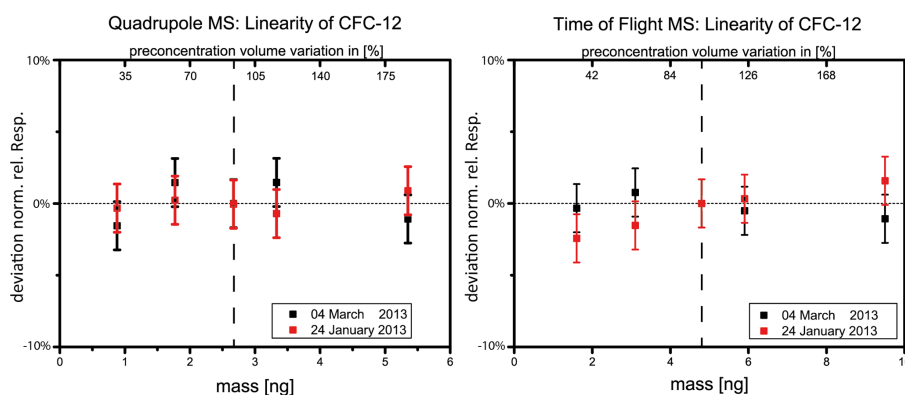
Figure 7. Same figure as Fig. 6 for the substance CFC-12 (CF_2Cl^+ fragment).

found for the QP MS but only for some species in the TOF MS. If the detector does not behave linearly, the relationship between the integrated peak area and the atmospheric concentration has to be approximated by a fit function. In order to generate this fit function, additional measurements with varying preconcentration volumes are necessary before each measurement series. This procedure was found to be necessary for the TOF MS. It lengthens measurement series, implies an additional error source and requires additional time for data processing.

5   Conclusions

A Markes International Bench TOF-dx was compared to an Agilent Technologies 5975 QP MS with respect to the measurement of halogenated trace gases in the atmosphere. Both detectors ran in parallel (66:34 split) after cryogenic

preconcentration and gas chromatographic separation of the air sample. The comparison included the mass resolution, mass accuracy, the limit of detection, the measurement precision (reproducibility) and the detector linearity. The TOF MS showed a resolution of 1000 and a Δm of 0.071 at mass 219.995 u with a mass accuracy of 50 to 170 ppm. Therefore it is able to qualitatively separate ion signals at different exact mass but equal unit mass (for example the mass 84.966 u from the mass 85.106 u by a Δm of 0.136). This qualitative mass separation of the TOF MS could be sufficient for improved substance identification and is an advantage over the QP MS. The QP MS does not allow for separation of exact masses as the mass resolution of QP MS instruments is generally too low ($R \approx 200$) for that purpose. The analysis of detection limits showed that the TOF MS is generally more sensitive than the QP MS (despite using selected ion monitoring mode). The LOD of the QP in the SCAN mode are up

to a factor of 12 higher than the LOD of the TOF MS. LOD of the TOF MS are lower by factors of up to 3 (Table 5) in comparison to the QP MS with operational SIM mode settings used for routine measurements. In the SIM mode with only one quantifier (optimised SIM mode) the TOF MS is similar to the QP MS. In that respect, the TOF MS with its very high sensitivity and full mass range information provides a considerable advantage compared to a QP MS. The reproducibility of both instruments was found to be on an equal level with slightly better reproducibilities of the QP MS at high signal-to-noise levels and slightly better reproducibilities of the TOF MS for low-concentrated species. Regarding detector linearity, the Bench TOF-dx in its current configuration could not compete with the QP MS. A high degree of linearity is, however, necessary for high accuracy measurements in trace gas analysis. The encountered non-linearities necessitate a correction which adds an error source, especially when there is a large concentration difference between sample and calibration measurement. It furthermore complicates measurements as well as data evaluation. For other applications where concentration variability is significantly higher than the non-linearity of the detector, the observed detector non-linearities might not be of such high relevance. In conclusion, the TOF MS does show advantages with respect to mass resolution and sensitivity without losing the full mass spectra information. Persisting non-linearities are a big disadvantage but might be conquered in the future by developments in detector electronics. With reduced non-linearities, TOF MS could well be the technology of the future for the analysis of halogenated trace gases in the atmosphere, despite the significantly higher costs of the TOF MS in comparison to QP MS instruments. These conclusions are only valid for the Markes International Bench TOF-dx E-24 MS and atmospheric trace gas measurements and might turn out differently for another field of research or another TOF MS.

References

Aydin, M. and De Bruyn, D. J. and Saltzman, E.: Preindustrial atmospheric carbonyl sulfide (OCS) from an Antarctic ice core, Geophys. Res. Lett., 29, 73, doi:10.1029/2002GL014796, 2002.

Brinckmann, S., Engel, A., Bönisch, H., Quack, B., and Atlas, E.: Short-lived brominated hydrocarbons – observations in the source regions and the tropical tropopause layer, Atmos.

Chem. Phys., 12, 1213–1228, doi:10.5194/acp-12-1213-2012, 2012.

Cohan, D. S., Sturrock, G. A., Biazar, A. P., and Fraser, P. J.: Atmospheric Methyl Iodide at Cape Grim, Tasmania, from AGAGE Observations, J. Atmos. Chem., 44, 131–150, doi:10.1023/a:1022481516151, 2003.

Cooke, K. M., Simmonds, P. G., Nickless, G., and Makepeace, A. P. W.: Use of Capillary Gas Chromatography with Negative Ion-Chemical Ionization Mass Spectrometry for the Determination of Perfluorocarbon Tracers in the Atmosphere, Anal. Chem., 73, 4295–4300, doi:10.1021/ac001253d, 2001.

Cunnold, D. M., Weiss, R. F., Prinn, R. G., Hartley, D., Simmonds, P. G., Fraser, P. J., Miller, B., Alyea, F. N., and Porter, L.: GAGE/AGAGE measurements indicating reductions in global emissions of CCl_3F and CCl_2F_2 in 1992–1994, J. Geophys. Res., 102, 1259–1269, doi:10.1029/96jd02973, 1997.

Derwent, R. G., Simmonds, P. G., O'Doherty, S., Grant, A., Young, D., Cooke, M. C., Manning, A. J., Utembe, S. R., Jenkin, M. E., and Shallcross, D. E.: Seasonal cycles in short-lived hydrocarbons in baseline air masses arriving at Mace Head, Ireland, Atmos. Environ., 62, 89–96, doi:10.1016/j.atmosenv.2012.08.023, 2012.

Farman, J. C., Gardiner, B. G., and Shanklin, J. D.: Large losses of total ozone in Antarctica reveal seasonal ClO_x/NO_x interaction, Nature, 315, 207–210, doi:10.1038/315207a0, 1985.

Hall, B. D., Engel, A., Mühle, J., Elkins, J. W., Artuso, F., Atlas, E., Aydin, M., Blake, D., Brunke, E.-G., Chiavarini, S., Fraser, P. J., Happell, J., Krummel, P. B., Levin, I., Loewenstein, M., Maione, M., Montzka, S. A., O'Doherty, S., Reimann, S., Rhoderick, G., Saltzman, E. S., Scheel, H. E., Steele, L. P., Vollmer, M. K., Weiss, R. F., Worthy, D., and Yokouchi, Y.: Results from the International Halocarbons in Air Comparison Experiment (IHALACE), Atmos. Meas. Tech., 7, 469–490, doi:10.5194/amt-7-469-2014, 2014.

Ivy, D. J., Arnold, T., Harth, C. M., Steele, L. P., Mühle, J., Rigby, M., Salameh, P. K., Leist, M., Krummel, P. B., Fraser, P. J., Weiss, R. F., and Prinn, R. G.: Atmospheric histories and growth trends of C_4F_{10}, C_5F_{12}, C_6F_{14}, C_7F_{16} and C_8F_{18}, Atmos. Chem. Phys., 12, 4313–4325, doi:10.5194/acp-12-4313-2012, 2012.

Jordan, A., Haidacher, S., Hanel, G., Hartungen, E., Märk, L., Seehauser, H., Schottkowsky, R., Sulzer, P., and Märk, T. D.: A high resolution and high sensitivity proton-transfer-reaction time-of-flight mass spectrometer (PTR-TOF-MS), Int. J. Mass Spectrom., 286, 122–128, doi:10.1016/j.ijms.2009.07.005, 2009.

Kim, Y.-H. and Kim, K.-H.: Ultimate Detectability of Volatile Organic Compounds: How Much Further Can We Reduce Their Ambient Air Sample Volumes for Analysis?, Anal. Chem., 84, 8284–8293, doi:10.1021/ac301792x, 2012.

Kundel, M., Huang, R.-J., Thorenz, U. R., Bosle, J., Mann, M. J. D., Ries, M., and Hoffmann, T.: Application of Time-of-Flight Aerosol Mass Spectrometry for the Online Measurement of Gaseous Molecular Iodine, Anal. Chem., 84, 1439–1445, doi:10.1021/ac202527a, 2012.

Laube, J. C. and Engel, A.: First atmospheric observations of three chlorofluorocarbons, Atmos. Chem. Phys., 8, 5143–5149, doi:10.5194/acp-8-5143-2008, 2008.

Laube, J. C., Hogan, C., Newland, M. J., Mani, F. S., Fraser, P. J., Brenninkmeijer, C. A. M., Martinerie, P., Oram, D. E., Röck-

mann, T., Schwander, J., Witrant, E., Mills, G. P., Reeves, C. E., and Sturges, W. T.: Distributions, long term trends and emissions of four perfluorocarbons in remote parts of the atmosphere and firn air, Atmos. Chem. Phys., 12, 4081–4090, doi:10.5194/acp-12-4081-2012, 2012.

Laube, J. C., Newland, M. J., Hogan, C., Brenninkmeijer, C. A. M., Fraser, P. J., Martinerie, P., Oram, D. E., Reeves, C. E., Röckmann, T., Schwander, J., Witrant, E., and Sturges, W. T.: Newly detected ozone-depleting substances in the atmosphere, Nat. Geosci., 7, 266–269, doi:10.1038/ngeo2109, 2014.

Law, K. S. and Sturges, W. T. L. A.: Global Ozone Research and Monitoring Report – Chapter 2, WMO, Geneva, Switzerland, 2011.

Lee, J. M., Sturges, W. T., Penkett, S. A., Oram, D. E., Schmidt, U., Engel, A., and Bauer, R.: Observed stratospheric profiles and stratospheric lifetimes of HCFC-141b and HCFC-142b, Geophys. Res. Lett., 22, 1369–1372, doi:10.1029/95gl01313, 1995.

Miller, B. R., Weiss, R. F., Salameh, P. K., Tanhua, T., Greally, B. R., Mühle, J., and Simmonds, P. G.: Medusa: A Sample Preconcentration and GC/MS Detector System for in Situ Measurements of Atmospheric Trace Halocarbons, Hydrocarbons, and Sulfur Compounds, Anal. Chem., 80, 1536–1545, doi:10.1021/ac702084k, pMID: 18232668, 2008.

Molina, M. J. and Rowland, F. S.: Stratospheric sink for chlorofluoromethanes: chlorine atomc-atalysed destruction of ozone, Nature, 249, 810–812, doi:10.1038/249810a0, 1974.

Montzka, S. A. and Reimann, S. L. A.: Global Ozone Research and Monitoring Report – Chapter 1, WMO, Geneva, Switzerland, 2011.

Montzka, S. A., Hall, B. D., and Elkins, J. W.: Accelerated increases observed for hydrochlorofluorocarbons since 2004 in the global atmosphere, Geophys. Res. Lett., 36, L03804, doi:10.1029/2008gl036475, 2009.

NIST: National Institute of Standards and Technology: Mass Spectral Search Program for the NIST/EPA/NIH Mass Spectral Library, Gaithersburg, MD, USA, 2014.

Prinn, R. G., Weiss, R. F., Fraser, P. J., Simmonds, P. G., Cunnold, D. M., Alyea, F. N., O'Doherty, S., Salameh, P., Miller, B. R., Huang, J., Wang, R. H. J., Hartley, D. E., Harth, C., Steele, L. P., Sturrock, G., Midgley, P. M., and McCulloch, A.: A history of chemically and radiatively important gases in air deduced from ALE/GAGE/AGAGE, J. Geophys. Res., 105, 17751–17792, doi:10.1029/2000jd900141, 2000.

Sala, S., Bönisch, H., Keber, T., Oram, D. E., Mills, G., and Engel, A.: Deriving an atmospheric budget of total organic bromine using airborne in situ measurements from the western Pacific area during SHIVA, Atmos. Chem. Phys., 14, 6903–6923, doi:10.5194/acp-14-6903-2014, 2014.

Solomon, S.: Progress towards a quantitative understanding of Antarctic ozone depletion, Nature, 347, 347–354, doi:10.1038/347347a0, 1990.

Vollmer, M. K., Reimann, S., Folini, D., Porter, L. W., and Steele, L. P.: First appearance and rapid growth of anthropogenic HFC-245fa ($CHF_2CH_2CF_3$) in the atmosphere, Geophys. Res. Lett., 33, L20806, doi:10.1029/2006GL026763, 2006.

Vollmer, M. K., Miller, B. R., Rigby, M., Reimann, S., Mühle, J., Krummel, P. B., O'Doherty, S., Kim, J., Rhee, T. S., Weiss, R. F., Fraser, P. J., Simmonds, P. G., Salameh, P. K., Harth, C. M., Wang, R. H. J., Steele, L. P., Young, D., Lunder, C. R., Hermansen, O., Ivy, D., Arnold, T., Schmidbauer, N., Kim, K.-R., Greally, B. R., Hill, M., Leist, M., Wenger, A., and Prinn, R. G.: Atmospheric histories and global emissions of the anthropogenic hydrofluorocarbons HFC-365mfc, HFC-245fa, HFC-227ea, and HFC-236fa, J. Geophys. Res., 116, D08304, doi:10.1029/2010jd015309, 2011.

Watson, N. and Davies, S. and Wevill, D.: Air Monitoring: New Advances in Sampling and Detection, The Scientific World JOURNAL, 11, 2582–2598, doi:10.1100/2011/430616, 2011.

iii. "An automated gas chromatography time-of-flight mass spectrometry instrument for the quantitative analysis of halocarbons in air"

Citation

Obersteiner, F., Bönisch, H., and Engel, A.: An automated gas chromatography time-of-flight mass spectrometry instrument for the quantitative analysis of halocarbons in air, Atmospheric Measurement Techniques, 9, 179-194, 2016. DOI: 10.5194/amt-9-179-2016

Own Contribution

Wrote the manuscript, which was proof-read by A. Engel and H. Bönisch as well as M. Gonin from Tofwerk AG. Prepared the answers-to-the-reviewers (proof-read by A. Engel and T. Schuck) as well as the final, revised version of manuscript and figures.

Developed the experimental design, partly together with H. Bönisch and A. Engel, conducted the experiments and evaluated and prepared the results for the publication.

Wrote the LabVIEW code which controls sample preconcentration, manages system states and can run fully automated measurement sequences.

Mechanical construction work was done by the workshop of the institute (F. Malkemper and L. Merkel).

Atmospheric
Measurement
Techniques

An automated gas chromatography time-of-flight mass spectrometry instrument for the quantitative analysis of halocarbons in air

F. Obersteiner, H. Bönisch, and A. Engel

Institute for Atmospheric and Environmental Science, Goethe University Frankfurt, Frankfurt, Germany

Correspondence to: F. Obersteiner (obersteiner@iau.uni-frankfurt.de)

Abstract. We present the characterization and application of a new gas chromatography time-of-flight mass spectrometry instrument (GC-TOFMS) for the quantitative analysis of halocarbons in air samples. The setup comprises three fundamental enhancements compared to our earlier work (Hoker et al., 2015): (1) full automation, (2) a mass resolving power $R = m/\Delta m$ of the TOFMS (Tofwerk AG, Switzerland) increased up to 4000 and (3) a fully accessible data format of the mass spectrometric data. Automation in combination with the accessible data allowed an in-depth characterization of the instrument. Mass accuracy was found to be approximately 5 ppm in mean after automatic recalibration of the mass axis in each measurement. A TOFMS configuration giving $R = 3500$ was chosen to provide an R-to-sensitivity ratio suitable for our purpose. Calculated detection limits are as low as a few femtograms by means of the accurate mass information. The precision for substance quantification was 0.15 % at the best for an individual measurement and in general mainly determined by the signal-to-noise ratio of the chromatographic peak. Detector non-linearity was found to be insignificant up to a mixing ratio of roughly 150 ppt at 0.5 L sampled volume. At higher concentrations, non-linearities of a few percent were observed (precision level: 0.2 %) but could be attributed to a potential source within the detection system. A straightforward correction for those non-linearities was applied in data processing, again by exploiting the accurate mass information. Based on the overall characterization results, the GC-TOFMS instrument was found to be very well suited for the task of quantitative halocarbon trace gas observation and a big step forward compared to scanning, quadrupole MS with low mass resolving power and a

TOFMS technique reported to be non-linear and restricted by a small dynamical range.

1 Introduction

The history of environmentally harmful airborne halocarbons and the need for monitoring them in the atmosphere goes back to the 1950s with the introduction of chlorofluorocarbons (CFCs) synthesized and promoted by Thomas Midgley (Midgley, 1937). The production of CFCs was banned by the Montreal Protocol in 1987 after highly rising emissions of CFCs and the subsequent discovery of the catalytic depletion of stratospheric ozone (Molina and Rowland, 1974) and the ozone hole (Farman et al., 1985). CFCs were replaced by partly halogenated hydrochlorofluorocarbons (HCFCs) and are nowadays replaced by a variety of hydrofluorocarbons (HFCs). HFCs do not destroy stratospheric ozone significantly (Ravishankara et al., 1994); nevertheless most of them are strong greenhouse gases with a global warming potential much larger than CO_2 (Velders et al., 2005). The ongoing introduction of new compounds and their release to the atmosphere (e.g. Arnold et al., 2012; Vollmer et al., 2011) leads to the need not only to monitor known compounds but also to identify new compounds. In the attempt to extend site measurements to emission surveillance, promising approaches have been made by combining measurement data with inverse modelling (e.g. Keller et al., 2011; Lunt et al., 2015; Maione et al., 2008; Simmonds et al., 2015; Stohl et al., 2010).

In the early days of halocarbon measurement, the electron capture detector was the instrument of choice

(Clemons and Altshuller, 1966). This choice moved to mass spectrometers later on as an additional dimension of information is added: molecule-specific fragmentation. Today, the most sophisticated instrumentation for the task is probably the Medusa GC-MS of the AGAGE (Advanced Global Atmospheric Gases Experiment) network described by Miller et al. (2008) with a quadrupole mass filter for detection. The Medusa systems have been applied for many investigations – from perfluorocarbons (Mühle et al., 2010), hydrocarbons (Grant et al., 2011) and nitrogen trifluoride (Arnold et al., 2012) to emerging HFCs just recently by Vollmer et al. (2015). In particular, quadrupole MS has been used by many others for halocarbon analysis (e.g. Grimsrud and Rasmussen, 1975; Sala et al., 2014; Simmonds et al., 1995) and sometimes also sector field MS (e.g. Laube et al., 2012; Lee et al., 1995). In contrast, TOFMS is much more widespread in other fields of research such as aerosol composition analysis (e.g. DeCarlo et al., 2006), measurements of volatile organic compounds (e.g. Graus et al., 2010) and proteomics (e.g. Bonk and Humeny, 2001). The big advantage of TOFMS over quadrupole MS and sector field MS is the intrinsic full mass range data acquisition without spectral skew. However, there were also two significant limitations to quantitative analysis with TOFMS observed in the past: limited dynamic range and non-linearity – e.g. as described by Emteborg et al. (2000), Rowland and Holcombe (2009) as well as Hoker et al. (2015) for the field of application of this work.

In this work, we go one step further from our first application of TOFMS for halocarbon analysis described in Hoker et al. (2015) using a BenchTOF-dx (Markes International Ltd, UK). A new GC-TOFMS system was set up including fully automated sample preconcentration and a Tofwerk EI-TOF model mass spectrometer with a significantly higher-than-nominal mass resolving power and data in a fully accessible data format. Technical descriptions regarding sample preparation, gas chromatography, mass spectrometry and data treatment are given in Sect. 2 of this paper. The presentation and discussion of characterization experiments and selected applications can be found in Sect. 3. The section is structured to go from basic parameters like mass accuracy (Sect. 3.1) over detection limits (Sect. 3.2) and measurement precision (Sect. 3.3) to non-linearities (Sect. 3.4) for which most aspects discussed before have to be considered. For quality assurance, we show results from a comparison to a reference instrument, a state-of-the-art GC-quadrupole MS (GC-QPMS), in Sect. 3.5.

2 Technical description

This section gives a technical overview of the GC-TOFMS discussed in this work. The instrument can be divided into three basic components (i) stream selection and sample preconcentration, (ii) gas chromatograph and (iii) mass

spectrometer. Explanations are given in Sects. 2.1 to 2.3. Section 2.4 gives information on instrument control and data processing.

2.1 Stream selection and sample preconcentration unit

The setup described in this work allows for the attachment of five different air samples, a calibration gas and a blank gas. Gas stream selection is realized by solenoid valves (Fluid Automation Systems, Switzerland) that allow for sample pressures up to 5 bars absolute; i.e. a pressure reducer has to be used for high-pressure flasks. All tubing ($1/8''$ stainless steel with Swagelok compression fittings, about 500 mm length) is heated to $> 100\,°C$ to reduce accumulation of water and other sample components on tubing walls. All samples with tropospheric water content were dried prior to preconcentration using magnesium perchlorate which was heated to $80\,°C$.

The very low mixing ratio range of the targeted analytes in the parts per trillion (ppt) to parts per quadrillion (ppq) mole fraction constitutes the requirement for a preconcentration before analysis with GC-MS. The usage of adsorptive material for that purpose is a widespread procedure in instrumental analytics. Cooling the adsorption material shifts the steady state of the adsorption–desorption process towards adsorption and is referred to as "cryotrapping" or "cryofocusing". The combination of cryofocusing–thermodesorption, i.e. rapidly heating the formerly cooled material for sample preconcentration and injection into an analytical instrument, has been quite common for nearly 20 years; see e.g. Simmonds et al. (1995), Kerwin et al. (1996) or Bassford et al. (1998) for the field of application related to this work.

A Sunpower CryoTel CT free-piston Stirling cooler (FPSC; Ametek Inc., USA) is used for cooling. On top of the cooler's cold tip, an anodized aluminium coldhead is placed which contains the sample loop, a $1/16''$ outer diameter and 1 mm inner diameter stainless steel tube. It is filled with HayeSep®D adsorption material (Vici Valco Inc., USA) over a distance of about 100 mm with a mesh size of 80/100 and a mass of about 20 mg adsorption material.

The adsorption temperature is set to about $-80\,°C$ to quantitatively trap the lowest-boiling substance separated by the GC column from CO_2 (HFC-23, CHF_3, boiling point: $-82.1\,°C$). For all measurements, a constant sample preconcentration flow rate of $100\,mL\,min^{-1}$ is set by a mass flow controller (MFC; EL-FLOW F-201CM, Bronkhorst, the Netherlands) mounted directly downstream of the sample loop. The MFC can also be used for sample volume determination (ΔV). All components of the sample air which are not trapped on the adsorption material are collected in a 2 L stainless steel flask ("reference volume") equipped with a pressure sensor (Baratron 626, 0–1000 mbar, accuracy including non-linearity 0.25 % of reading, MKS Instruments, Germany) for sample volume determination (Δp). Tubing

and reference volume are evacuated with a Vacuubrand MD-1 vario-SP membrane pump (Vacuubrand GmbH & Co. KG, Germany) before each preconcentration step. For desorption, the sample loop is heated to about 220 °C and flushed with carrier gas for 3 min to transport formerly trapped analytes onto the GC column. A similar sample preconcentration setup was described by Sala et al. (2014) and Hoker et al. (2015).

2.2 Gas chromatograph

An Agilent Technologies 7890B gas chromatograph is used to separate analytes before detection. A 0.32 mm ID Gas Pro PLOT column of 30 m length is used for chromatographic separation with purified helium 6.0 as carrier gas (Praxair Technologies Inc., German supplier. Purification System: Vici Valco HP2). The column is divided into a backwards flushable 7.5 m precolumn and a 22.5 m main column. Column head pressure was adjusted so that at maximum flow (lowest column temperature), the pressure inside the ionization chamber of the TOFMS is suitable ($< 5 \times 10^{-5}$ mbar) and that on the other hand chromatographic peaks are kept sharp at minimum flow (highest column temperature). The head pressure of the carrier gas flow in line with the MS is kept constant at all times.

The gas chromatographic runtime is 16 min, with an additional 3 min cooldown before the next run, which results in a total of 19 min per measurement. The initial oven temperature is 45 °C, which is held for 2.3 min and ramped linearly afterwards with 25 °C min^{-1} to 200 °C and held until 16 min. The precolumn is set to backflush position after the analyte with highest retention time t_R has reached the main column after 11 min to keep the gas chromatographic system free of contaminations with higher boiling compounds. The main column is connected to the MS with a 0.1 mm ID fused silica transfer line (length: about 350 mm) inside the GC oven. The capillary feedthrough into the ionizer of the MS is kept at 210 °C at all times.

Gas flow switching (backflush, injection, etc.) is implemented with two Valco 1/16″ 6-port/2-position valves (Vici Valco Inc., USA) which are kept at 180 °C outside the GC oven. Valco stainless steel 1/16″ connectors with Valcon T ferrules are used for fused silica tubing (Vici Valco Inc., USA). Carrier gas flow, as determined by the Agilent Technologies flow calculator, is 4.0 mL min^{-1} at the beginning and 2.3 mL min^{-1} at the end of the run. However, actual flow rates should lie slightly lower, as the calculation only includes column and transfer line to the MS but no additional restrictions in the flow path like e.g. two Valco 2-position valves, the sample loop and column connectors.

Within the chromatographic runtime of 16 min, a total of 68 substances were detected and identified (most of them halocarbons) in different air samples. The substance with the shortest retention time is HFC-23 (CHF_3, $t_R = 3$ min); the latest detectable substance is CH_2I_2 at $t_R = 15$ min.

2.3 Time-of-flight mass spectrometer

The mass spectrometer used in this work is a Tofwerk EI-TOF (model EI-003, Tofwerk AG, Switzerland) – an orthogonal extraction, single reflectron TOFMS with an electron ionization (EI) ion source, a quadrupole high-pass filter and a Photonis multichannel plate (MCP) electron multiplier (Photonis, USA). The PCIe data acquisition card records 1.6 GS s^{-1} with a 14 bit s^{-1} ADC (analog-to-digital converter) using an on-board averaging firmware. Ions are extracted orthogonally with a rate of 22 kHz into the flight chamber; about 5500 resulting waveforms are averaged to form one mass spectrum that is transferred to the PC and saved to the hard disk. Extraction frequency and number of averaged waveforms give a full spectra rate of 4 Hz. A mass range of up to 600 Th (Thomson; $1\,\mathrm{Th} = 1\,u/e$; u: unified atomic mass unit, e: atomic charge unit) is recorded, which corresponds to a maximum flight time of about 40 µs at the given dimensions of the flight tube, acceleration voltage, etc.

The choice of spectra rate is a compromise between chromatographic signal integration demands and minimum noise levels. For the described gaschromatographic setup, chromatographic peaks typically have a minimum width of about 4 s ($\pm 2\sigma$ assuming Gaussian peak shape). As TOFMS in contrast to the quadrupole MS is not a scanning technique, the intensity of the chromatographic peak is sampled by the extraction rate (22 kHz in this case) and is therefore not subject to spectral skew – i.e. a relative change of ion signal intensity during the time it takes to scan the mass spectrum. A spectra rate of 4 Hz giving roughly 15 data points per chromatographic peak was chosen for comparability with our other GC-MS systems (see e.g. Hoker et al., 2015; Sala et al., 2014). For the TOFMS, a lower spectra rate should be possible due to the lack of spectral skew. However, the identification of the lowest possible and of the optimal spectra rate is beyond the scope of this work.

The current data acquisition hardware of the TOFMS theoretically allows for spectra rates of up to 1 kHz (PCIe $\times 4$ port). However, as the extraction rate is constant (22 kHz in this case) and determined by the flight time of the heaviest ion produced in the ion source, a higher extraction rate causes fewer individual waveforms to be averaged which in consequence increases the noise level, assuming a relative error of mean of the counting events given as $1/\sqrt{n}$, with n being the number of waveforms in a spectrum.

The ionizer temperature was kept at 240 °C. Ionization energy was set to 70 eV with an emission current of 0.5 mA. Pressure inside the ionization chamber varied between 2.4×10^{-5} and 4.2×10^{-5} mbar, and pressure inside the flight chamber varied from 5.2×10^{-7} to 8.4×10^{-7} mbar – both depending on GC runtime and column outflow. The quadrupole high-pass filter was set to attenuate N_2^+ and O_2^+

signals and completely exclude ions lighter than 15 Th. This filter setting was kept constant during all chromatographic runs.

The MS is equipped with a calibrant pulser valve (Tofwerk AG, Switzerland) which can be programmed to release a few nanograms of a calibration substance (perfluoroperhydrophenanthrene, $C_{14}F_{24}$, CAS 306-91-2) into the ionization chamber. To ensure mass axis stability, calibrant pulses were triggered at the beginning of each chromatogram, prior to the elution of any compound. By this procedure, the mass axis can be recalibrated in each chromatogram as part of data processing.

2.4 Automation and data processing

The analytical system can run a fully automated sequence of measurements. The automation is based on a LabVIEW cRIO system (National Instruments Inc., USA) which controls the system state (preconcentration, desorption, etc.) and can start GC and MS to record the chromatogram.

The analysis of high-resolution mass spectrometric data is performed in the IDL programming environment (Exelis Inc., USA) using asymmetric Lorentzian fits on mass peaks to determine peak width for mass resolving power and peak centre for mass accuracy.

Intensities of specific masses in each mass spectrum recorded during the chromatographic run are calculated by summing specified intervals of the mass axis. Both nominal and accurate mass intensities are derived from the same raw data. For nominal mass intensities, an interval of ± 0.3 Th around the integer mass is used. For accurate mass intensities, an interval of ± 0.0250 Th around the calculated exact mass is used unless noted otherwise.

Determination of noise levels and integration of chromatographic signals is done in IDL with a custom-written widget-based software named IAU_Chrom. Previous versions of this software were used by Sala et al. (2014) and Hoker et al. (2015). IAU_Chrom was extended to include import and processing tools as well as viewing functionality for the HDF5 file format of the Tofwerk MS data. Chromatographic noise levels are calculated as the 3-fold standard deviation of the residuals between data points and a second-degree polynomial fit through these data points. This calculation is performed routinely for all quantifier masses on baseline sections with a typical length of 25 s which includes 100 data points in the calculation. Chromatographic peaks are integrated with a custom routine using the IDL "gaussfit" function. Signal heights used in signal-to-noise ratio calculation are also taken from this Gaussian fit.

Mixing ratios in the measured samples are determined by a relative calibration scheme, i.e. substance signals in sample chromatograms are referenced against respective signals in calibration gas chromatograms obtained from a high-pressure flask of ambient air with known mixing ratios.

A linear proportionality of injected amount and detector response is assumed. In a series of measurements, each sample measurement (or block of repeated measurements of the same sample) is bracketed by calibration gas measurements.

3 Characterization

Four aspects of the instrument are described in this section to give the reader an impression of the system's capabilities: mass accuracy and mass resolving power (Sect. 3.1), sensitivity and limits of detection (Sect. 3.2), measurement precision and reproducibility (Sect. 3.3) and non-linearity (Sect. 3.4). All results are based on GC-TOFMS data with recalibrated mass axis using signals from the calibrant pulser described in Sect. 2.3.

3.1 Mass accuracy and resolving power

Mass accuracy as used here refers to mass measurement accuracy, i.e. the accuracy of a measured mass-to-charge ratio m_{meas}/Q compared to the corresponding calculated mass-to-charge ratio m_{calc}/Q. The relative mass error E_{mac} is calculated as $E_{mac} = \frac{m_{meas} - m_{calc}}{m_{calc}}$; multiplication by 10^6 gives E_{mac} in ppm, which is the quantity that is referred to by mass accuracy. The term mass or ion mass is used synonymously to m/Q with $Q = 1$. The term mass resolving power is used according to the full width at half maximum (FWHM) definition of IUPAC (2014) as

$$R = \frac{m}{\Delta m} = \frac{m_{meas}}{\text{FWHM}(m_{meas})}.$$

Mass accuracy and resolving power are both core parameters of the MS. They are the basic determinants (in addition to sensitivity, see Sect. 3.2) of data quality with respect to measurement precision from a chromatographic point of view and the benefits from having accurate mass information for chemical identification. From an application point of view, mass resolving power determines whether neighbouring signals from ions of different masses can be separated and mass accuracy describes the uncertainty of the measured mass. Insufficient mass accuracy cannot be compensated by high mass resolving power and vice versa. In fact, low mass accuracy can render a high mass resolving power "unexploitable" to some extent as it represents the uncertainty of a found accurate mass.

Data from five different measurement series were analysed to determine what the achievable mass axis calibration quality is (minimum E_{mac}) and how E_{mac} varies over time – i.e. during one measurement series and between different measurement series. Different configurations of the TOFMS giving different average mass resolving powers were tested to determine how mass accuracy, mass resolving power and signal intensity are correlated.
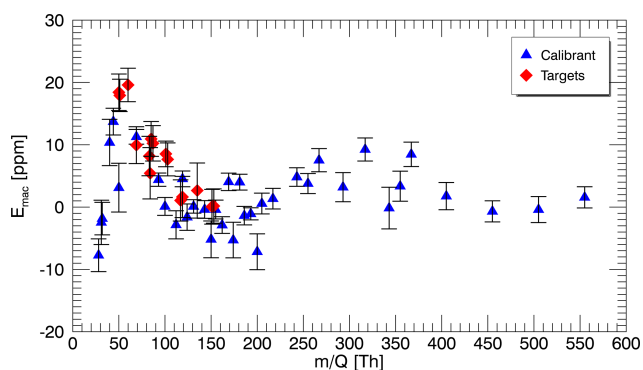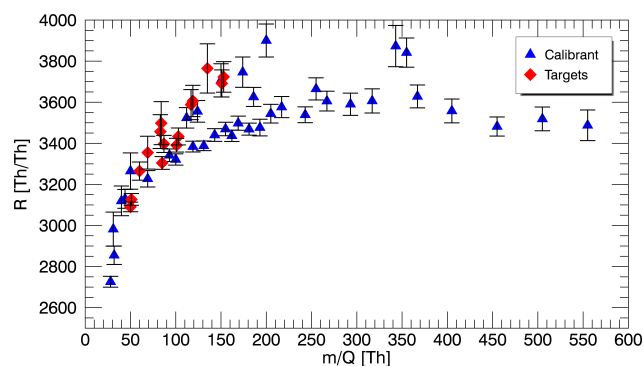
Figure 1. Mass accuracy (E_{mac}) in ppm over the whole mass range as determined for calibrant masses and masses of target substances during a measurement series. Error bars: 1-fold standard deviation from 44 individual measurements. Mean mass resolving power used in this measurement series: $R = 3500$.

Figure 2. Mass resolving power over the whole mass range as determined for all mass axis calibration masses found in calibrant pulses during a measurement series as well as 15 target masses from analyte molecules. Error bars: 1-fold standard deviation of each mass over 44 individual measurements.

3.1.1 Mass accuracy

Experimental values for the mass accuracy of calibrant masses (28–555 Th) were found to be $E_{mac} = (4 \pm 0.3)$ ppm as the arithmetic mean $\pm$ 1-fold standard deviation derived from five measurement series (186 measurements in total, based on absolute values of E_{mac}). Target substance masses (51–174 Th) within those measurement series showed a mean E_{mac} of (8 ± 0.8) ppm. Exemplary results for individual masses are shown in Fig. 1.

The variation of mass accuracies over the mass range is quite large relative to the mean value but generally not worse than 20 ppm, which is the manufacturer specification given as an absolute mass error of ± 0.002 Th at 100 Th. This specification can be considered as a worst-case estimate, especially when signals are very small. The underlying mass axis calibration model was chosen from a selection readily available from the manufacturer to yield best results over the whole mass range. The observed systematic dependency of E_m on m/Q (Fig. 1) is likely an artifact of the chosen model; different models might be better suited for individual sections of the mass axis.

For the target masses from analytes, only a slightly elevated E_{mac} was found compared to mass accuracies of calibrant masses used for mass axis calibration curve fitting. Mass accuracy also did not change significantly over the chromatographic runtime. Furthermore, mass accuracy was found to be stable over time, i.e. no significant trend over one measurement series or on average over different measurement series within a time span of multiple months as long as the same MS tuning was used. However, changes of ~ 100 ppm were observed during the first 1 to 2 hours of continuous measurement series (3–4 runs), probably caused by instrument warm-up and material elongation. This effect was compensated by the routinely executed recalibration of

the mass axis in each chromatogram, thereby achieving the mass accuracies discussed above.

3.1.2 Mass resolving power

In TOFMS, mass resolving power is anti-proportional to sensitivity to a certain extent. Assuming an optimal ion beam focusing, higher sensitivity would require more ions of equal mass to reach the detector – which in turn would cause a higher arrival time distribution per mass (Guilhaus, 1995). To optimize sensitivity at the given spectra rate and sample volume, a configuration giving an average of $R = 3500$ over the whole mass range was chosen. For further discussion of the effect of changes in mass resolving power on sensitivity, see Sect. 3.2.

Mass resolving power in general showed a stable behaviour over time, i.e. no significant trend during a measurement series or over multiple measurement series conducted with the same settings. Figure 2 shows the distribution of mass resolution along the mass axis. Resolving power for lighter ions is reduced compared to the average resolving power. This effect is known in TOFMS (e.g. Coles and Guilhaus, 1994) and caused mainly by the limited detection system bandwidth which determines single ion signal width. If a higher overall mass resolving power is enforced by instrument tuning (i.e. creating a narrower ion arrival time distribution), this limitation becomes clearly visible for lighter ions while heavier ions might not yet be affected. From an application point of view, this aspect has to be considered when very light ions (mass < 30 Th) are the focus of the analysis.

Based on an analysis of the mass axis calibration masses in routine measurement data (default resolving power setting $R = 3500$), a slight negative correlation of mass resolving power and ion signal height was found with a Spearman rank correlation coefficient of $\rho = -0.4$ ($p < 0.05$) in mean over the five analysed measurement series. The correlation

Table 1. Experimentally determined fragmentation and measured ion masses of fragments from HFC-1234yf (CH_2CFCF_3) in an air sample from a parking lot. Approximate HFC-1234yf mixing ratio in this sample: 3–4 ppt. For identification, the maximum intensity spectrum was chosen within the chromatographic peak.

Fragment	CF_3^+	$C_2H_2F_2^+$	$C_3H_2F_4^+$	$C_3H_2F_3^+$
m_{calc}/Q [Th]	68.9947	64.0119	114.0087	95.0103
m_{meas}/Q [Th]	68.9958	64.0116	114.0091	95.0126
E_{mac} [ppm]	+16	−5	+3	+24
Experimental relative abundance	1	0.78	0.64	0.40

between mass accuracy and ion signal height was found to be $\rho = +0.2$ but with very high p values > 0.1 and therefore of low significance. The correlation was more pronounced with $\rho = -0.8$ (resolving power) and $\rho = +0.8$ (mass accuracy) for the target ions from analyte molecules, both correlations with p values < 0.01.

The correlation of mass resolving power and intensity implies that a very small signal has an above-average mass resolution as smaller signals get effectively narrower due to decreased ion velocity disturbance by other ions of equal mass. This effect is clearly visible for the target substance ions and also selected calibrant masses displayed in Fig. 2; every mass with an elevated mass resolution compared to an interpolated mass-to-R curve in Fig. 2 was found to have below-average signal intensity (calibrant as well as targets). When becoming even smaller, signals are on the other hand afflicted with below-average mass accuracy as counting statistics quality decreases.

3.1.3 Exemplary identification of HFC-1234yf

Substance HFC-1234yf (CH_2CFCF_3, CAS 754-12-1) was introduced as a replacement for HFC-134a (CH_2FCF_3) in mobile air conditioning systems in 2011 and can already be detected at remote measurement sites as published by Vollmer et al. (2015). The identification of emerging substances like the one used as an example here is often difficult due to an unknown fragmentation. However, the CH_2CFCF_3 molecule should form CF_3^+ (69 Th), CH_2CF^+ (45 Th), $CH_2CF_2^+$ (64 Th), $CH_2CFCF_3^+$ (114 Th) and related ions. Likelihood of identification can then be significantly increased by using accurate mass information. Table 1 shows experimentally determined fragmentation and measured masses of the four most abundant fragments observed in an air sample with an elevated concentration of HFC-1234yf; the chromatographic peak of HFC-1234yf is shown in Fig. 3. Thanks to the all-time full mass range data acquisition of the TOFMS, no dedicated mass filter settings are necessary for identification as would be the case with a quadrupole MS.
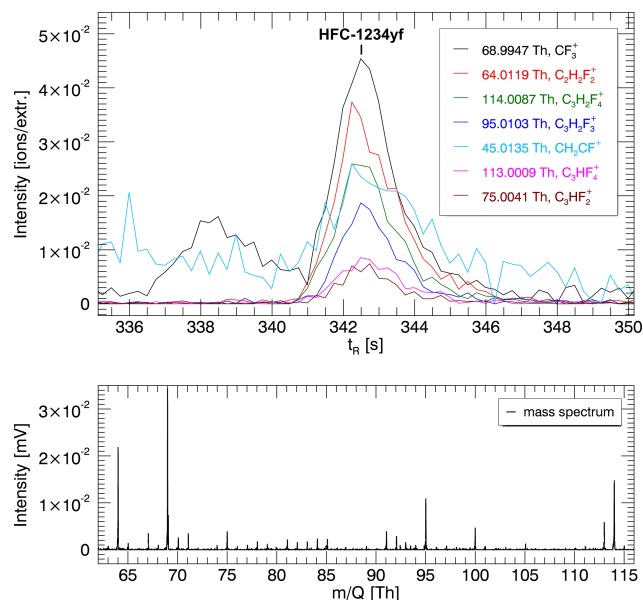
Figure 3. Upper graph: chromatographic signal of HFC-1234yf (CH_2CFCF_3) at a retention time (t_R) of 343 s observed in an air sample from a parking lot. Lower graph: mass spectrum excerpt at the chromatographic peak apex. Y axis unit conversion, lower to upper graph: divide by the number of extractions per spectrum and the signal intensity of a single ion (determined separately).

3.2 Sensitivity and limits of detection

To characterize the analytical system in respect to its sensitivity, the lowest detectable amount of a substance (limit of detection, LOD) is the quantity of interest. Due to the general applicability to all signals caused by substances with known mixing ratios in the sample, a signal-to-noise ratio (S/N; signal represented by the signal height) of 2 : 1 was chosen as detection limit in accordance with IUPAC (1998).

As the instrument discussed here offers the possibility to increase sensitivity by trading off mass resolving power (see also Sect. 3.1), changes in sensitivity were analysed relative to different mass resolving power settings of the MS. Furthermore, the detector is not independent of the chromatographic system; its effects on noise levels are therefore discussed based on the analysis of different baseline sections from a sample measurement series. To answer the question of where the actual limits of detection lie, a practical example is given for the substance Halon-1202 (CF_2Br_2) which was detected at $S/N \approx 2$. Additional LOD for different substances were derived from measurements of different ambient air samples to include possible sample matrix effects on LOD. A description of the applied noise level and signal height determination was given in Sect. 2.4.

Table 2. Comparison of different resolving power settings with regard to changes in sensitivity. Values based on 10 measurements per setting and 37 calibration masses for resolution calculation (avg. R, ΔR). Changes in S/N ($\Delta S/N$) determined as the mean relative change in S/N for 39 substances. From the total of 68 identified substances, a variable fraction could be integrated depending on the resolving power setting as shown in the last column (n subst. integrated). All values were determined with accurate mass intensities.

avg. R	ΔR	$\Delta S/N$	n subst. integrated
2577	-27%	$+38\%$	59 ($+9\%$)
3545	100%	100%	54
4477	$+26\%$	-64%	39 (-28%)

3.2.1 Sensitivity and its interdependence on mass resolving power

As pointed out before, an increase in sensitivity of the TOFMS goes along with reduced mass resolving power (see Sect. 3.1). The task for the user is to choose a resolving power setting which gives optimum sensitivity and data density for the desired application and spectra rate.

Table 2 shows a comparison of three different mass resolving power settings and the resulting changes in sensitivity, represented by a change in S/N relative to the default setting. While mass resolving power changed by approximately $\pm 25\%$ relative to the commonly used setting $R = 3500$, the changes in S/N are more pronounced with $+38$ and -64%. This implies that the anti-correlation between resolving power and sensitivity is not linear and has an optimum that depends on the user's requirements. The final column of Table 2 gives a more practical view on the experiment: the number of integrable substance signals substantially decreases with increasing mass resolving power. However, the change in number of integrable substances does not totally reflect the change in S/N. This can be related to the integration method and/or individual properties of the chosen substances.

3.2.2 Dependence on chromatographic effects

A key parameter in the discussion of sensitivity is the noise level. A special property of a chromatographic system is that noise levels can change over the chromatographic runtime with changing column temperature and pressure due to increased mobility of high-boiling compounds, column bleeding, etc. In most cases, column temperature and noise level are positively correlated. Furthermore, the correlation strength also depends on ion mass.

For the GC-MS system discussed here, Table 3 shows a comparison of three different ion masses typically formed by halocarbons and their change of noise level depending on the baseline section where noise is calculated. It has
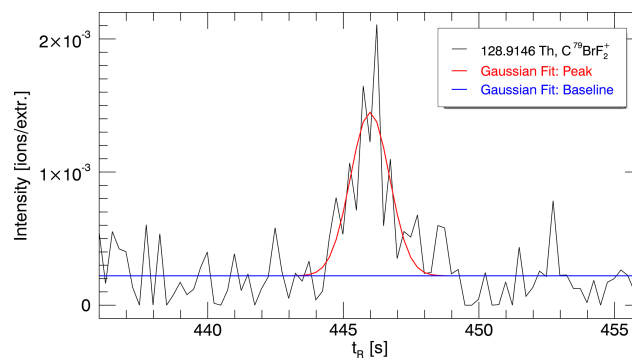
Figure 4. Chromatographic signal of Halon-1202 (CF_2Br_2) on mass 128.9146 Th ($C^{79}BrF_2^+$ fragment) at a retention time (t_R) of 446 s. Sample: H-218 flask AGAGE calibration gas, 490 mL preconcentration volume.

to be pointed out that noise levels change by factors of ~ 3 depending on the position in the chromatogram. Limits of detection based on S/N are therefore dependent on the retention time and qualifier/quantifier ion of the substance of interest. The detection limits of substances with ion masses displayed in Table 3 seem to be limited by the chromatographic system (and not the MS) towards higher retention times as noise levels tend to increase over the chromatographic runtime.

To illustrate the benefit of the use of accurate mass information on noise levels, Table 4 shows a comparison of the noise levels for m/Q 69 Th, comparing intensities derived from the nominal mass interval (69 ± 0.3 Th) to intensities derived from narrow mass interval around the calculated mass of the CF_3^+ ion (68.9947 ± 0.025 Th). This ion mass is known to be quite noisy relative to other ion masses, especially later in the chromatogram as demonstrated in Table 3 (column 3 vs. column 2).

Two things can be observed: first, noise levels are significantly reduced by ca. 70 % in all samples when using the accurate mass intensities instead of the nominal mass intensities. Second, the relative comparison of the noisiest sample (S_01) shows that the elevation in noise level, compared to the other samples, is strongly reduced when the accurate mass is used (70 % elevation on nominal mass intensities vs. 12 % elevation on accurate mass intensities). The analytical system gains independence from sample matrix effects by the usage of accurate mass intensities.

3.2.3 Detection limits derived from quantified substances

To demonstrate detection limits from a practical point of view, Fig. 4 shows the integrated signal of Halon-1202 (CBr_2F_2) which was detected and integrated at a signal-to-noise ratio of ≈ 2.

A mixing ratio of (0.035 ± 0.006) ppt was determined for the sample shown here (calibration scale of Halon-1202:

Table 3. Intra-sample comparison of noise levels on three typical halocarbon ion masses (nominal mass intensities). For each ion mass, two baseline sections were chosen for noise calculation, at the beginning and towards the end of the chromatogram. Noise levels and according 1σ standard deviations were determined over 40 chromatograms measuring the same reference gas and constant sample volume of 0.66 L. The Δ Noise row shows noise on late baseline section divided by noise on early baseline section.

Mass:	69 Th nominal		85 Th nominal		101 Th nominal	
Baseline section [s]	200–225	930–950	200–225	930–950	200–225	800–825
(Noise $\pm 1\sigma$) $\times 10^{-3}$	4.5 ± 0.50	17 ± 2.0	1.5 ± 0.13	4.1 ± 0.35	0.96 ± 0.076	3.2 ± 0.21
Δ Noise (late/early)	3.7		2.7		3.3	

Table 4. Inter-sample comparison of noise levels on nominal mass (69 ± 0.3) Th and accurate mass 68.9947 ± 0.025 Th (CF_3^+) for four different samples. Both signals were extracted from the same raw data as described in Sect. 2.4. Noise levels were calculated as means over five measurements per sample on a baseline section from 870 to 895 s chromatographic time. Errors given as the corresponding 1-fold standard deviations. All samples were measured in one measurement series with constant sample volume and the same MS settings.

Sample	S_01	S_02	S_03	S_04
Nominal 69 Th: (noise $\pm 1\sigma$) $\times 10^{-3}$	32 ± 0.7	19 ± 1.3	19 ± 1.7	17 ± 0.9
CF_3^+, 68.9947 Th: (noise $\pm 1\sigma$) $\times 10^{-3}$	7.2 ± 0.32	6.4 ± 0.20	6.8 ± 0.75	6.3 ± 0.32
Noise ratio, nominal/accurate	4.4	3.0	2.8	2.7

UEA-2009). For a 1 L air sample, the calculation gives a LOD of (0.016 ± 0.003) ppt, which equals (0.138 ± 0.024) pg Halon-1202 per litre of air at standard temperature and pressure.

LOD were found in the sub-ppt and sub-pg range for all analysed substances and even go down to the low ppq or fg range for some species. Detection on accurate mass instead of detection on nominal mass yields LOD improvements by factors of 5 and more. Table 5 shows an excerpt from calculated LOD for six different substances roughly covering the mass and retention time range of the chromatogram.

LOD were calculated as arithmetic means of five different samples measured five times each during one measurement series as well as the calibration gas to include sample matrix effects on detection limits.

From Table 5 it can be observed that the compounds Halon-1301 ($CBrF_3$) and HCFC-22 ($CHClF_2$), both detected on fluorinated fragments, show less improvement in LOD on accurate mass compared to the other three compounds. An explanation could be that the noise on nominal mass 51 and 69 Th is caused mainly by the CHF_2^+ and CF_3^+ fragments, especially for the corresponding relatively early baseline sections (see also Table 4). In comparison, the $CH_2^{35}Cl_2^+$ and $CH_2^{79}Br^{81}Br^+$ from dichloromethane (CH_2Cl_2) and dibromomethane (CH_2Br_2) show much more pronounced improvements as most of the noise is potentially not produced by those fragments.

In general, we cannot quantify how much sensitivity will be gained for which ion mass. A strong positive correlation was found between retention time and mass over the full substance range with $r = 0.70$ ($p < 10^{-7}$). It is therefore very difficult to disentangle, if there also is e.g. a significant correlation between gain in S/N and mass (attributing the effect to the MS) or gain in S/N and t_R (attributing the effect to the chromatographic system).

3.3 Precision and reproducibility of quantification

In order to quantify small trends of long-lived species like CFC-12, CFC-11 or CFC-113 (Carpenter et al., 2014) with only a few individual measurements, a high measurement precision is necessary. Additionally, high measurement precision is a prerequisite to analyse systematic effects and potential systematic errors like system non-linearities in measurement data.

Measurement precision as variability of the measured values around a mean value (random error) is analysed with so-called precision experiments consisting of up to 50 measurements of the same reference gas with constant sample volume. Within this series, a subset of measurements is treated as calibration points and another subset as samples. This gives blocks of repeated sample measurements between bracketing calibration points. Calibration is achieved by linear interpolation between calibration points and referencing the bracketed samples to the calibration, giving a relative response for every sample measurement. An ideal measurement should give a relative response of 1; i.e. the spread around 1 represents the measurement precision. Measurement precision of an individual measurement is then taken to be the mean standard deviation of all sample subsets of the series. To gain information about the reproducibility of the measurement precision derived from individual experiments, multiple precision experiments as well as routine sample measurement series were taken into consideration. A normal sample measurement is principally

Table 5. Limits of detection for six different species with different retention times and fragment masses: values derived from the analysis of five different air samples calibrated against a secondary standard of the AGAGE network (flask H-218) as well as the calibration gas itself (mean LOD shown). Sample volume was extrapolated from approximately 490 mL to 1 L. LOD were calculated based on an evaluation of the respective (1) nominal and (2) accurate mass intensities (see Sect. 2.4 for details). Errors were derived from mean errors of noise and height calculation for each sample. The ratio of nominal mass LOD to accurate mass LOD is shown in the last column.

| Substance	t_R [s]	Fragment	m_{calc}/Q [Th]	(1) nominal LOD [ppt]	(1) nominal LOD [pg]	(2) accurate LOD [ppt]	(2) accurate LOD [pg]	nom./acc.
Halon-1301	232	CF_3^+	68.9947	0.107 ±0.0076	0.644 ±0.0453	0.105 ±0.0071	0.631 ±0.0428	1.0
HCFC-22	313	CHF_2^+	51.0041	0.079 ±0.0040	0.277 ±0.0138	0.066 ±0.0043	0.230 ±0.0150	1.2
Halon-1211	379	$CF_2^{35}Cl^+$	84.9651	0.078 ±0.0346	0.517 ±0.2306	0.054 ±0.0038	0.357 ±0.0253	1.4
Dichloromethane	491	$CH_2^{35}Cl_2^+$	83.9528	0.123 ±0.0039	0.421 ±0.0132	0.022 ±0.0018	0.075 ±0.0063	5.6
Halon-2402	516	$C_2F_4^{79}Br^+$	178.9114	0.008 ±0.0003	0.086 ±0.0029	0.003 ±0.0003	0.034 ±0.0028	2.5
Dibromomethane	606	$CH_2^{79}Br^{81}Br^+$	173.8497	0.018 ±0.0011	0.128 ±0.0078	0.004 ±0.0004	0.030 ±0.0027	4.3

the same as a precision experiment with the exception that a real air sample instead of a reference gas is analysed in a sample block.

3.3.1 Measurement precision

Measurement precision in regard to analyte quantification for a single measurement was found to be better than 1 % for about 15 out of 47 analysed substances and in good correlation with the signal-to-noise ratio of the respective substances. Best values were achieved for CFC-12 at exact ion mass 84.9651 ($CF_2^{35}Cl^+$) with 0.15 % individual measurement precision and 0.08 % error of mean for sample blocks of three subsequent measurements of the same sample (evaluation of accurate mass).

Figure 5 illustrates the precision range of the instrument for 47 analysed substances (mostly halocarbons, evaluation of nominal mass intensities) and their correlation with the signal-to-noise ratio. It can be observed that measurement precision exponentially improves with exponentially increasing signal-to-noise ratio with a good correlation coefficient of $r^2 = 0.86$. The quality of the correlation was underlined during routine measurements by the fact that outliers did indicate "problematic" substances like e.g. methyl iodide which was found in the system blank.

The lower end of precision ($> 10\%$) is limited by signal quality – i.e. signals with a signal-to-noise ratio < 3 constitute a problem for the integration routine used to determine signal area. At the high end of precision, a very large increase in S/N seems to be necessary to achieve higher precision, i.e. approximately doubling the sample volume from 0.66 to 1.33 L to improve precision from 0.2 to 0.1 %. A precision
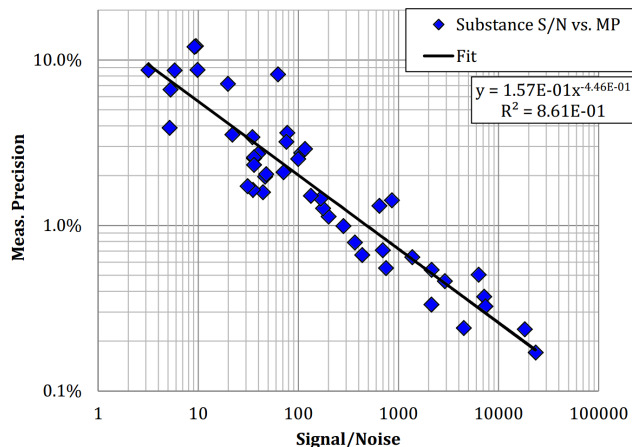
Figure 5. Correlation of measurement precision (y axis, MP) and signal-to-noise ratio (x axis) on a double-logarithmic plot. Data derived from repeated measurements of the same reference gas at constant sample volume of about 0.66 L; evaluation based on nominal mass intensities.

experiment with a preconcentration volume of about 1.38 L showed that this theoretical extrapolation of the correlation is not valid. S/N did increase but not linearly and measurement precision was even lower in mean although it was improved for some species, mostly in the lower S/N regime < 100. These findings imply that chromatographic effects play an important role and that there is an optimum sample volume if overall measurement precision should be maximized with a given chromatographic setup.
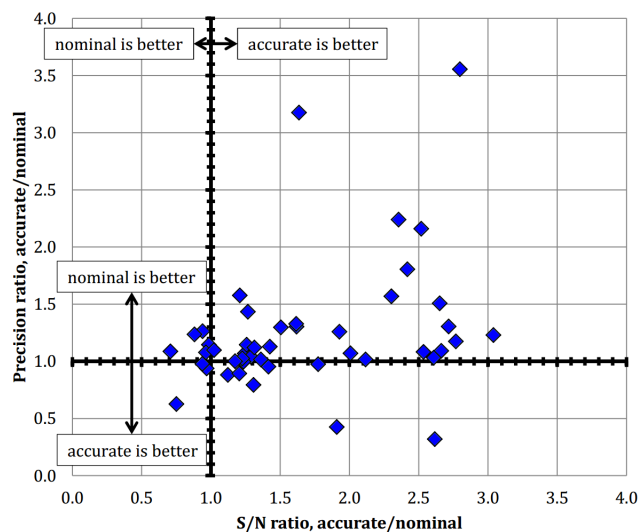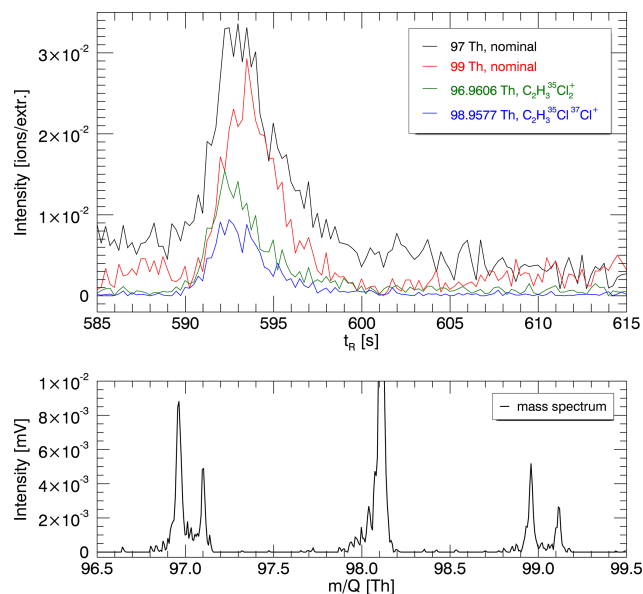
Figure 6. Corresponding ratios of signal-to-noise (*x* axis) and measurement precision (*y* axis) of values determined with accurate mass intensities relative to values determined with nominal mass intensities. Each diamond represents a substance which was evaluated on both nominal and accurate masses. Data based on repeated measurements of the same reference gas at constant sample volume of about 0.66 L, see Fig. 5. While S/N is improved for almost all substances using the accurate mass intensities, a slight decrease in measurement precision is observed compared to values derived with nominal mass intensities.

Figure 7. Upper graph: chromatographic signal of methyl chloroform (CH_3CCl_3) on ion masses 97 and 99 Th, nominal mass intensities shown in black and red, accurate mass intensities shown in green and blue. Lower graph: mass spectrum excerpt at the chromatographic peak apex. A coeluting substance with matching retention time and nominal masses 97 and 99 Th leads to a systematic error in mixing ration determination if the nominal mass intensity is used for substance quantification. Unit conversions, *y* axis of lower to upper graph: see Fig. 3.

3.3.2 Benefits from accurate mass information

As the Tofwerk AG mass spectrometer allows the use of the information gained by a significantly higher than nominal mass resolving power, the question arises of how signal-to-noise ratios and measurement precision are influenced by the use of accurate mass information for further data processing.

Accurate masses comprise mass accuracy as an additional error source if fixed mass intervals are used to obtain them. Consequently, the correlation of measurement precision and signal-to-noise ratio is less pronounced ($r^2 = 0.75$) for the same experiment shown in Fig. 5 and overall measurement precision is slightly decreased (10 out of 53 vs. 15 out of 47 better than 1 %), even if it is also increased for some species. Signal-to-noise ratios are increased in almost all cases using accurate masses. The changes in both quantities, measurement precision and signal-to-noise, relative to values determined for nominal masses are shown in Fig. 6.

While S/N is mostly increased by factors up to 3 when comparing accurate mass to nominal mass evaluation, a coinciding decrease in measurement precision can be observed (upper right quadrant of Fig. 6). However, this is not strictly true for all analysed substances; some are improved in both quantities by using the accurate mass information instead of the nominal mass information (lower right quadrant of Fig. 6). A possible explanation is the

interference from other ions with matching nominal mass caused by an unknown substance in the specific retention time window. This interference can be compensated by the use of accurate masses, if the accurate ion masses from known and unknown compound differ in that case. Only very few substances show better S/N and better measurement precision on nominal masses (upper left quadrant of Fig. 6) and only one substance exhibits a better measurement precision on the accurate mass together with a decreased S/N ratio (lower left quadrant of Fig. 6). The substance was identified to be methyl chloroform (CH_3CCl_3).

This substance is an example of how the accuracy of substance quantification can be improved in some cases by using the accurate mass information as illustrated in Fig. 7. A narrow mass interval can compensate the coelution of a substance with matching nominal mass but deferring accurate mass. In such cases, the accurate mass from the GC-TOFMS system is likely to give a mixing ratio much closer to the true value.

3.3.3 Reproducibility and instrument stability

To demonstrate measurement precision over a longer time period and varying conditions, Table 6 displays mean single measurement precision of 10 selected substances derived from five idealized precision experiments and four routine

Table 6. Mean measurement precision and relative drift in calibration of 10 selected substances which were chosen according to a precision of generally better than 1 %. Data are based on five different precision experiments using different reference gases and sample volumes from 0.49 to 1.38 L as well as four routine measurement series including four to five samples per series. Precision values were calculated as the arithmetic mean of all sample blocks per measurement series. Drift calculated as minimum to maximum range of normalized chromatographic signal areas of calibration measurements within the routine measurement series (10–16 h total duration). Errors are displayed as the 1-fold standard deviation over all values used per substance. All measurements were conducted with a TOFMS configuration giving an R of 3500 in mean.

Substance	Measurement precision, idealized experiments	Measurement precision, routine measurements	Drift in calibration, routine measurements
CFC-12	(0.22 ± 0.06) %	(0.30 ± 0.09) %	(5.49 ± 4.24) %
Chloromethane	(0.28 ± 0.08) %	(0.45 ± 0.20) %	(6.01 ± 3.56) %
CFC-11	(0.28 ± 0.08) %	(0.29 ± 0.04) %	(5.62 ± 4.37) %
HCFC-22	(0.30 ± 0.06) %	(0.49 ± 0.22) %	(5.23 ± 3.82) %
Carbonylsulfide	(0.42 ± 0.10) %	(0.39 ± 0.17) %	(8.47 ± 7.99) %
Dichloromethane	(0.52 ± 0.10) %	(0.48 ± 0.24) %	(8.07 ± 3.35) %
HFC-134a	(0.54 ± 0.23) %	(0.55 ± 0.15) %	(6.05 ± 5.15) %
CFC-113	(0.55 ± 0.08) %	(0.39 ± 0.11) %	(6.48 ± 3.99) %
HCFC-142b	(0.67 ± 0.15) %	(0.83 ± 0.06) %	(5.54 ± 5.23) %
Tetrachloromethane	(0.68 ± 0.21) %	(0.65 ± 0.09) %	(6.31 ± 4.77) %

measurement series. Only values derived from nominal mass evaluation are shown, as these serve as an internal reference to us and are directly comparable to our GC quadrupole MS instrument (e.g. Hoker et al., 2015).

The selection and order within Table 6 is based on best average measurement precision within the underlying precision experiments. Measurement precision in routine ambient air sample measurement series is subject to a greater variability as sample matrix, water content etc. also varies. This can be observed in column 3 of Table 6, where precision values derived from routine measurement series are shown. Precision values are slightly elevated compared to values derived from idealized experiments, as expected. However, all values are in good agreement considering the standard deviation of the estimated single measurement precision of the selected substances.

Column 4 of Table 6 shows maximum to minimum differences for normalized signal areas of calibration measurements for each substance to give information about instrument drift over routine measurement series, which typically took 10–16 h of continuous operation. The instrument was found to be less stable (10–20 % drift) if highly contaminated (e.g. by hydrocarbons) and/or very moist samples were measured or if measurements were conducted directly after start-up of the MS, e.g. after downtime due to ion source cleaning and filament replacement.

3.4 Non-linearity

As described in Sect. 2.4, a linear proportionality of mixing ratio in the sample and detector response is assumed for quantification. If mixing ratios in sample and calibration gas differ and the detector features significant non-linearities within the observed concentration range, measurement accuracy is decreased by the degree of the non-linearity. A correction of non-linearities as a post-processing step is only possible if non-linearities are systematic or very well understood. In any case, non-linearity correction adds an additional error source and is very time consuming and often complex as it can be different for every target substance.

To analyse non-linearity of the GC-TOFMS, volume variation experiments were conducted similar to the precision experiments described in Sect. 3.3 only that different volumes from the same high-pressure flask (reference gas) were preconcentrated and used as "samples". Variation volumes of 0.1–1.0 L from the reference gas were compared to 0.5 L calibration points (reference volume). For volume determination, the MFC installed in the system (see Sect. 2.1) was used. Volumes determined in parallel by the MFC and by the pressure sensor derived from Δp were found to correlate linearly ($r^2 > 0.999998$). All volume-corrected chromatographic signal areas (A/V) were normalized ($n(A/V)$) by dividing them by the drift-corrected calibration A/V. The ratio of any sample $n(A/V)$ to the calibration $n(A/V)$ at that point within the measurement series, which was calculated by linear interpolation of the bracketing calibration $n(A/V)$, should give a relative response (rR) of 1 in case of a linear system. A deviation of up to the 3-fold measurement precision from a relative response of 1 was still considered to be linear behaviour. Substances with known memory or blank effects were excluded from the analysis.

Figure 8 shows exemplary results from the volume variation experiment described in the previous paragraph of this section. Two exemplary substances are shown: CFC-12 and HFC-134a (reference gas mixing ratios: 522 and 113 ppt).
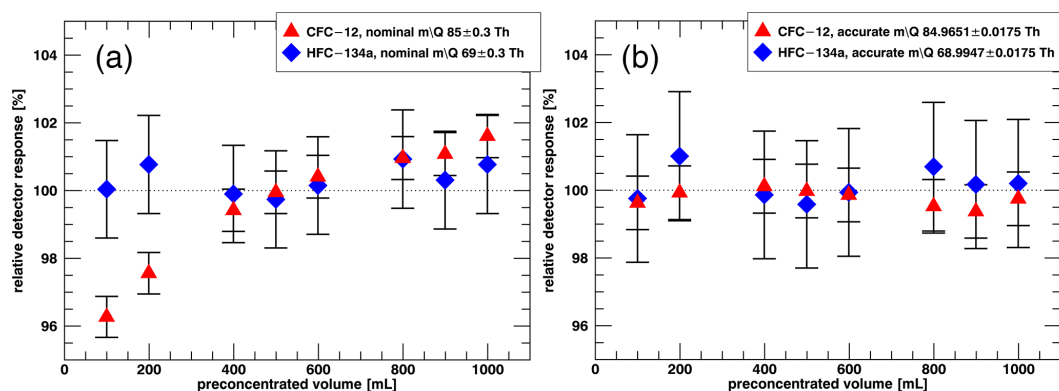
Figure 8. Relative detector responses (*y* axis) derived for different preconcentration volumes (*x* axis) of the same reference gas. Relative responses were calculated relative to the detector response of calibration points with a preconcentrated volume of 0.5 L. Error bars: 3-fold measurement precision of the respective substance. **(a)** Results based on nominal mass data; **(b)** results based on accurate mass data. While HFC-134a (blue diamonds) does not deviate significantly from linearity in either of the panels, a systematic non-linearity is observed for CFC-12 (red triangles) in **(a)**.

While HFC-134a shows no deviations from the expected linear response within the 3-fold measurement precision, a systematic deviation from linearity is observed for CFC-12 if the calculation of relative responses is based on nominal mass intensities, i.e. integer mass of the ion serving as quantifier ± 0.3 Th (Fig. 8a). The mixing ratio of CFC-12 in smaller sample volumes would be systematically underestimated while the mixing ratio in larger volumes would be systematically overestimated. Although most pronounced for CFC-12, this systematic deviation from linearity was also found for four other substances with similar chromatographic peak heights (0.5 L preconcentrated volume, peak heights given relative to the peak height of CFC-12): CH_3Cl (74.5 % relative height), CFC-11 (CCl_3F, 56.7 % relative height), HCFC-22 ($CHClF_2$, 32.6 % relative height) and COS (25.7 % relative height). All substances with peak heights of $\leq \sim 15$ % relative to CFC-12 did not reveal a systematic deviation from linearity like e.g. HFC-134a with 10.1 % relative height. For the correlation of chromatographic peak height and the deviation from linearity expressed as the *n*-fold measurement precision, a Spearman rank correlation coefficient of $\rho = +0.78$ ($p < 0.0001$) was found. This suggests that the degree of non-linearity correlates positively with the maximum number of fragment ions formed by ionization of a substance eluting from the GC.

The systematic non-linearity found for the species named above mostly disappears if the calculation of relative responses is based on accurate mass intensities – i.e. the exact ion mass of the ion serving as quantifier ± 0.0175 Th, as exemplarily shown in Fig. 8b for CFC-12. The results for other substances like HFC-134a do not change significantly compared to the results based on nominal mass intensities.

The difference of nominal and accurate mass intensities can possibly be assigned to a (potentially instrument-specific) signal reflection at high intensities, presumably in the high-frequency line between MCP and pre-amplifier or also within the pre-amplifier itself. As illustrated in Fig. 9, a "shoulder" appears to the right of the ion signal. As both results displayed in Fig. 9 are based on chromatograms of the same reference gas, a neighbouring ion signal should appear in both chromatograms (0.1 and 1.0 L preconcentrated volume). The hypothesis of a signal reflection can furthermore be supported by the finding that a longer signal cable between MCP and pre-amplifier moves the "shoulder" further away from the actual signal. As the reflected signal travels through the cable multiple times, the relative offset towards the actual signal is increased if the duration of a single pass-through is increased by a longer cable. This observation is displayed in Figure 10 for the high-intensity signal on mass 69 of the CF_3^+ ion from the mass axis calibration substance (see Sect. 2.3 for a description of the calibration pulser).

If signals are summed up over an interval of ± 0.3 Th around the integer mass, the area of the artificial "shoulder" is included in the nominal mass intensity, creating a positive offset which increases with the number of ions reaching the detector (i.e. sample volume) according to the results discussed above. Consequently, the response from a larger sample volume is overestimated and the response from a smaller sample volume is underestimated as the comparison is done relative to the response from a fixed sample volume of 0.5 L. The fact that no non-linearities were found below a certain signal height ($\leq \sim 15$ % relative to CFC-12 signal height) suggests that the signal reflection becomes insignificant at low intensities. Note that in the example discussed above, we had to use a narrower mass interval to calculate the accurate mass intensity and exclude the reflection (± 0.0175 Th instead of ± 0.0250 Th used by default, see Sect. 2.4).
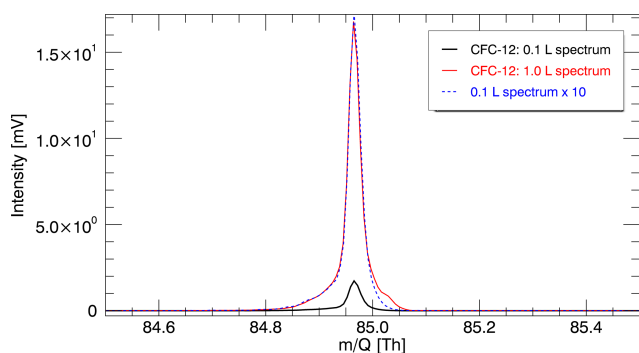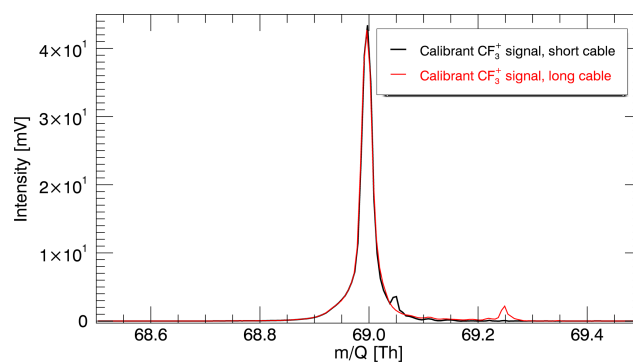
Figure 9. Comparison of $CF_2^{35}Cl^+$ signals taken from the chromatographic peak apex of CFC-12. The solid lines in black and red show intensities of a 0.1 and 1.0 L sample, both from preconcentrations of the same reference gas. Towards high intensities (1.0 L spectrum), a "shoulder" appears to the right of the ion signal, which is not detectable at low intensities (0.1 L spectrum). The blue dashed line shows the intensity of the 0.1 L spectrum multiplied by 10 for comparison. No "shoulder" is visible in this calculated spectrum.

Figure 10. CF_3^+ signals obtained from the mass axis calibration substance (perfluoroperhydrophenanthrene; see also Sect. 2.3), with signal intensity displayed on the y axis and m/Q displayed on the x axis. The signal drawn in black was obtained with a short connection cable between MCP and pre-amplifier (ca. 150 mm); the signal drawn in red was obtained with a long cable between MCP and pre-amplifier (ca. 1500 mm). No chromatographic run was active at the time of recording. The signal elevation to the right of the actual ion signal is clearly shifted to the right if the signal travel time is increased by a longer cable.

From a practical point of view, the non-linearities observed are problematic if the following conditions are met: (1) the analysis is done with nominal mass intensities and (2) the signal intensity generated by the quantifier ion of a substance reaches a certain level (which has to be determined by dedicated experiments). Condition (2) can also be met for substances like HFC-134a which did not exhibit non-linear behaviour in the experiment described above but might show large variability of mixing ratio in different samples. However, suppression of the non-linearity by the use of accurate mass intensities is possible without a significant decrease in measurement precision (Fig. 8b). Furthermore, the open data format of the used TOFMS does offer many options to correct the non-linearity by exploiting the accurate mass information. Narrow mass intervals is just one straightforward approach and other procedures like a mass peak fitting using prescribed peak shapes or a mathematical deconvolution of signal peak and reflected peak would also be possible.

3.5 Comparison to reference instrument

For quality assurance, we compared the instrument to our laboratory GC-QPMS, which showed consistent results with the NOAA network (National Oceanic and Atmospheric Administration) in Hall et al. (2014) and has been used before by Laube et al. (2010), Brinckmann et al. (2012) and Hoker et al. (2015). During the currently ongoing InGOS (Integrated non-CO_2 Greenhouse gas Observation System) Halocarbon Round Robin Intercomparison (IHRRI), four ambient air flask samples were analysed on both instruments using the same calibration gas. A relative comparison is therefore not afflicted by calibration gas mixing ratio

uncertainties or calibration scale differences. Please note that no official IHRRI results have been published at the time of preparation of this paper so we will not name any specific mixing ratios.

Thirty-four substances were analysed on both the GC-QPMS and the GC-TOFMS and compared subsequently. One substance, tetrachloroethene (C_2Cl_4), was excluded from comparison due to contamination issues at the GC-TOFMS (blank residues > 20 %). The mean absolute deviation over all four samples between both instruments was calculated for each substance. Furthermore, the mean ratio of both instruments over all substances was analysed for each sample to check for systematic deviations. The mean ratio did not deviate significantly from 1 within one standard deviation. An overall systematic deviation between both instruments is therefore not evident.

Figure 11 shows results for the 33 substances compared. A substance-specific error estimate was calculated by Gaussian error propagation of the 1σ measurement precision of both instruments. Nineteen of 33 substances (58 %) are in very good agreement (within 1-fold error) and 12 substances are in good agreement (within 2-fold error) at both instruments, giving a total of 94 % within the 2-fold error. For only two substances, the differences in mixing ratio lay further apart than the 2-fold error: trichloroethene (C_2HCl_3, 2.5-fold error) and methyl chloroform (2.1-fold error). Trichloroethene is systematically elevated in chromatograms of the GC-TOFMS; therefore, a contamination problem similar to tetrachloroethene is likely, however not confirmed by blank residues. A significant difference in methyl chloroform mixing ratio between both instruments is only observed in one sample of the round robin series (likely
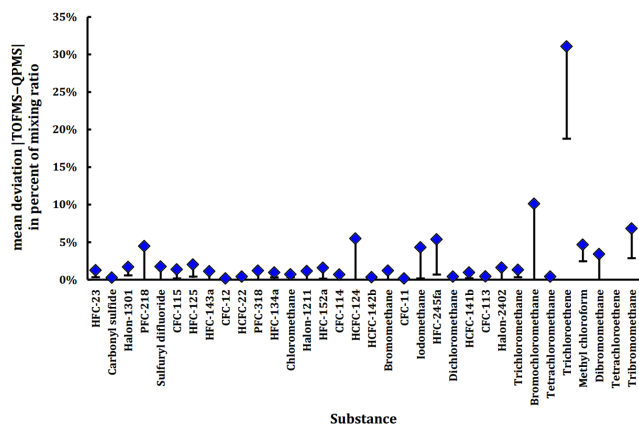
Figure 11. Mean deviation of mixing ratios determined with the GC-QPMS and the GC-TOFMS in the four InGOS round robin flasks. *X* axis: list of the 33 substances analysed, order based on retention times on the GC-quadrupole MS. *Y* axis: average absolute deviation of both instruments in [%]. GC-TOFMS results were derived from accurate mass intensities. Error bars: uncertainty calculated by Gaussian error propagation of the 1σ measurement precision of both instruments.

polluted air). Results shown earlier in this work (Sect. 3.3) suggest that the GC-TOFMS could provide better accuracy in the case of methyl chloroform.

4   Summary and conclusion

In this work, a newly developed GC-TOFMS system designed for the quantitative analysis of halogenated trace gases was characterized. Besides a state-of-the-art GC and TOFMS, the setup comprises a self-built sample preconcentration unit. It is routinely operated with an adsorption temperature of $-80\,°C$, but allows $-120\,°C$ (tested) and depending on the cycle time of cooling and heating even lower adsorption temperatures, without needing a cooling agent like liquid nitrogen. The thermodesorption of the preconcentrated sample directly onto the warm GC column together with a cool-down time back to adsorption temperature of less than 60 s allows a high cycle time. The combination of automated sample selection, preconcentration and measurement sequencing, as well as the fully accessible data format of the TOFMS, enabled us to gain in-depth understanding of the analytical instrument with focus on the mass spectrometer.

The medium-level mass resolving power of approximately 4000 allows the quantitative separation of e.g. many hydrocarbon fragments from halogenated fragments. This makes the analysis more independent from sample matrix effects and can therefore increase accuracy of quantification. The latter is mandatory for reliable quantification, as needed for many atmospheric halocarbon analyses (attribution of trends, sources etc.). It also gives the instrument an

advantage over quadrupole mass spectrometers in chemical identification, although it cannot compete with instruments built specifically for this task with mass resolving powers of multiple tens of thousands. Mass accuracy determined for the characterized instrument was found to support the benefits from the mass resolving power of the instrument in respect to unambiguous fragment identification. The calibrant pulser of the TOFMS was found to be a very valuable innovation as it offers the option to establish automated recalibration of the mass axis.

The mass spectrometer was also found to be very sensitive, especially when using the accurate mass information. This allows for relatively small and easy-to-handle sample sizes of 0.5–1.0 L and also the early detection of emerging compounds with very low atmospheric mixing ratios in the range of a few ppt to ppq. At the upper end of the concentration range, no saturation effect of the detector was observed for any of the analysed species; the largest preconcentration volume tested was 10.0 L corresponding to about 5.2 ppb (ca. 25.5 ng) of the highest concentrated halocarbon CFC-12.

A measure for the measurement precision needed for atmospheric trace gas analysis, here mainly halocarbons, is the capability of resolving atmospheric variability and trends. One of the most challenging tasks is the attribution of atmospheric trends of major long-lived halocarbons, at least on yearly base. The instrument is capable of classifying most sample mixing ratios into the yearly trend of the respective substances (Carpenter et al., 2014) based on a single measurement. There are only a few exceptions of substances with very small trends, e.g. CFC-114 with $-0.2\,\%\,yr^{-1}$ ($-0.01\,ppt\,yr^{-1}$).

Instrument non-linearities were found to be negligible for the low and medium mixing ratio range analysed ($<150\,ppt$ at 0.5 L preconcentration volume). At higher concentration levels, significant non-linearities were found, in positive correlation with signal intensity. These non-linearities could be suppressed by setting narrow mass intervals around mass signals and thereby excluding artificially elevated parts of the signal. At this time, it is not clear whether this issue is specific to our instrument or affects a series of EI-TOFMS. A hardware solution is ongoing work at Tofwerk and also in cooperation with us to fully understand and solve the problem.

Overall, the instrument was found to be very well suited for the quantitative analysis of halocarbons in air, also supported by the results of a comparison to a reference instrument. A big step forward was made compared to common quadrupole and TOFMS with low resolving power ≤ 1000. The availability of accurate mass information at medium mass resolving power has proven to be very valuable due to the simplified substance identification, the gain in sample matrix independence and measurement accuracy and also in respect to the exclusion of non-linearities induced by the detection system of the MS. Within the described

field of application, both the general limitations being low dynamic range and non-linearity of TOFMS seem to be overcome by the Tofwerk instrument. Together with the always present high-sensitivity full mass range, these aspects make TOFMS in general an ideally suited method for digital air archiving. This work is only focused on halocarbons in atmospheric air samples, but in principle there is much more information in the chromatograms recorded with full mass range. We have just started to look into other substance classes like hydrocarbons and the GC-TOFMS data look very promising for future (re-)analysis of many more substances than discussed here.

References

Arnold, T., Mühle, J., Salameh, P. K., Harth, C. M., Ivy, D. J., and Weiss, R. F.: Automated measurement of nitrogen trifluoride in ambient air, Anal. Chem., 84, 4798–4804, 2012.

Bassford, M. R., Simmonds, P. G., and Nickless, G.: An automated system for near-real-time monitoring of trace atmospheric halocarbons, Anal. Chem., 70, 958–965, 1998.

Bonk, T. and Humeny, A.: MALDI-TOF-MS analysis of protein and DNA, Neuroscientist, 7, 6–12, 2001.

Brinckmann, S., Engel, A., Bönisch, H., Quack, B., and Atlas, E.: Short-lived brominated hydrocarbons – observations in the source regions and the tropical tropopause layer, Atmos. Chem. Phys., 12, 1213–1228, doi:10.5194/acp-12-1213-2012, 2012.

Carpenter, L. J., Reimann, S., Burkholder, J. B., Clerbaux, C., Hall, B. D., Hossaini, R., Laube, J. C., and Yvon-Lewis, S. A.: Ozone-Depleting Substances (ODSs) and other gases of interest to the Montreal Protocol, in: Scientific Assessment of Ozone Depletion: 2014, Global Ozone Research and Monitoring Project – Report No. 55, 416 pp., World Meteorological Organization, Geneva, Switzerland, 2014.

Clemons, C. A. and Altshuller, A. P.: Responses of electron-capture detector to halogenated substances, Anal. Chem., 38, 133–136, 1966.

Coles, J. N. and Guilhaus, M.: Resolution limitations from detector pulse width and jitter in a linear orthogonal-acceleration time-of-flight mass spectrometer, J. Am. Soc. Mass Spectrom., 5, 772–778, doi:10.1016/1044-0305(94)80010-3, 1994.

DeCarlo, P. F., Kimmel, J. R., Trimborn, A., Northway, M. J., Jayne, J. T., Aiken, A. C., Gonin, M., Fuhrer, K., Horvath, T.,

Docherty, K. S., Worsnop, D. R., and Jimenez, J. L.: Field-deployable, high-resolution, time-of-flight aerosol mass spectrometer, Anal. Chem., 78, 8281–8289, 2006.

Emteborg, H., Tian, X., Ostermann, M., Berglund, M. and Adams, F. C.: Isotope ratio and isotope dilution measurements using axial inductively coupled plasma time of flight mass spectrometry, J. Anal. Atom. Spectrom., 15, 239–246, 2000.

Farman, J. C., Gardiner, B. G., and Shanklin, J. D.: Large losses of total ozone in Antarctica reveal seasonal ClO_x/NO_x interaction, Nature, 315, 207–210, 1985.

Grant, A., Yates, E. L., Simmonds, P. G., Derwent, R. G., Manning, A. J., Young, D., Shallcross, D. E., and O'Doherty, S.: A five year record of high-frequency in situ measurements of non-methane hydrocarbons at Mace Head, Ireland, Atmos. Meas. Tech., 4, 955–964, doi:10.5194/amt-4-955-2011, 2011.

Graus, M., Müller, M., and Hansel, A.: High resolution PTR-TOF: quantification and formula confirmation of VOC in real time, J. Am. Soc. Mass Spectr., 21, 1037–1044, 2010.

Grimsrud, E. P. and Rasmussen, R. A.: Survey and analysis of halocarbons in the atmosphere by gas chromatography-mass spectrometry, Atmos. Environ., 9, 1014–1017, 1975.

Guilhaus, M.: Special feature: Tutorial, principles and instrumentation in time-of-flight mass spectrometry, physical and instrumental concepts, J. Mass Spectrom., 30, 1519–1532, 1995.

Hall, B. D., Engel, A., Mühle, J., Elkins, J. W., Artuso, F., Atlas, E., Aydin, M., Blake, D., Brunke, E.-G., Chiavarini, S., Fraser, P. J., Happell, J., Krummel, P. B., Levin, I., Loewenstein, M., Maione, M., Montzka, S. A., O'Doherty, S., Reimann, S., Rhoderick, G., Saltzman, E. S., Scheel, H. E., Steele, L. P., Vollmer, M. K., Weiss, R. F., Worthy, D., and Yokouchi, Y.: Results from the International Halocarbons in Air Comparison Experiment (IHALACE), Atmos. Meas. Tech., 7, 469–490, doi:10.5194/amt-7-469-2014, 2014.

Hoker, J., Obersteiner, F., Bönisch, H., and Engel, A.: Comparison of GC/time-of-flight MS with GC/quadrupole MS for halocarbon trace gas analysis, Atmos. Meas. Tech., 8, 2195–2206, doi:10.5194/amt-8-2195-2015, 2015.

IUPAC: Compendium of Analytical Nomenclature (the "Orange Book"), Blackwell Science, Ltd., Oxford, UK, 1998.

IUPAC: Compendium of Chemical Terminology – Gold Book, available at: http://goldbook.iupac.org/PDF/goldbook.pdf (last access: 14 September 2015), 2014.

Keller, C. A., Hill, M., Vollmer, M. K., Henne, S., Brunner, D., Reimann, S., O'Doherty, S., Arduini, J., Maione, M., Ferenczi, Z., Haszpra, L., Manning, A. J., and Peter, T.: European emissions of halogenated greenhouse gases inferred from atmospheric measurements, Environ. Sci. Technol., 46, 217–225, 2011.

Kerwin, R. A., Crill, P. M., Talbot, R. W., Hines, M. E., Shorter, J. H., Kolb, C. E., and Harriss, R. C.: Determination of atmospheric methyl bromide by cryotrapping-gas chromatography and application to soil kinetic studies using a dynamic dilution system, Anal. Chem., 68, 899–903, 1996.

Laube, J. C., Kaiser, J., Sturges, W. T., Bönisch, H., and Engel, A.: Chlorine isotope fractionation in the stratosphere, Science, 329, 1167, doi:10.1126/science.1191809, 2010.

Laube, J. C., Hogan, C., Newland, M. J., Mani, F. S., Fraser, P. J., Brenninkmeijer, C. A. M., Martinerie, P., Oram, D. E.,

Röckmann, T., Schwander, J., Witrant, E., Mills, G. P., Reeves, C. E., and Sturges, W. T.: Distributions, long term trends and emissions of four perfluorocarbons in remote parts of the atmosphere and firn air, Atmos. Chem. Phys., 12, 4081–4090, doi:10.5194/acp-12-4081-2012, 2012.

Lee, J. M., Sturges, W. T., Penkett, S. A., Oram, D. E., Schmidt, U., Engel, A., and Bauer, R.: Observed stratospheric profiles and stratospheric lifetimes of HCFC-141b and HCFC-142b, Geophys. Res. Lett., 22, 1369–1372, 1995.

Lunt, M. F., Rigby, M., Ganesan, A. L., Manning, A. J., Prinn, R. G., O'Doherty, S., Muhle, J., Harth, C. M., Salameh, P. K., Arnold, T., Weiss, R. F., Saito, T., Yokouchi, Y., Krummel, P. B., Steele, L. P., Fraser, P. J., Li, S., Park, S., Reimann, S., Vollmer, M. K., Lunder, C., Hermansen, O., Schmidbauer, N., Maione, M., Arduini, J., Young, D., and Simmonds, P. G.: Reconciling reported and unreported HFC emissions with atmospheric observations, P. Natl. Acad. Sci. USA, 112, 5927–5931, 2015.

Maione, M., Giostra, U., Arduini, J., Belfiore, L., Furlani, F., Geniali, A., Mangani, G., Vollmer, M. K., and Reimann, S.: Localization of source regions of selected hydrofluorocarbons combining data collected at two European mountain stations, Sci. Total Environ., 391, 232–240, 2008.

Midgley, T.: From the Periodic Table to production, Ind. Eng. Chem., 29, 241–244, 1937.

Miller, B. R., Weiss, R. F., Salameh, P. K., Tanhua, T., Greally, B. R., Muhle, J., and Simmonds, P. G.: Medusa: a sample preconcentration and GC/MS detector system for in situ measurements of atmospheric trace halocarbons, hydrocarbons, and sulfur compounds, Anal. Chem., 80, 1536–1545, 2008.

Molina, M. J. and Rowland, F. S.: Stratospheric sink for chlorofluoromethanes: chlorine atomc-atalysed destruction of ozone, Nature, 249, 810–812, 1974.

Mühle, J., Ganesan, A. L., Miller, B. R., Salameh, P. K., Harth, C. M., Greally, B. R., Rigby, M., Porter, L. W., Steele, L. P., Trudinger, C. M., Krummel, P. B., O'Doherty, S., Fraser, P. J., Simmonds, P. G., Prinn, R. G., and Weiss, R. F.: Perfluorocarbons in the global atmosphere: tetrafluoromethane, hexafluoroethane, and octafluoropropane, Atmos. Chem. Phys., 10, 5145–5164, doi:10.5194/acp-10-5145-2010, 2010.

Ravishankara, A. R., Turnipseed, A. A., Jensen, N. R., Barone, S., Mills, M., Howard, C. J., and Solomon, S.: Do hydrofluorocarbons destroy stratospheric ozone?, Science, 263, 71–75, 1994.

Rowland, A. and Holcombe, J. A.: Evaluation and correction of isotope ratio inaccuracy on inductively coupled plasma time-of-flight mass spectrometry, Spectrochim. Acta B, 64, 35–41, 2009.

Sala, S., Bönisch, H., Keber, T., Oram, D. E., Mills, G., and Engel, A.: Deriving an atmospheric budget of total organic bromine using airborne in situ measurements from the western Pacific area during SHIVA, Atmos. Chem. Phys., 14, 6903–6923, doi:10.5194/acp-14-6903-2014, 2014.

Simmonds, P. G., O'Doherty, S., Nickless, G., Sturrock, G. A., Swaby, R., Knight, P., Ricketts, J., Woffendin, G., and Smith, R.: Automated gas chromatograph/mass spectrometer for routine atmospheric field measurements of the CFC replacement compounds, the hydrofluorocarbons and hydrochlorofluorocarbons, Anal. Chem., 67, 717–723, 1995.

Simmonds, P. G., Derwent, R. G., Manning, A. J., McCulloch, A., and O'Doherty, S.: USA emissions estimates of CH_3CHF_2, CH_2FCF_3, CH_3CF_3 and CH_2F_2 based on in situ observations at Mace Head, Atmos. Environ., 104, 27–38, 2015.

Stohl, A., Kim, J., Li, S., O'Doherty, S., Mühle, J., Salameh, P. K., Saito, T., Vollmer, M. K., Wan, D., Weiss, R. F., Yao, B., Yokouchi, Y., and Zhou, L. X.: Hydrochlorofluorocarbon and hydrofluorocarbon emissions in East Asia determined by inverse modeling, Atmos. Chem. Phys., 10, 3545–3560, doi:10.5194/acp-10-3545-2010, 2010.

Velders, G. J. M., Madronich, S., Clerbaux, C., Derwen, R., Grutter, M., Hauglustaine, D., Incecik, S., Ko, M., Libre, J.-M., Nielsen, O. J., Stordal, F., and Zhu, T.: Chemical and radiative effects of halocarbons and their replacement compounds, in: IPCC/TEAP 2005 – Safeguarding the Ozone Layer and the Global Climate System: Issues Related to Hydrofluorocarbons and Perfluorocarbons, Cambridge University Press, Cambridge, UK, 133–180, 2005.

Vollmer, M. K., Miller, B. R., Rigby, M., Reimann, S., Mühle, J., Krummel, P. B., O'Doherty, S., Kim, J., Rhee, T. S., Weiss, R. F., Fraser, P. J., Simmonds, P. G., Salameh, P. K., Harth, C. M., Wang, R. H. J., Steele, L. P., Young, D., Lunder, C. R., Hermansen, O., Ivy, D., Arnold, T., Schmidbauer, N., Kim, K.-R., Greally, B. R., Hill, M., Leist, M., Wenger, A., and Prinn, R. G.: Atmospheric histories and global emissions of the anthropogenic hydrofluorocarbons HFC-365mfc, HFC-245fa, HFC-227ea, and HFC-236fa, J. Geophys. Res., 116, D08304, doi:10.1029/2010jd015309, 2011.

Vollmer, M. K., Reimann, S., Hill, M., and Brunner, D.: First observations of the fourth generation synthetic halocarbons HFC-1234yf, HFC-1234ze(E), and HCFC-1233zd(E) in the atmosphere, Environ. Sci. Technol., 49, 2703–2708, 2015.